

The copyright of this thesis vests in the author. No quotation from it or information derived from it is to be published without full acknowledgement of the source. The thesis is to be used for private study or non-commercial research purposes only.

Published by the University of Cape Town (UCT) in terms of the non-exclusive license granted to UCT by the author.

4

# **Geomagnetically Induced Currents and its Presence in the Eskom Transmission Network**



Prepared by:

Jacko Koen,  
MSc Electrical Engineering Student,  
University of Cape Town

Prepared for:

Prof. C T Gaunt,  
Department of Electrical Engineering,  
University of Cape Town,  
22 February 2000

Submitted to the Department of Electrical Engineering, University of Cape Town, in  
partial fulfilment of the requirements for the degree of Master of Science in Engineering

*“The most beautiful experience we can have is the mysterious.  
It is the fundamental emotion which stands at the cradle of true  
art and true science.*

*Whoever does not know it and can no longer wonder, no longer  
marvel, is as good as dead, and his eyes are dimmed.”*

*- Albert Einstein, 1931 [4]*

# Terms of Reference

This project was commissioned by Mr A C Britten of Eskom TSI and supervised by Prof. C T Gaunt of the University of Cape Town. The final instructions given on 1 February 1999, were:

1. To undertake a thorough literature search on the mechanism of Geomagnetically Induced Currents and its effect on power network equipment.
2. Review prevailing solar activity and identify the potential benefits of monitoring GICs and its effects.
3. Investigate correlation (if any) between previous system events and geomagnetic storms.
4. Understand the modelling process necessary to theoretically predict expected levels of GIC in the Eskom MTS.

Instruction 3 was necessary to establish whether the Eskom MTS might be susceptible to GICs. Instruction 4 was done based on a method developed at the Finnish Meteorological Institute. The final thesis reflects work for all four instructions.

## Declaration

This thesis could not have been carried without substantial help from expertise from the University of Cape Town, Eskom and the Finnish Meteorological Institute, all whom have been mentioned in the acknowledgements. The breakdown of work on various aspects of the thesis was as follows:

### Literature Search

Although the literature review was done by myself I would not be able to do it thoroughly without the input and guidance of Prof. C T Gaunt (UCT), Mr A C Britten (Eskom, TSI), Prof. R Pirjola (Finnish Meteorological Institute) and Mr C King (Eskom, Transmission).

### Investigation of Past Events

The investigation into possible correlation between system events and GICs would not be possible without data received from Dr P Sutcliffe (Hermanus Magnetic Observatory) and Mr E Stokes-Waller (Eskom, National Control). Guidance to identify such events was provided by Prof. C T Gaunt (UCT).

### Modelling Technique

The understanding and application of the necessary method to completely model the effect of GICs on power networks would not be possible without the support and guidance of Prof. R Pirjola and Dr A Viljanen both of the Finnish Meteorological Institute.

Signature:

Signed by candidate

Date: 28/02/2000

# Abstract

This thesis serves to describe the findings of the investigation into the possible existence and occurrence of Geomagnetically Induced Currents (GICs) in the Eskom MTS. The project commenced in January 1999 and is a joint collaboration between Eskom, the University of Cape Town and EPRI.

Eskom has been aware since about 1990, that occasional severe geomagnetic storms in the Southern Cape might disrupt the MTS in that area. At that time no correlation was observed between disruptions at selected sites of the Eskom MTS and geomagnetic activity. (The sites selected were based on the knowledge at that time.) However, there is now evidence that the sites most susceptible are not at the conventionally accepted locations, and that damage and disruption may have occurred where it was not expected.

For this project a thorough literature search was done to understand the source and effects of GICs. An investigation was conducted into the past events on the Eskom MTS, which was compared with geomagnetic activity to check for correlation. Finally, the modelling process of a network that would indicate its susceptibility to GICs was studied.

Typical disruptions that would indicate the existence of GICs include Buchholz trips, interwinding faults, permanent failure due to internal faults, etc. From this investigation there is circumstantial evidence that equipment damage may have occurred due to geomagnetic activity during the previous solar cycle peak

# Acknowledgements

I am indebted first and foremost to my supervisor, Prof. Trevor Gaunt for his guidance and support with the project. His numerous discussions, advice and comments have greatly helped me in the course of this work.

I owe many thanks to Mr Tony Britten of Eskom TSI who approached me with this project. I appreciate the opportunity he gave me as well as his interest and support of the project.

My sincere appreciation goes to Prof. Risto Pirjola and Dr Ari Viljanen of the Finnish Meteorological Institute for their help and support. Prof. Pirjola went out of his way to help and guide me; his patience and friendly support is greatly appreciated.

I own many thanks to Mr Colin King of Eskom Transmission for our many discussions and his comments. I would also like to thank Dr Peter Sutcliffe of the Hermanus Magnetic Observatory. Dr Sutcliffe was always available to discuss and provide information regarding geomagnetic disturbances. Mr Edmund Stokes-Waller of Eskom National Control supplied the data on past system events, which is greatly appreciated. I also own thanks to Mr Archie Graham for providing help with illustrations and software.

This project would not be possible without the financial support of Mr Logan Pillay (Eskom TSI) and the Eskom Transmission Group Steering Committee for which I am very grateful.

I wish to express my gratitude to my parents for their continuous support and to my fiancée Willina, who has been a constant source of encouragement through the many years of my studies.

Above all my eternal gratitude for the love that transcends all understanding bestowed on me by God the Father, the Son and the Holy Spirit.

# Contents

## List of Illustrations

<b>Introduction</b>	<b>1</b>
<b>1. Geomagnetic Storms</b>	<b>3</b>
1.1 Introduction	3
1.2 The Sun	4
1.2.1 History	4
1.2.2 The Solar Atmosphere and Solar Wind	7
1.2.3 The Solar Cycle	9
1.3 The Earth's Magnetic Field	15
1.4 Solar Wind Interaction with the Magnetosphere	16
1.5 Disrupting the Magnetic Field	23
1.6 Magnetic Field Measurements	24
<b>2. GIC Effects on Power Systems</b>	<b>26</b>
2.1 Introduction	26
2.2 Protective Relaying Effects	27
2.3 Saturation of Power Transformers and Reactors	28
2.4 Transformer Heating	30
2.5 Harmonic Generation in Transformers	32
2.6 The Expected Performance of Eskom Power Transformers	33



<b>3.</b>	<b>Historical Background</b>	<b>35</b>
3.1	Introduction	35
3.2	Disrupting Technology	35
3.3	Disrupting Power Systems	37
3.3.1	International Incidents Related to GICs	37
3.3.2	The Relation of Geomagnetic Storms and Network Equipment Failure in South Africa	41
3.3.2.1	Shunt Capacitors	41
3.3.2.2	Transformers and Reactors	41
<b>4.</b>	<b>Modelling and Predicting GICs</b>	<b>44</b>
4.1	Introduction	44
4.2	Network Calculation	44
4.2.1	Model Description	44
4.2.2	Network Configuration	47
4.3	Geophysical Calculation	51
4.4	Example of Calculating GICs	53
4.4.1	Network Constants	53
4.4.2	Magnetic Data and GIC	57
4.4.3	Interpretation of Results	58
<b>5.</b>	<b>Measurements and Mitigation</b>	<b>60</b>
5.1	Introduction	60
5.2	Measurements	61
5.3	Mitigation	63
5.3.1	Passive Devices	63
5.3.2	Active Devices	63
5.3.3	Operational Mitigation	63
<b>6.</b>	<b>Conclusions and Recommendations</b>	<b>65</b>

<b>References</b>	<b>67</b>
-------------------	-----------

<b>Appendixes</b>	<b>i</b>
-------------------	----------

<b>A</b>	<b>Literature Review</b>	<b>74</b>
<b>B</b>	<b>Trip Report on Visit to United States and Scandinavia</b>	<b>82</b>
<b>C</b>	<b>Data of Geomagnetic Activity (K-index)</b>	<b>86</b>
<b>D</b>	<b>Report on Failure of Reactors at Beta</b>	<b>100</b>
<b>E</b>	<b>Calculating the Electric Field</b>	<b>122</b>
<b>F</b>	<b>Magnetic Data Used for Example</b>	<b>123</b>

# List of Illustrations

1	Induced voltage drives GIC through the neutral ground points of power transformers	1
1.1	Galileo used observations of the changing position of sunspots to prove that the sun rotated	5
1.2	Sunspot numbers through the last four cycle's	6
1.3	The various components of the Sun's atmosphere	7
1.4	Solar corona seen during a total solar eclipse	8
1.5	A composite photograph of the sun showing several forms of activity	9
1.6	Formation of sunspots	10
1.7	The sunspot "butterfly pattern"	11
1.8	A typical sunspot, showing the dark umbra and a penumbra	11
1.9	A solar flare in comparison to the size of the earth	12
1.10	Coronal Mass Ejection	13
1.11	Plages are due to moderate concentrations of magnetic flux	14
1.12	Quiescent prominence	14
1.13	The earth's dipole magnetic field	15
1.14	Particles are trapped forming regions known as the Van Allen radiation belts	15
1.15	Magnetospheric convention with a southward directed interplanetary magnetic field	16
1.16	Diffuse Aurora as seen from space	18
1.17	Sketch showing the main features of the magnetosphere	18
1.18	Sequence of changes of magnetic field and plasma configuration during a substorm	19
1.19	Schematic of the northern half of the magnetospheric current system that flows during a substorm in the Auroral Oval	20

1.20	The spectacular Aurora Borealis	21
1.21	The Northern and Southern Auroral Ovals	21
1.22	The earth is surrounded by a dynamically changing region	22
1.23	Idealised H-component variations during a geomagnetic storm	23
1.24	Histogram indicating the number of occurrences of major and severe geomagnetic storms as measured at Hermanus since 1989	24
1.25	The diagram illustrates the rate of change of the vertical component of the magnetic field as measured at the HMO during the severe storm on 13 March 1989	25
2.1	Transformer magnetisation curve in the presence of GIC	28
2.2	Relationship of Exciting Current without GIC present, and with GIC that saturates the transformer	29
2.3	GIC flow can severely disrupt the flux path in power transformers	30
2.4	Damage caused to a transformer winding due to GIC	31
2.5 a	DC flux return path for a single phase transformer	33
2.5 b	DC flux return path for a three phase, five limb transformer	33
4.1	Induced voltage drives GIC through the neutral ground points of power transformers.	45
4.2 a	Sample network to illustrate modelling procedure	46
4.2 b	DC model of sample network	46
4.3	Definition of symbols used for a transmission network	47
4.4	The closed loop between two nodal points $p_i$ and $p_j$	49
4.5	Single line diagram of model	53
4.6	<i>Top panel:</i> X and Y at substation 5 during very severe storm of 13 March 1989 <i>Middle panel:</i> $dX/dt$ and $dY/dt$ <i>Bottom panel:</i> Predicted GICs at substation 5.	57

# Introduction

During solar storms, enormous flares of energy on the sun's surface hurl dense waves of charged particles through space. These emissions are called Coronal Mass Ejection's (CME's) and the flow of plasma, called the solar wind, may reach the earth several days later, where it interacts with and disrupts the earth's magnetic field, known as a geomagnetic storm.

It has been known since the early 1940's that large transient fluctuations of the earth's magnetic field can produce quasi-dc currents in electric power systems through the grounded neutral of transformers. These geomagnetically induced currents (GICs) cause half-cycle saturation of power transformers resulting in increasing reactive power requirements and the generation of harmonics. During intense geomagnetic disturbances there have been unusual swings in real and reactive power flow, excessive voltage fluctuations, frequency shifts, undesired relay operations, and high harmonic currents [1, 2, 3].

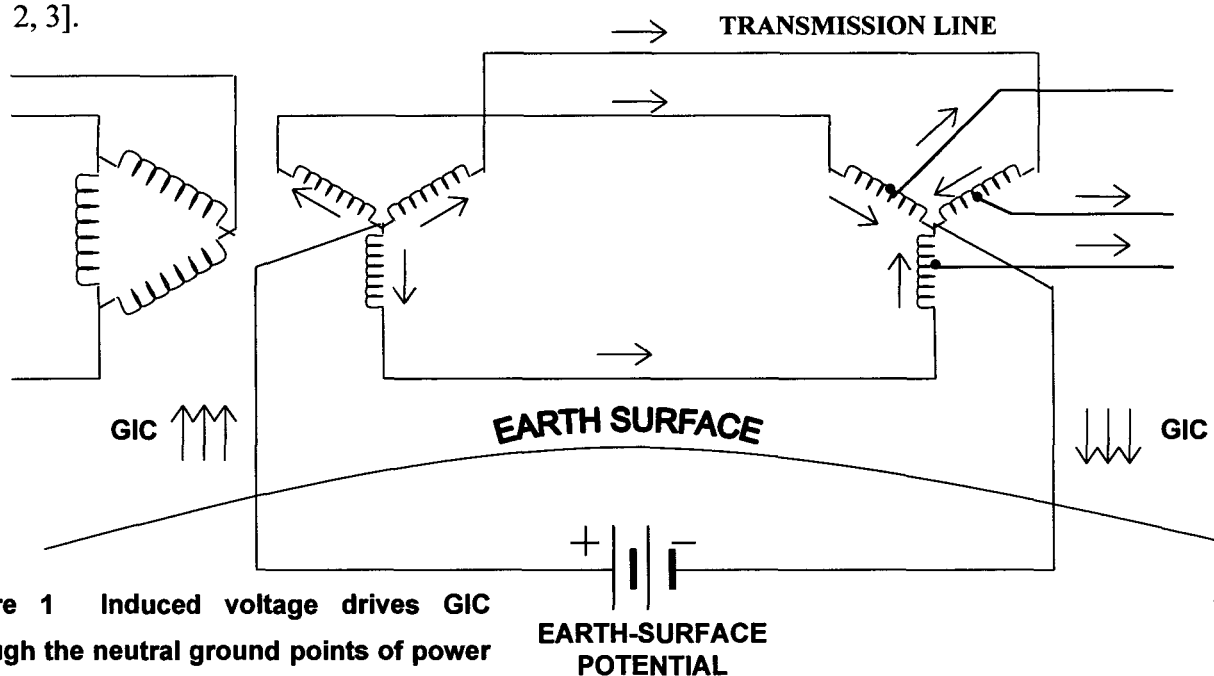


**Figure 1** Induced voltage drives GIC through the neutral ground points of power transformers.

**EARTH-SURFACE  
POTENTIAL**

The most dramatic recent impact occurred in March 1989 with Solar Cycle 22 when virtually the entire Canadian province of Quebec was plunged into darkness. In total 21500 MW of load and generation was lost and it lasted more than 9 hours to fully restore the supply. The same geomagnetic disturbance affected several large power transformers elsewhere, and caused hundreds of maloperations of relays and protective systems. Power systems suffered voltage depressions and unusual swings in real and reactive power flow [1, 3].

Power networks are more vulnerable today because of the continual expansion and increase in interconnections, thus linking large cumulative earth surface potentials. Networks situated above igneous rock geology are most vulnerable since the relatively high resistance encourages more current to flow in alternative conductors such as the power lines located above these formations. Power systems adjacent to coastal areas are also more susceptible to GICs due to the large induced currents in the highly conductive seawater.

The greatest GIC problem occurs at high latitudes in or near the auroral zones. In these areas the geomagnetic storms are most intense and frequent since the ionospheric source is typically a localised electrojet. The occurrence of these storms statistically follows the sunspot cycle (ca. 11 years), so definite and reliable conclusions of GICs require recordings and observations of at least this time. Countries at mid-latitude such as South Africa are located far from the magnetic pole and therefore do not experience the same severity of geomagnetic disturbances as North America or Scandinavia. However, long transmission lines, high resistance rock geology and coastal areas could present a risk during a very severe storm. This project serves to introduce the phenomenon as part of Eskom's preparation for the next solar peak. The solar peak is expected in the first quarter of 2000 with intense geomagnetic activity expected in the 3 following years.

# Chapter 1

## Geomagnetic Storms

### 1.1 Introduction

Coronal mass ejections are violent discharges of electrically charged gas from the Sun. Such an explosion can hurl up to 10 billion tons of gas into space at up to three million kilometres per hour [11]. Particles from solar flares disrupt power systems, communication technology, space technology etc. The radiation from the flares can even give passengers in aeroplanes a dose of radiation equivalent to a medical X-ray [12].

On March 13, 1989 a severe geomagnetic disturbance occurred affecting various technology systems worldwide. This was due to a gigantic solar flare that erupted from a large sunspot only three days earlier. Within two days, massive amounts of protons and electrons from the blast was captured by the earth's magnetic field, producing brilliant auroras and disrupting electric power systems, orbiting satellites and communication systems.

The March 13 geomagnetic storm caused more havoc on U.S. and Canadian power systems than any other in history did [4]. Some of these disturbances include the blackout of the entire Hydro-Quebec power system, severe damage to large power transformers and hundreds of misoperations of relays and protective systems. Power systems also suffered voltage fluctuations and unusual swings in real and reactive power flow. Transformers were damaged by severe tank heating and melted copper conductor

well as everyday experience, he failed to convince his principal successors. Only in 1510 did Nicolaus Copernicus (1473-1543) began work on a sun-centred system and went far beyond Aristarchus by providing detailed models of the revolution of planets around the sun.

According to his law of centripetal force, Isaac Newton (1642-1727) estimated the mass and density of the sun. While his initial estimate of the sun's mass turned out to be too small by an order of magnitude, his result for the sun's relative density was within 2 percent of the modern value. By revising some of the observational parameters, he later made a more accurate estimate of the sun's mass which was within 32 percent of the modern value. In 1796 Laplace came within 1 percent of the 1976 accepted value which is 332,946 times the earth's mass.

By 1780, after a century of increasingly sophisticated attempts to determine the scale of the solar system, the astronomers had a fairly reliable set of figures. In fact, the solar distance of 24,000 earth radii and solar radius of 112 earth radii were within 10 percent of modern values. [6].

Johannes Fabricius published the first paper on sunspots in Germany during 1611 after observing it with a telescope. One year later Galileo Galilei (1564-1642) wrote a paper on sunspots arguing that the motion of sunspots proved the sun rotated.

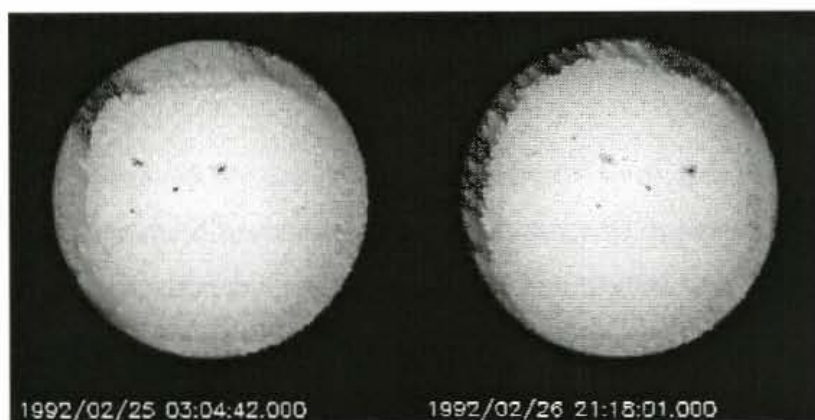


**Figure 1.1** Galileo used observations of the changing position of sunspots to prove that the sun rotated [13].



In 1826 Heinrich Schwabe (1789-1875) started a daily record of the number of sunspots and sunspot groups. As his data accumulated he observed a cyclic pattern in the number of sunspots. After observing two maxima and two minima of what appeared to be a 10-year cycle he sent a report of his discovery to an astronomical journal. This report was however passed over by most of his contemporaries, evidently he was too far outside the astronomical mainstream for his work to receive the attention it deserved. Soon after, his observation became significant when it was found that these sunspot variations were identical to magnetic variations. J. Rudolf Wolf (1816-93) then reviewed sunspot observations since Galileo's day and reported that the cycle's typical duration was in fact eleven years. He also reported correlation between sunspot cycles and magnetic variations.

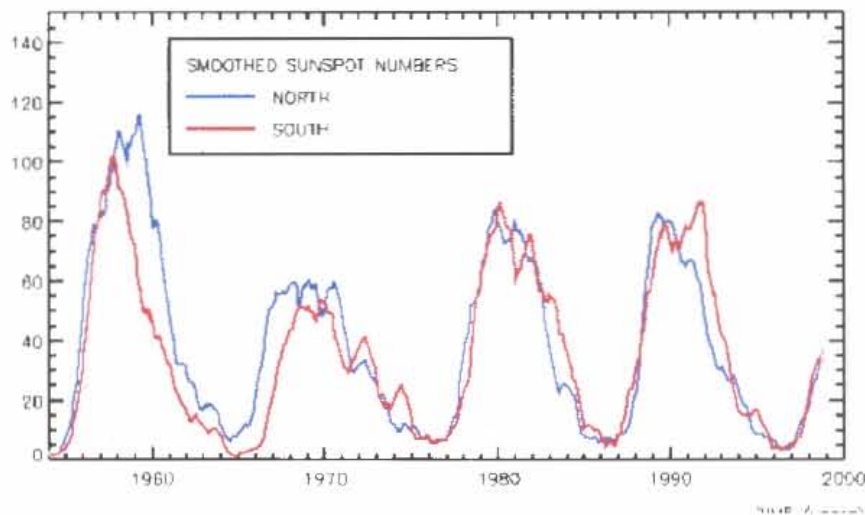


**Figure 1.2** Sunspot numbers through the last four cycle's [14].

These sunspot cycles are very significant since they are the directly related to the geomagnetic disturbances that induces currents in pipelines and cause havoc on power, communication and satellite systems. The next section describes the solar structure and dynamics.

### 1.2.2 The Solar Atmosphere And Solar Wind

The various components and thickness of the Sun's atmosphere are discussed in this section and depicted in fig. 1.3. The visible solar atmosphere consists of three regions with different physical properties. Optical photons originate in a thin layer of plasma, a region known as the photosphere. Within this region the temperature of the gas decreases from a value of 6500 K at the base to a minimum of 4400 K about 500 km higher up, at the top of the photosphere. Above this point the temperature begins to rise again.

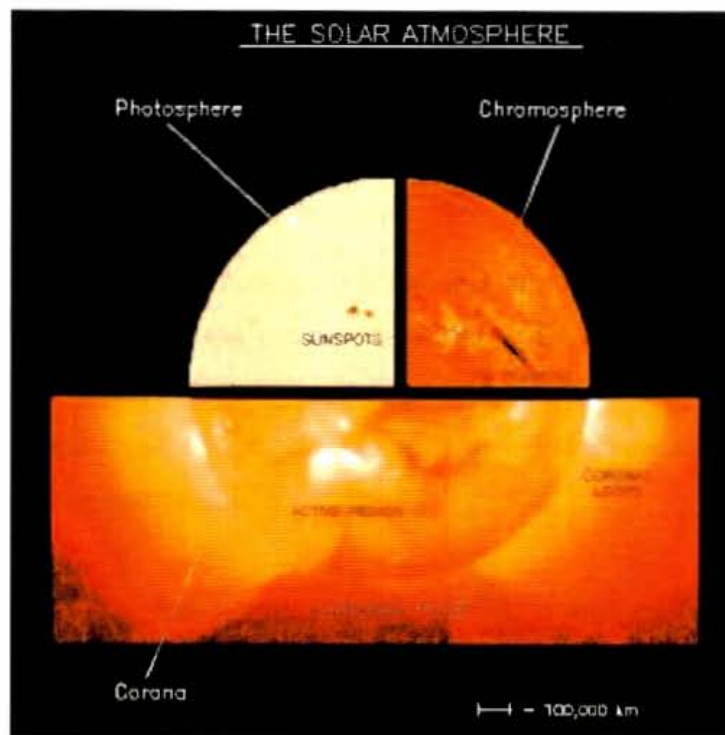


**Figure 1.3** The various components of the Sun's atmosphere [15].

Above this region lies the more transparent chromosphere with an intensity that is only about  $10^{-4}$  of the value of the photosphere. It extends upwards for approximately 2000 km with the temperature increasing from 4400 K to about 25,000 K.

Corona extends from the top of a narrow transition region to the earth and beyond. In this transition region the temperature rises very rapidly reaching more than  $10^6$  K before the temperature gradient flattens. During a total solar eclipse the radiation from the faint corona becomes visible as shown in fig. 1.4.

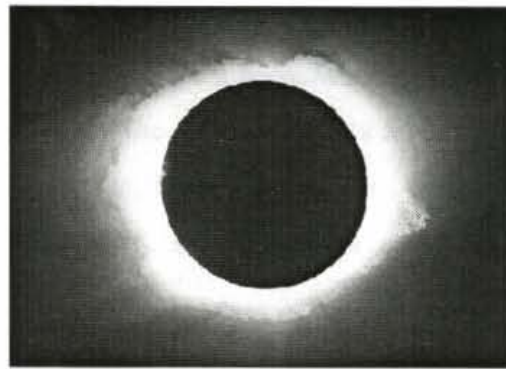


**Figure 1.4** Solar corona seen during a total solar eclipse (taken by Greg Babcock) [16]

The sun does not only emit the heat we can feel and light we can see but also various other radiations. These radiations control variations in the Earth's magnetic field and ionosphere and they include electromagnetic radiation, such as radio waves, ultraviolet radiation, X-rays and charged particle radiation consisting mainly of protons and electrons, known as the solar wind.

The magnetic field of the sun is not a perfect dipole, it appears to be squashed and confined to the equatorial plane due to a solar equatorial current sheet. The average position of the current sheet is tilted relative to the solar equator and contains folds. From X-ray images of the sun it can be seen that the X-ray emission is not uniform, but that dark regions called coronal holes exists. Coronal holes corresponds to those parts of the magnetic field where the magnetic field lines are open extending out to great distances from the sun. These holes source the solar wind, a continuous stream of ions and electrons following the magnetic lines out and away from the sun, moving through interplanetary space at a mean velocity of  $300$  to  $400 \text{ km s}^{-1}$  [9]. Coronal holes occur mostly at the solar poles, which will not influence the earth lying in the sun's equatorial

plane. They do however move down towards this plane in a cyclic pattern and thus, similar to solar flares, increases the solar wind density and velocity.

By observing the tails of comets this ongoing mass loss from the sun can be seen. The latter are generally composed of two parts, a curved dust tail and a straight ion tail, both of which are always pointed away from the sun. The force exerted on the dust grains by radiation pressure is sufficient to push it back, while the electric force between the ions of the solar wind and the ions in the comet accounts for the direction of the ion tail. The aurora borealis and the aurora australis (the northern and southern lights, respectively) are also products of the solar wind, this phenomena is explained in the section 3.

### 1.2.3 The Solar Cycle

Quiet sun conditions are intermittently disrupted by a variety of transient features, some of which are illustrated in fig. 1.5.

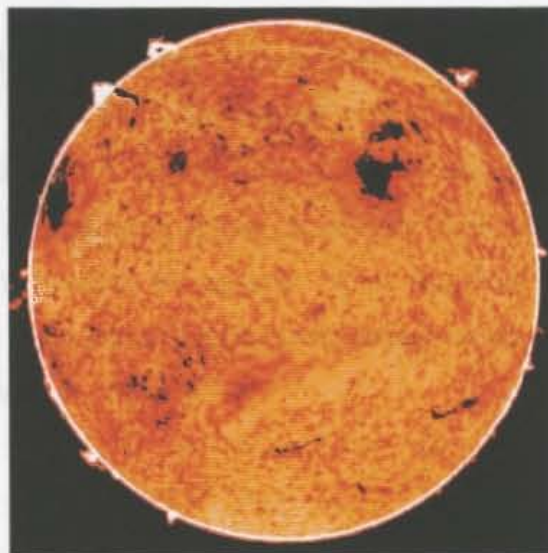


**Figure 1.5** A composite photograph of the sun showing several forms of activity (U.S. National Solar Observatory at Kitt Peak (Arizona) [30 APR 1999 15:37:34]) [17].



The surface of the photosphere is usually marked with dark spots of intense magnetic field, called sunspots. Their occurrence follows an 11-year cycle, going from minimum to maximum in about 4 years. Their formation can be explained with the aid of fig 1.6. At the beginning of the cycle, the lines of magnetic force run north and south between the Sun's magnetic poles. This is the period of minimum magnetic activity called the "Solar Minimum". As the Sun rotates, the Convection Zone spins faster at the equator than at the poles. Beneath the Convection Zone, the Radiation Zone spins as a solid mass. The different ways that these two zones move causes the Sun's magnetic field lines to be drawn out.

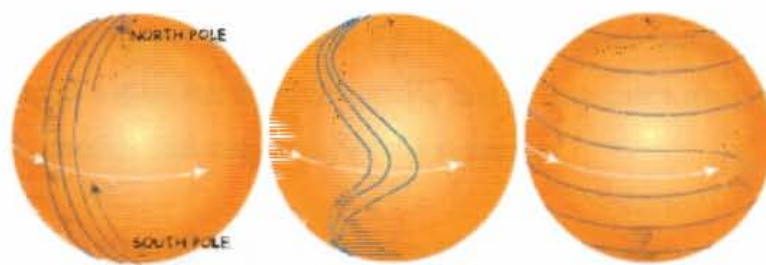


**Figure 1.6** Formation of sunspots [26]

Spot pairs in opposite hemispheres have opposite magnetic polarity and the same polarity as the nearer pole. The entire magnetic field of the sun reverses after such a cycle and therefore the sun is said to have a 22-year cycle. The initial spots at the beginning of a new sunspotcycle appear at relative high latitudes and as the cycle progresses, drift slowly towards the equator. Spots that form later in the cycle appear closer to the equator. This pattern is fairly symmetrical across the equator and forms the "butterfly pattern" as shown in fig. 1.7.

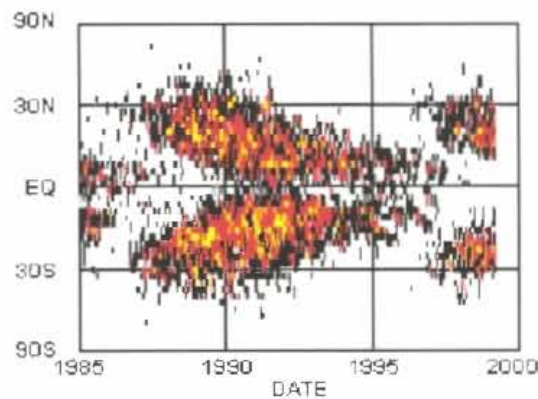


**Figure 1.7** The sunspot “butterfly pattern” [14].

Individual sunspots are short-lived features, typically not surviving more than one month or so [7]. A typical sunspot is shown in fig. 1.8. The darkest centre part is called the umbra that can have a diameter more than twice that of the earth’s diameter. The umbra is surrounded by another dark region called the penumbra.

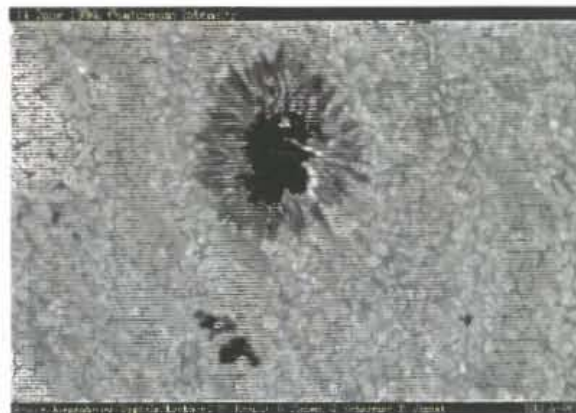


**Figure 1.8** A typical sunspot, showing the dark umbra and a penumbra [19].

Sunspots appear dark because they are cooler than the surrounding gas. The photosphere has a temperature of about 5500 degrees Celsius and a typical sunspot has a temperature about 3900 degrees Celsius. Their lifetime can be as short as an hour or two or as long as several months.

Solar flares are eruptive events occurring near sunspots. It's a brilliant region of intense emission and represents the violent instability of part of an active-region magnetic field and the resulting release of increased amounts of radiation and energetic particles. Flares have enormous dimensions with large flares reaching 100,000 km in length. Flares develop in regions of great magnetic intensity from which they draw their energy, namely sunspot groups, and the enhanced radiation due to them reaches the earth 8 minutes later [8]. Solar flares increase solar wind density and velocity, and when reaching the earth 12 to 48 hours later, the wind causes a sudden compression of the magnetic field, which is called a sudden impulse.

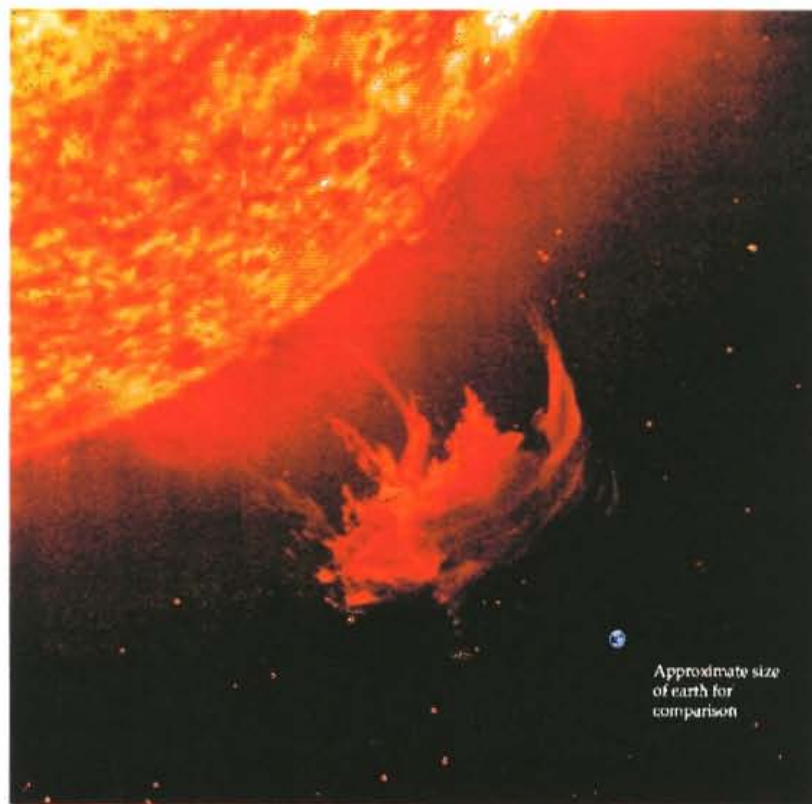


**Figure 1.9** A solar flare in comparison to the size of the earth [20].

Sometimes energetic particles and magnetic storms are observed at Earth without any exceptional flare activity preceding them, but they may be associated with a different solar phenomenon called "Coronal Mass Ejections" (CMEs). CMEs are huge bubble-shaped disturbances rising above active sunspot regions, expanding as they rise.

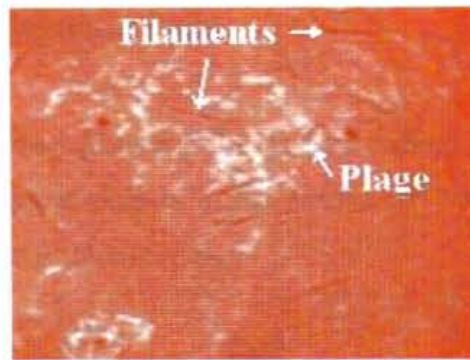


**Figure 1.11** Plages are due to moderate concentrations of magnetic flux [21].

A solar prominence is also related to the Sun's magnetic field. Quiescent prominences are curtains of ionised gas that reach well into the corona region. Prominences are made up of material that collected along the magnetic field lines of an active region, therefore the gas is cooler and less dense than that of the surrounding coronal gas. It will then “rain” back down into the chromosphere causing a spectacular sight.

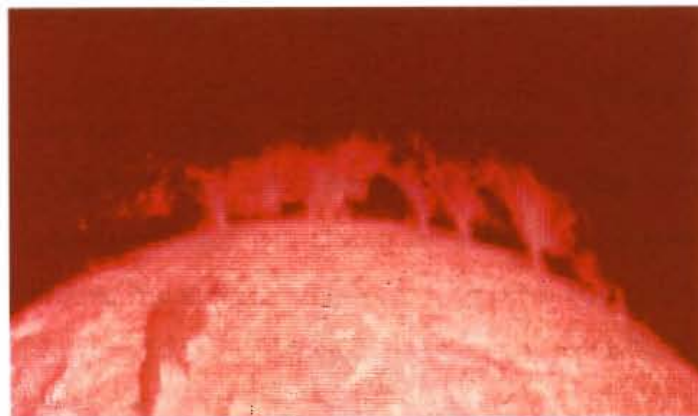


**Figure 1.12** Quiescent prominence [21].



### 1.3 The Earth's Magnetic Field the Magnetosphere

The earth has a rather strong planetary dipole field, which is roughly aligned with the spin axis (the north magnetic pole is in the Northwest Territories in Canada and the south magnetic pole in the Antarctic region).

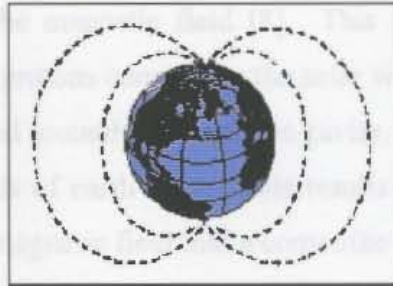


**Figure 1.13** The earth's dipole magnetic field [22].

The geomagnetic field is produced and maintained in the molten iron-nickel outer core by the self-exciting dynamo operation of the earth. The working principal is similar to that of a car's alternator. The rotating earth induces the current into the electrically conducting outer core, which creates the dipole magnetic field.

Emissions from the sun confine the Earth's magnetic field to region called the magnetosphere with its boundary called the magnetopause. This magnetic field protects the planet from incoming charged particles in the solar wind, as well as ionised cosmic rays. Instead of striking the surface some of the particles become trapped in the field where they bounce back and forth between the North and South Poles. These regions of trapped particles are known as the Van Allen radiation belts.

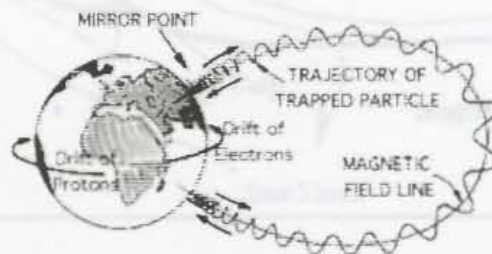


**Figure 1.14** Particles are trapped forming regions known as the Van Allen radiation belts [23].

## 1.4 Solar Wind Interaction with the Magnetosphere

The Earth's magnetic field carves out a cavity in the flow of hot plasma from the sun, or the so-called solar wind. It will push against the magnetosphere on the dayside with the magnetopause occurring roughly at about 10 earth radii where the plasma pressure of the solar wind is balanced by the magnetic field [8]. This is where the transition region occurs and the electrons and protons composing the solar wind can penetrate no closer to earth and are mostly deflected around the magnetic cavity. On the nightside the field is elongated extending hundreds of earth radii. This results from particle "friction" with the solar wind dragging the magnetic field into a cometlike tail.

The interplanetary magnetic field (due to the sun) has a component perpendicular to the ecliptic plane of the sun. Since the earth lies in this plane which contains many folds this component can vary between north or south in a couple of hours. When it points south it will merge with the Earth's magnetic field, which allows the plasma to enter through that region thereby "energising" the magnetosphere.

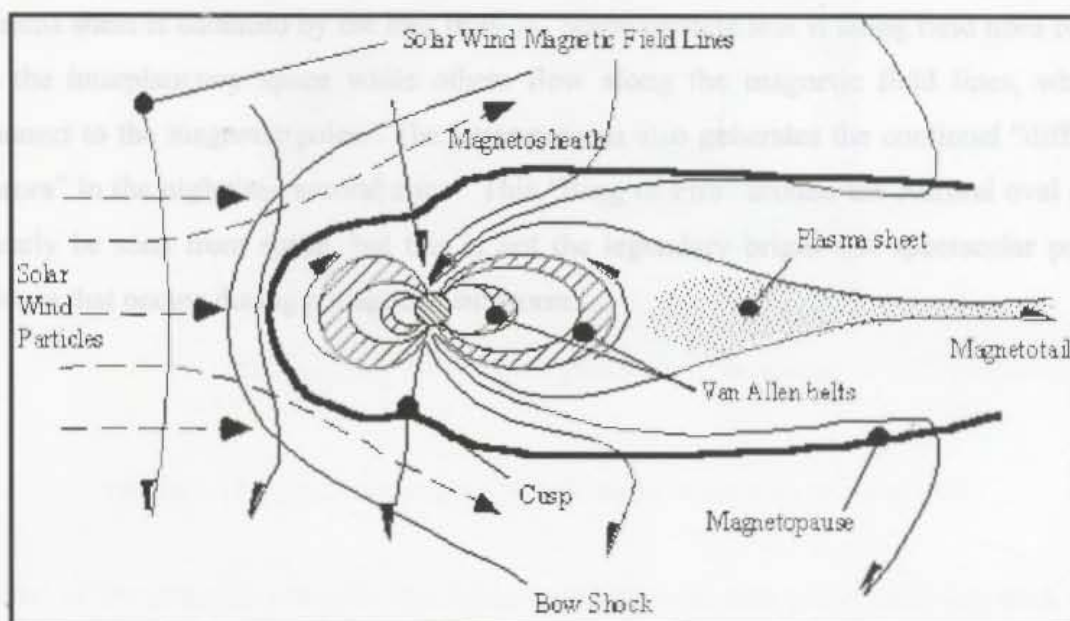


**Figure 1.15** Magnetospheric convection with a southward directed interplanetary magnetic field [24].

Another large fraction of the solar wind particles gain access at the front of the dayside magnetosphere by penetrating the bowshock, while the remainder are diverted around the magnetospheric cavity as illustrated in fig. 1.15.

The magnetic cusp region is where the Earth's magnetic field lines change from closed (joined to the other hemisphere) to open (swept into the magnetic tail). This forms a natural access funnel for some of the recently entered plasma into the Earth's dayside atmosphere, see fig 1.15. Dayside aurora is then formed as these particles collide with the oxygen and nitrogen of the upper atmosphere. The participating particles only have enough energy to penetrate down to height of about 250 km, hence they are red in colour since that's where the red spectral emission from atomic oxygen dominates.

The plasma that streams along the flanks of the magnetic tail forms the "mantle". The tail reconnects in the distance causing particles to accumulate in its central region and thus forming the plasma sheet. This is a stable situation as long as the build-up of the plasma sheet is balanced by the loss from it. Some particle loss is along field lines back to the interplanetary space while others flow along the magnetic field lines, which connect to the magnetic poles. The latter process also generates the continual "diffuse aurora" in the nighttime auroral zone. This "Ring of Fire" around the Auroral oval can clearly be seen from space, but this is not the legendary bright and spectacular polar corona that occurs during a magnetic substorm.

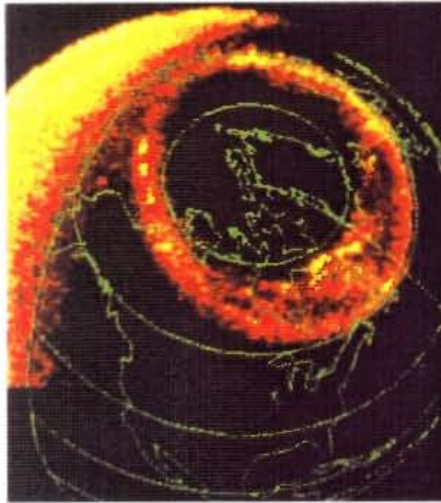


**Figure 1.16** Diffuse Aurora as seen from space (Picture taken by the Dynamics Explorer 1 Spacecraft) [28].

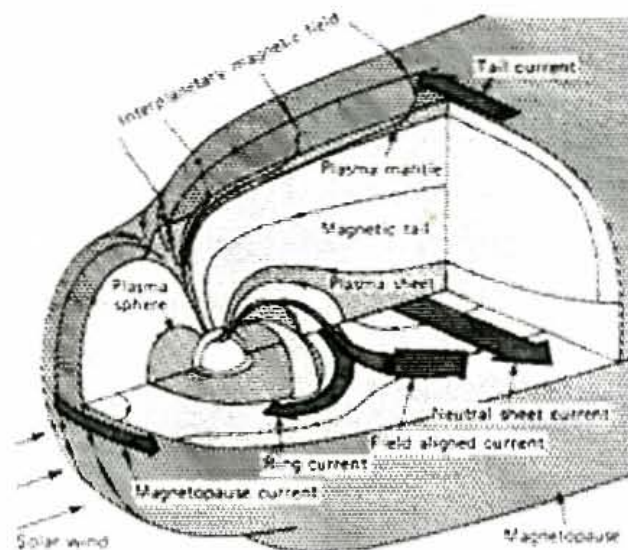


**Figure 1.17** Sketch showing the main features of the magnetosphere [25].

Some of the particles join the Van Allen radiation belts and while bouncing back and forth between the poles will drift around the earth, electrons eastward and protons westward. It occurs in the equatorial plane at distances of 3 to 7 earth radii above the



earth's surface [8]. This is called the ring current and significantly decreases the vertical component (H) of the earth's magnetic field over a period of hours.

The tail current divides the magnetopause into two lobes. It is the source of the stretched, parallel, magnetic field lines on the nightside. This current flows across the neutral plane at the equator, closing the circuit across the plasma sheet.

Magnetospheric substorms create the really bright and spectacular auroras, as well as disruptions on power and communication networks. It occurs when the sun is very active (large number of sunspots or coronal holes) and is the process where particles derived from the substorms and stored in the tail is released into the earth's atmosphere.

A magnetospheric substorm is explained with the aid of fig. 1.18. In the quiet state the plasma sheet thickness tapers off with increasing distance to the neutral point N. During a substorm the thinning of the plasma sheet occurs near to the centre of the tail (N') since the plasma sheet is unable to contain any further increases. The configuration is highly unstable and quickly relaxes to a more stable state during an explosive process that usually takes only 10 - 30 minutes. This process converts the accumulated magnetic energy into kinetic energy causing the particles in the plasma sheet to shoot away from the neutral point (N') towards the earth.

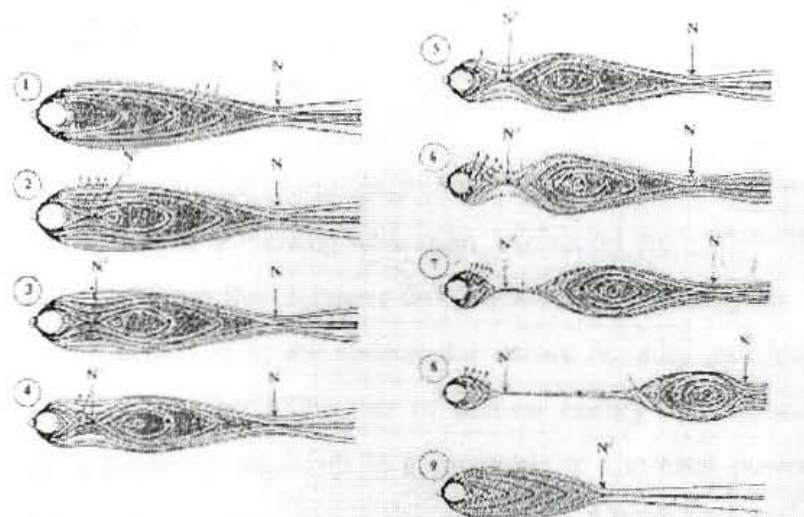


**Figure 1.18** Sequence of changes of magnetic field and plasma configuration during a substorm [8].

During a substorm the electrical particles is moved across the magnetic field lines and, similar to the process in the alternator of a car, an electric current will flow. This process will set up a large-scale convection motion toward the earth along the highly conductive field lines. The current can easily flow along the conductive strip in the auroral zone ionosphere. This gigantic current thus flows inward along magnetic field lines to the morning polar ionosphere, westward along the high conductivity strip in the ionosphere, and then along the magnetic field lines back to the equatorial plane as shown in fig 1.19.

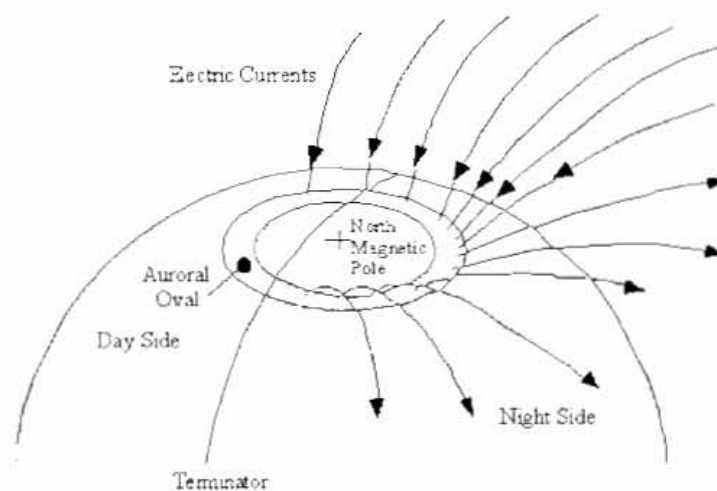


**Figure 1.19** Schematic of the northern half of the magnetospheric current system that flows during a substorm in the Auroral Oval [24].

The protons and electrons guided along magnetic field lines will collide with nitrogen and oxygen in high atmosphere causing ionisation, excitation etc. When the atoms or molecules recombine, or when the electrons drop back to lower energy levels, light are emitted which is then observed as the spectacular aurora borealis (northern lights) or aurora australis (southern lights). The rate of auroral energy release into the upper atmosphere during a moderate substorm is comparable to the total power-generating capacity of all man-made power plants in the world and this represents perhaps only 0.1% of the energy that precipitates the atmosphere [4].



**Figure 1.20** The spectacular Aurora Borealis (photographs by David Miller) [29].

A similar current wedge is formed in both hemispheres creating a remarkable similar auroral form under the same magnetic line [4]. The non-uniform auroral currents, or electrojets, follows general circular paths around the two magnetic poles at altitudes of 100 km or more and can have magnitudes of 1 million amperes. This can severely distort the earth's magnetic field; during the March 1989 disturbance compass needles was noticeable deflected [1].

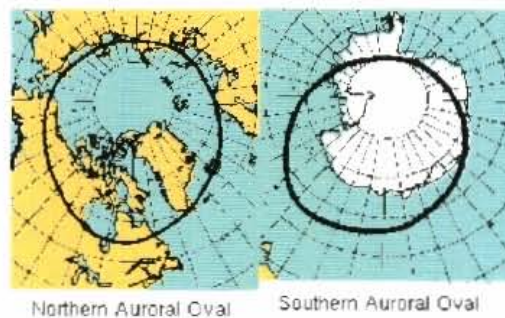


**Figure 1.21** The Northern and Southern Auroral Ovals [18].

Clearly, unlike we sometimes imagine, the earth is not just a small planet in the endless black void of empty space, but surrounded by a dynamically changing region of charged electrical particles and magnetic and electric fields.

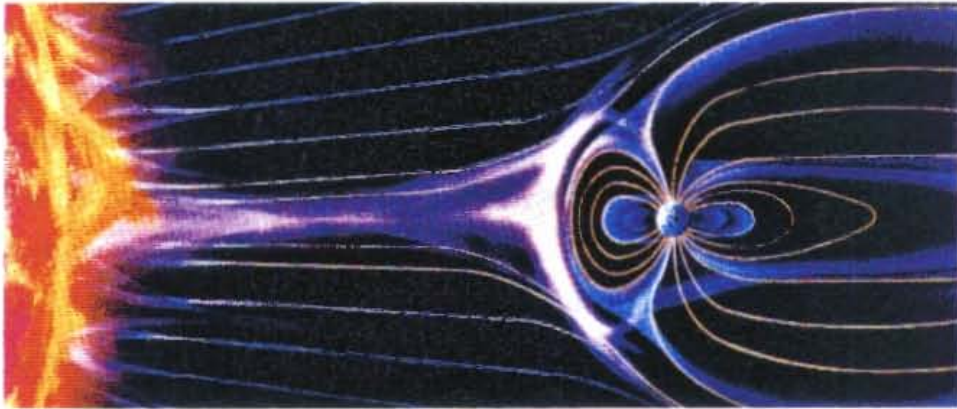


**Figure 1.22** The earth is surrounded by a dynamically changing region (Illustration by K. Endo. © Nikkei Science Inc.) [30].



## 1.6 Magnetic Field Measurements

The K index represents the deviation of the earth's magnetic field from normal at a specific geographic location. It serves as an indicator of the maximum variation of the magnetic field in a three-hour interval on the basis of a quasi-logarithmic scale (see table 1.1) with integer values from 0 (minimum activity) through 9 (super storm). Note that the amplitude ranges are unique to a particular station because of the latitude dependence of magnetic storms.

**Table 1.1** Limits of amplitude ranges (nT) for defining the K index at the Hermanus Magnetic Observatory [8].

K index	0	1	2	3	4	5	6	7	8	9
Range (nT)	3	6	12	24	42	72	120	198	300	

Magnetic storm conditions are considered to prevail when the degree of magnetic activity is taken to be a K-index of 5 or greater. It is considered a major storm when  $K=6$  and a severe storm when K exceeds 6. The histogram in figure 1.24 indicates the number of major and severe geomagnetic storms over the past decade as measured at Hermanus. Note that the general trends and variations as measured at Hermanus are similar all over South Africa [8]. For reference purposes the K-indexes of the previous solar peak (1/01/89 – 31/12/92) can be found in appendix C.

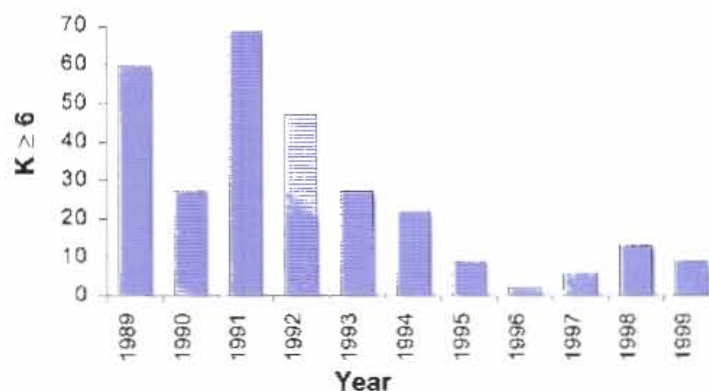


**Figure 1.24** Histogram indicating the number of occurrences of major and severe geomagnetic storms as measured at Hermanus since 1989.

The figure also illustrate the correlation with the previous sunspot peak (cycle 22) in 1991. Geomagnetic storms can take place at any time, however the probability of it occurring is higher during the occurrence of a large number of sunspots. Based on the statistics of previous cycles the next peak, that of cycle 23, is expected in the first quarter of 2000.

It is important to note that not so much the intensity but that the sustained rate of change of the magnetic field is an important factor [39, 40, 41]. Faraday's Law can explain this: the electric field is associated with the time derivative of the magnetic field, not with the variation amplitude. Fig 1.25 shows the rate of change of the magnetic field over 24 hours during a severe storm. This diagram also show how the K-index is not sufficient to determine the severity of the impact on the power system since the K-index of 9 after 9 hours was not at all similar in magnitude to the K-9 after 21 hours.

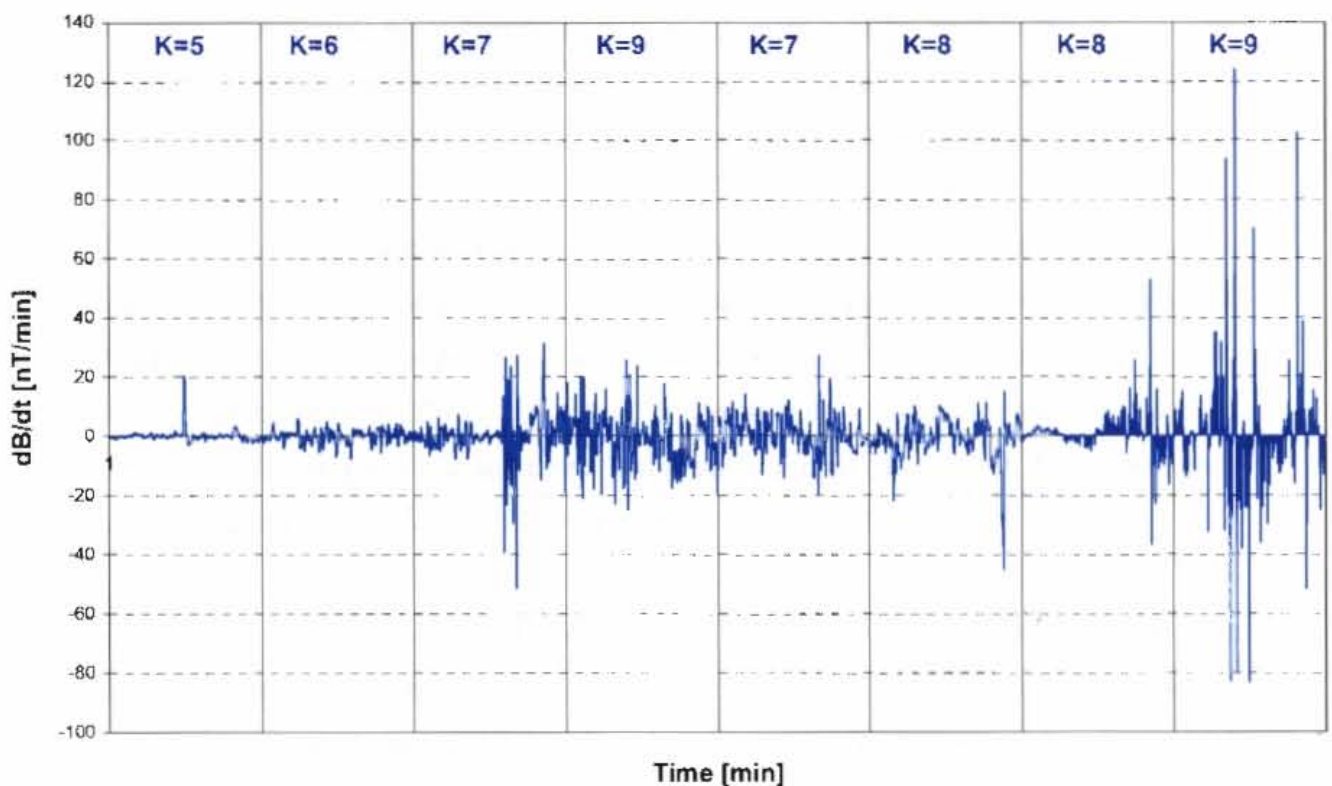


**Fig 1.25** The diagram illustrates the rate of change of the vertical component of the magnetic field as measured at the HMO during the severe storm on 13 March 1989.

## **Chapter 2**

# **GIC Effects on Power Systems**

### **2.1 INTRODUCTION**

Power networks are more vulnerable today because of the increase in extent and interconnections, thus linking large cumulative earth surface potentials. Networks situated above igneous rock geology are most vulnerable since the relatively high resistance encourages more current to flow in alternative paths, such as the power lines located above these formations. Power systems adjacent to coastal areas are also more susceptible to GICs due to the large induced currents in the highly conductive seawater.

The GIC, having a fundamental period of approximately 5 to 15 minutes [34], are a quasi-dc, resulting in the simultaneous ac and dc excitation of energised transformers. Typical perturbations to power systems due to GICs include, fluctuations in system voltage, increased var flow, generation of harmonics, relaying problems, localised heating in transformers and increased audio noise output [1; 34]. In North America, voltage fluctuations in excess of 10% have been reported [78].

Countries at mid-latitude such as South Africa are located far from the magnetic pole and therefore do not experience the same severity of geomagnetic disturbances such as in Canada, North America or Scandinavia. However, long transmission lines, high resistance rock geology and coastal areas could present a risk during very severe storms.

This chapter will elaborate on the effect of GICs on power systems, with emphasis on the GIC induced half-cycle saturation of power transformers, the primary cause of perturbations on the power system.

## **2.2 Protective Relaying Effects**

The high level of harmonic distortion caused by GICs may cause conventional protection systems to provide inadequate protection for capacitors, transformers and generators [80, 83]. The transformer differential relaying scheme has apparently been the most vulnerable to GICs [80]. Considers a star-delta transformer with GIC flowing on the star side; if the GIC cause saturation it will effectively reduce the magnetisation impedance which will result in a current unbalance in the relay circuit.

A risk associated with distance relays is that the saturation of a transformer can reduce the apparent impedance seen by the relay. If this apparent impedance is within the operating zone of the relay, an unnecessary tripping may occur [78, 80].

Another factor is the increased dependence of power systems on reactive power compensation such as shunt capacitors. These shunt capacitors are protected with neutral overcurrent relays. Harmonics caused due to transformer saturation will see these devices as a low impedance to ground and it may trip due to overcurrent. However, this should not be labelled a false trip since shunt capacitors need to be protected against overload due to harmonics.

Transformer neutral overcurrent relays need to be filtered against harmonics since triplen harmonics may appear as zero sequence currents and provide a “false” overcurrent to the relay [2; 35]. Undervoltage relays can also misoperate due to depressed voltage conditions [80].

The effect of GICs on protection current transformers (CT) is of less concern. Since the core of these CT's are designed to handle large fault currents they are unlikely to saturate due to GIC. The only time a problem may occur is during the unlikely event that a fault occur at the same time as a GIC event. To date, no significant threat to reliable CT performance was found [2].

## 2.3 Saturation of Power Transformers and Reactors

A transformer core is made of high permeability ferromagnetic material. Its purpose is to provide a well-defined low reluctance path for magnetic flux. During normal operation, the majority of the flux will stay in the core. However, in the presence of GICs the core becomes saturated which lead to operation in the extremely non-linear portion of the core steel saturation curve (see fig.2.1). Excitation current is normally very small for large power transformers (less than 1% of rated load current) and they are designed to operate near the saturation point. These two characteristics will cause low values of GICs to push the core into saturation. Due to the quasi-dc nature of GICs, saturation will occur for one half of the ac cycle, hence the term half-cycle saturation, the root-cause of all power system problems that occur during geomagnetic storms.

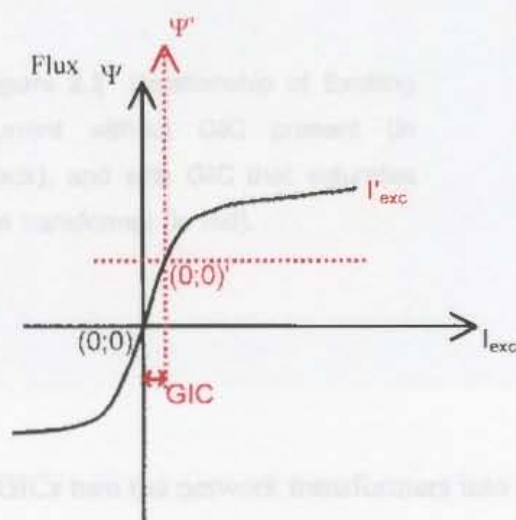
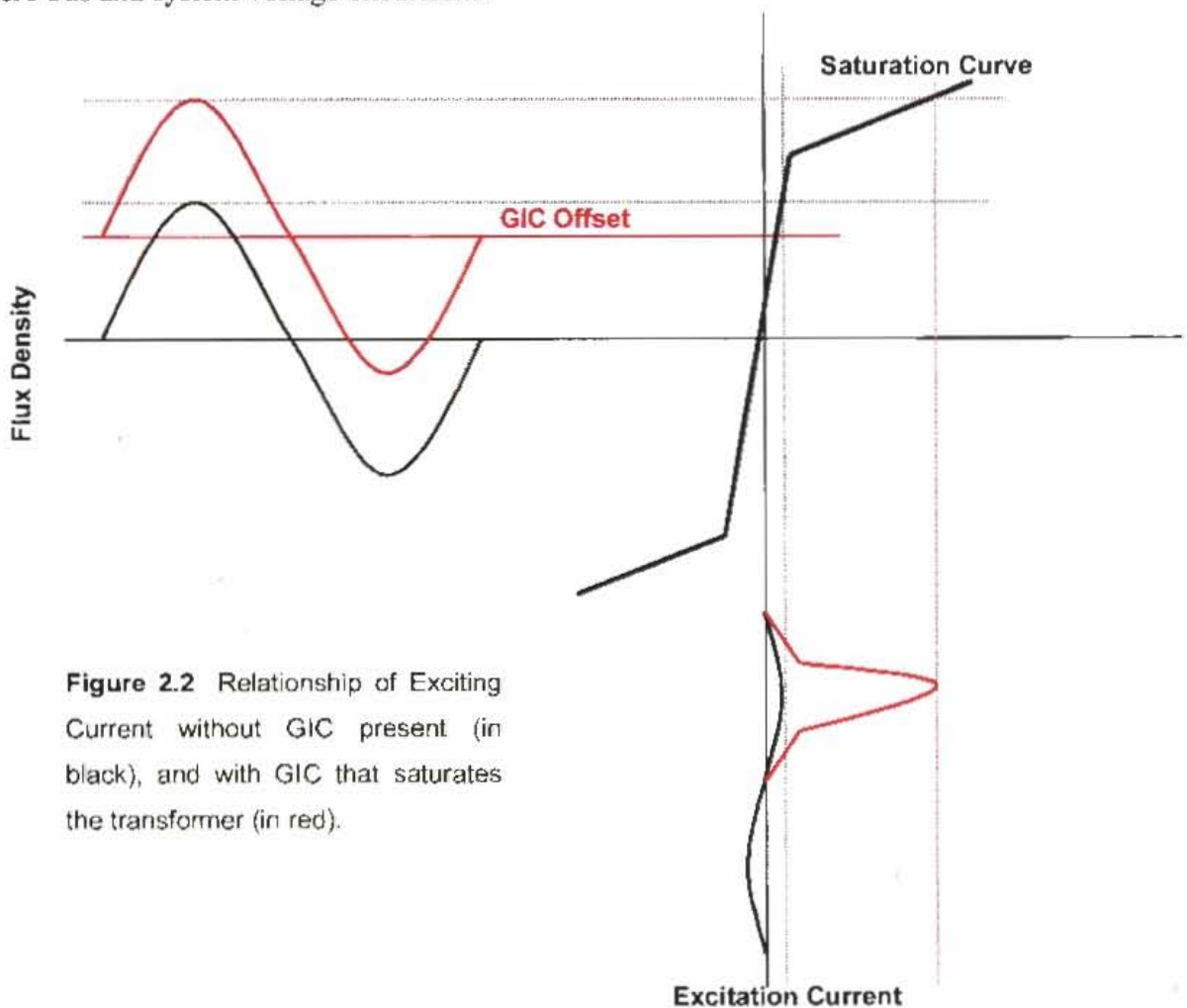


Figure 2.1 Transformer magnetisation curve in the presence of GIC.



Under GIC bias the saturated core becomes a much higher reluctance path which requires more ampere-turns to produce the same amount of flux required. This will cause the transformer to draw an extremely large exciting current (see fig 2.2), rich in even and odd harmonics. The increased exciting current will cause a reactive power demand much greater than during normal operation for a single transformer. When a large number of transformers experience saturation due to GICs it will increase the reactive power demand significant when compared to either the total transformer demand or the total area connected load. VAR demands of this magnitude can cause severe bus and system voltage excursions.



**Figure 2.2** Relationship of Exciting Current without GIC present (in black), and with GIC that saturates the transformer (in red).

In effect, GICs turn the network transformers into sinks of reactive power and sources of harmonic currents. Typical problems during a geomagnetic storm are unusual real and reactive power flows, voltage fluctuations, frequency shifts and undesired relay and

protective system operation [34]. GICs will increase generator output, decrease total system generation, increase transmission losses and reduce tie-line transfer capabilities.

## 2.4 Transformer Heating

The saturation of the magnetic core will also cause flux to exit the core steel for alternative paths, such as the tank wall, flux shields, clamps and other structural steel members of the transformer (see fig 2.2).



**Figure 2.3** GIC flow can severely disrupt the flux path in power transformers [3]

The leakage flux due to core saturation will initiate eddy current heating in components linked by it and create hot spots. Hot spots can melt structural steel members and are likely to cause a cumulative damaging effect on the transformer winding insulation,

leading to premature transformer failure. An example of such damage occurred during the March 1989 storm to an 1200 MVA generator step-up (GSU) transformer at a nuclear plant in New Jersey which was damaged beyond repair (see fig. 2.3) [3]. At the same time the increased excitation current and higher harmonic content will add additional heating due to  $i^2R$  losses.

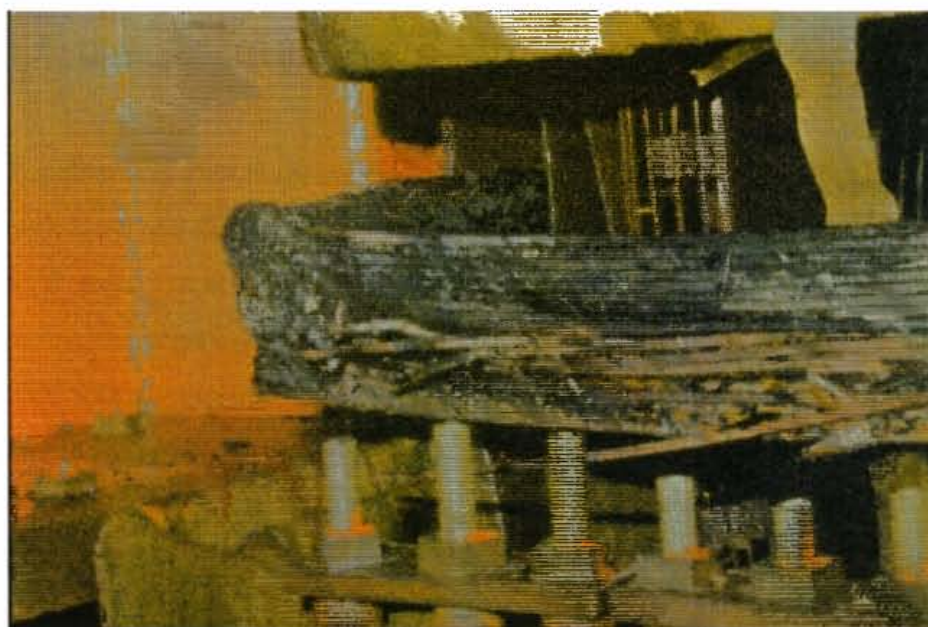


**Figure 2.4** Damage caused to a transformer winding due to GIC [3]

Transformer heating due to stray flux is governed by the following factors [2, 35]:

- stray flux magnitude
- material characteristics (e.g. permeability and conductivity)
- size of the object (e.g. clamp) perpendicular to the stray flux
- heat transfer away from the object.

On a well-monitored transformer at a different site the temperature increased on a hot spot from  $60^\circ$  to  $175^\circ$  in less than 10 minutes [3]. This can lead to very severe damage since geomagnetic storms can last for several hours repeated over several days which will lead to the deterioration of insulation and subsequent decrease in life span of transformers and reactors. It was found that the failure rate of GSU transformers are 60% higher in the Northeastern US (the area of highest GIC susceptibility) than the rest of the US [3]. The same study showed that the failure pattern of these transformers



virtually mimics the cyclic pattern of the geomagnetic storm cycle with a time lag of approximately 3 years). GSU transformers of base load substations are most vulnerable since they are usually loaded to rated values and have limited margins to absorb additional heating stress [35].

## **2.5 Harmonic Generation in Transformers**

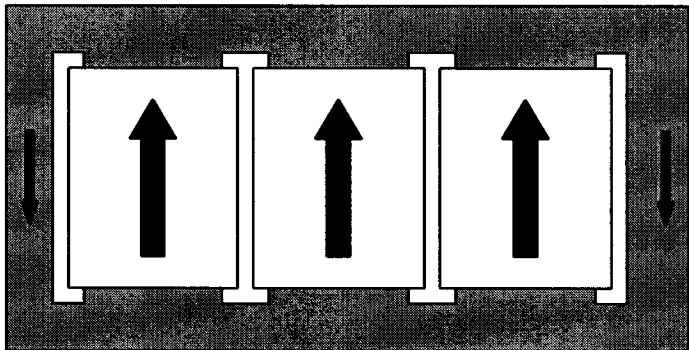
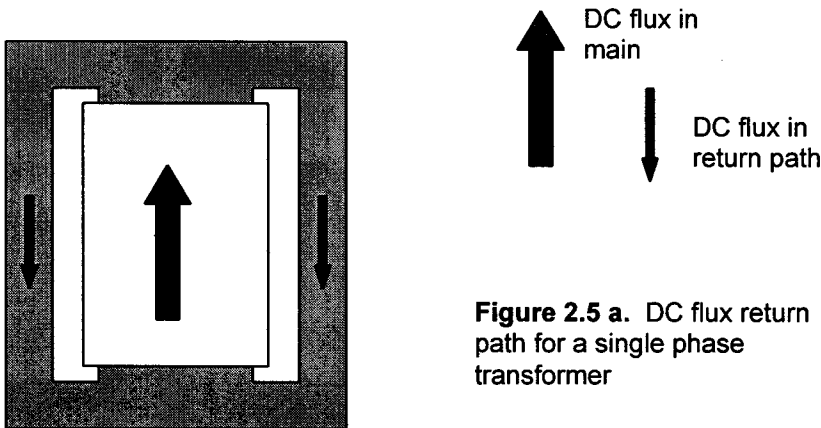
The distorted excitation current drawn during transformer half-cycle saturation is full of both even and odd harmonics. This can cause misoperation of protective relays such as SVC overcurrent relays. This was the primary cause of the Hydro-Quebec blackout during the severe geomagnetic storm in March 1989. The harmonics generated caused 7 SVC's to trip on overload since their capacitive legs acted as sinks for it. Coincided with that the reactive power demand increased due to the half-cycle saturated transformers on the network. This led to severe voltage regulation problems, and ultimately to the collapse of the network [1].

The harmonic spectrum produced by transformers are generally unique to their construction type (five-leg core form, single phase units, etc.). The resulting current waveform of single-phase units will tend to be the same since they are subjected to the same waveform. However, transformers such as five leg core form or three phase shell form may produce very different waveforms since the individual phases will not experience the same saturation due to unbalanced magnetics [2].

The asymmetry caused by the dc offset in the transformer magnetisation lead to both odd and even harmonics. Normally utilities are well aware of odd harmonics in the power systems but few are prepared to handle the uncommon even harmonics. In general, the magnitude of harmonics decreases with an increase in the harmonic number and the magnitude of these harmonics increase almost linearly with an increase in the GIC magnitude [2].

## 2.6 The Expected Performance of Eskom Power Transformers

All single phase and three phase transformer designs are susceptible to GICs, and the saturation is determined by both the core configuration and the relative core leg dimensions [53]. The HV transformers most commonly used by Eskom are three phase, five limb autotransformers as well as a few single-phase units. Comparing the performance of all transformers the single-phase transformers are most affected by GICs since there are no opposing fields in the adjacent limbs [52, 53]. As far as three phase transformers are concerned the five legged type have showed to be the more susceptible to GICs by drawing more excitation current than the three legged core [52, 53]. Three-phase three-leg core-form transformers experience the least adverse effects to GICs since they offer no return path to the dc flux. This is since the GIC in the neutral will split evenly into the three phases, and since they are in phase will induce an opposing, equal flux [84].



Note that with autotransformers it is more difficult to make a theoretical prediction of the location of GICs in the power system since the current does not necessarily terminate at the earthing point. It can bypass the earthing point by flowing through the common winding to the next transformer. Therefore the GIC measured in the neutral of an autotransformer does not necessarily indicate its level of saturation since the measured value might only be a small fraction of the GIC in the series winding. The saturation of these transformers can be determined more accurately by rather monitoring the effects of GICs such as harmonics and reactive power flow.

# **Chapter 3**

## **Historical Background**

### **3.1 Introduction**

Power networks are not the only technology affected by geomagnetic storms. In fact, the impact of these storms dates back from 1846 with reports of disruptions on the early telegraph systems [1]. Eventually, engineers and scientists were finding effects almost everywhere they looked. The first section of this chapter describes some of the disturbances to various technology systems during severe storms of the past. Section 3.2 is divided into two subsections and it's focussed on past incidents related to the effect on power systems. Its first subsection describes some of the events known to have occurred internationally due to GICs. The second subsection describes the results of an investigation into past incidents to equipment of the Eskom MTS that can be correlated with geomagnetic storms.

### **3.2 Disrupting Technology**

The effect of geomagnetic storms was reported on the early telegraph system with reports dating back to 1859 when operators in Boston and Portland were able to disconnect their batteries and “for more than one hour held communication with the aid of celestial batteries alone” [63]. GICs has been so severe at times that at times it started fires at telegraph stations. It has also produced outages of phone cables as well as alternating sound levels on transatlantic cables.

Another technology greatly effected is that of pipelines. The greatest problem is the effect on the cathodic protection designed to prevent electrolytic corrosion at flaws in the pipeline coating. During a severe storm the pipe-to-soil potential vary rapidly making pipeline surveying almost impossible and exposing the pipeline to possible corrosion [39].

Following is a list of some of the effects during March 1989 when a number of massive solar flares occurred; causing some of the largest magnetic storms ever recorded (not including effects on power system, see following section) [8].

### **Surface Technology Problems**

- South African geophysical exploration chief reported “conditions unlike any I’ve ever seen before; nothing worked.”
- Mineral survey worker in Western Australia reported a totally disrupted survey, “never seen conditions quite like it.”
- Pipeline surveying company in Australia could not understand their pipe-to-soil potential records and became concerned about probability of increased pipeline corrosion due to induced currents and potentials to ground.
- Power supply cables to undersea fibre-optic telecommunication cables monitored large voltage swings (500-600 V).

### **Space Technology Problems**

- Stable low-altitude satellite began uncontrolled tumbling.
- GOES-7 high orbiting satellite had communications circuit anomaly on 12 March 1989, and lost imagery and communications on the next day.
- Aerospace engineer concerned over power panel problems.
- Japanese high orbiting communications satellite permanently lost half of its communications circuitry.
- Ageing low orbiting NASA satellite has dropped in altitude “as if it hit a brick wall”. Dropping almost 5 km during the entire period.

## **Ionosphere Communications Problems**

- March 6 - NBC warned affiliates of potential relay problems during the following two weeks.
- US Coast Guard reported many LORAN and HF-radio problems.
- US Navy MARS (10-20 MHz) circuits out world-wide but 144-148 MHz transceivers received signals from unusual long distances.
- Australia - many reports of poor HF-radio conditions on 13-14 March 1989. Polar to midlatitude circuits was useless and equatorial circuits very weak and noisy.

## **3.3 Disrupting Power Systems**

Power networks are more vulnerable today because of the continual expansion and increase in interconnections, thus linking large cumulative earth surface potentials. Networks situated above igneous rock geology are most vulnerable since the relatively high resistance encourages more current to flow in alternative conductors such as the power lines located above these formations. Power systems adjacent to coastal areas are also more susceptible to GICs due to the large induced currents in the highly conductive seawater.

### **3.3.1 International Incidents Related to GICs**

The Finnish Meteorological Institute (FMI) in collaboration with the Fingrid Power Company have monitored and studied GICs in the Finnish power system since 1977, i.e. for a longer time than the 11 year sunspot cycle. The largest GIC ever measured during this period occurred at Rauma on March 24, 1991. The one-minute mean value was 201A [36]. Also during this period the largest time derivative to be measured in southern Finland was 40nT/s, this occurred on July 13 to 14, 1982. Despite these large values, the Finnish power network has not experienced any significant disruptions due to GICs. This appears to be due to the transformer type and specific design being used.

They pay a lot of attention to leakage flux path to minimise the occurrence of hot spots and the transformers are generally only operated a half its rated value [51].

It is interesting to note that the Finnish neighbours, Sweden has not being as fortunate in escaping the detrimental effects of GICs. For instance, during the July 1982 storm mentioned above, they had 4 transformers and 15 lines tripped [36]. In fact, the first observations of GICs in Nordic countries was observed in Sweden, more than 70 years ago [44]. A comparison of the two networks (Sweden and Finland) has being done [44]. The main differences are listed in table 3.1.

**Table 3.1** The main differences between the Finish and Swedish power systems

	<b>Finland</b>	<b>Sweden</b>
<b>Transformers</b>	Five limb, core type, full wound three phase transformers (400/400/125 MVA, 400/120/21 kV, Ynyn0d11).	400/130 kV, and 400/220 kV three phase autotransformers.
<b>Earthing</b>	The 110 kV network is earthed through current limiting reactors.	The 130 kV system is solidly earthed due to the autotransformers.
<b>Reactive Power</b>	Compensation through reactors connected to the tertiaries of the system transformers	Compensation mainly through 400 kV shunt reactors connected to substation busbars.

Note that previously the differential relays used in Sweden were not stable in the presence of harmonics, this has now been corrected [44].



It is interesting to note that GIC values are generally lower in North America than in Scandinavia, however their transformers are more sensitive to these currents which is evident from the number of problems they have had. One of their earliest disturbances occurred on 24 March 1940 [80]. In the northern United States and eastern Canada they had disturbances on 10 separate power systems, of which misoperation of transformer differential relays the most common problem. In 1957 saturation of power transformers saturated causing excessive harmonics and another storm in 1958 caused widespread voltage and power flow variations [80]. Also in 1958 the Bowater Power Company experienced outages on 4 generators. More differential relay maloperations was reported occurred in 1967, 1968 and 1970. A severe impact occurred in August 1972 which caused transformers to trip on differential relay, a capacitor bank on overcurrent, undervoltage breaker operation as well as unwanted supervisory operation [80].

To date, probably the most dramatic effect of GICs on power systems was the Hydro-Quebec collapse in Canada during a very severe storm in March 1989. The blackout affected more than 6 million customers. A total of 21 500 MW of load and generation was lost taking more than 9 hours to completely restore. Following is a description of the events that took place [1]:

The geomagnetic disturbance occurred early in the morning of 13 March 1989 causing GICs in the system. This caused excessive harmonics in the system which flowed into nearby static VAR compensators, whose capacitive legs is a low impedance to ground for the high frequency harmonics.

The harmonics overloaded the capacitors to such an extent that protective systems took the static VAR compensators off-line to prevent possible damage. Within a minute of storm onset, all seven static VAR compensators on the Hydro-Quebec 735 kV La Grande network tripped. This left the 9500 MW La Grande Hydroelectric complex without the support of voltage regulation and reactive power compensation. This, together with the increased reactive power demand by half-cycle saturated transformers contributed to voltage regulation problems.

About 8 seconds after the loss of the compensators, one of the five 735 kV La Grande lines tripped, almost immediately followed by the remaining 4 lines. This completely cut-off 9500 MW from the rest of the network. Frequency and voltage throughout the network fell. Automatic load shedding was not fast enough to restore a balance between load and generation available and in less than 30 seconds the entire network collapsed.

The same storm also caused unrepairable damage to a generation step-up (GSU) transformer in New Jersey. The 1200 MVA, 500 kV transformer overheated due to stray flux causing hot spots at certain concentrations. This kind of damage can be cumulative and a statistical analysis of GSU transformers in the U.S. showed that the failure rate was 60 percent more in GIC susceptible areas [3]. It is estimated that another storm of this magnitude could have a \$3-6 billion loss in gross domestic product in the northeastern United States only [33].

A network seemingly even more sensitive to GICs is that of the UK. With a neutral dc current of only 5-25A, they have reported [85]:

- MVAR swings on generators
- Voltage changes  $\pm 5\%$
- Demand tripping by under voltage
- Generator negative sequence alarms
- Increased harmonic levels
- Bucholz trips / Transformer damage
- Communication channel failures

### **3.3.2 The Relation of Geomagnetic Storms and Network Equipment Failure in South Africa**

The investigation into correlation between past system events and geomagnetic storms was conducted for the peak period of activity during the previous cycle, i.e. 1989 through 1994. The only available data was that of events concerning shunt capacitor banks, transformers and reactors. This data is unfortunately not sufficient to proof the possible existence or absence for that matter of GICs in the Eskom MTS. Data such as voltage change, generator MVAR swings, increased harmonic levels etc. will be essential to establish conclusive proof of the existence of GICs.

#### **3.3.2.1 Shunt Capacitors**

No correlation between shunt capacitor trips and geomagnetic storms was found, which could be for numerous reasons such as network geometry, protection settings, magnitude of GICs, etc. It does not prove beyond doubt that there has not been any GIC related incidents at shunt capacitors on the network.

#### **3.3.2.2 Transformers and Reactors**

The results of the investigation into transformer and reactor events that could be GIC related are shown in table 3.2. The table also lists all major to severe storms (K-index > 5)<sup>1</sup> which have occurred close to the date of an incident. See appendix C for all K-index data from 1989 through 1992.

---

<sup>1</sup> The K-index (a 1-digit number) is a 3 hourly indication of geomagnetic activity. See section 1.6 for a more thorough explanation.

**Table 3.2** Results of investigation between past system events and geomagnetic storms [86].

Date	K-index sequence	Name	Description
13 Mar 1989	5679 7889		
14 Mar 1989	9765 3466		
15 Mar 1989	6443 3332	Poseidon- Neptune Reactor	Permanent fault on the reactor; interwinding fault
28 July 1990	2456 6566	Beta Reactor 4	Internal fault; reactor was removed on 8/09/90
24 Mar 1991	2866 5378		
25 Mar 1991	6643 4555		
26 Mar 1991	6555 7443	Hydra Transformer 21	Permanent fault; reason unknown
18 Apr 1991		Beta Reactor 4	Neutral earthing reactor faulted
18 Apr 1991		Beta Reactor 2	Internal fault
19 Jun 1991		Hydra Reactor 2 <sup>2</sup>	Permanent fault, reactor was removed
14 Aug 1991		Beta Reactor 4	Neutral earthing reactor faulted and was disconnected
19 Aug 1991	4375 4322	Hydra Transformer 21	Permanent transformer fault; transformer removed
25/05/92		Hydra Transformer 3	Transformer tripped on Buchholz protection
06 May 1993		Hydra Reactor 1	Reactor faulted internally. To be replaced.
14 Dec 1993		Beta Alpha 2 Reactor	Red phase winding faulted.
21 Mar 1994		Hydra Poseidon 1 Reactor	Reactor faulty and replaced

<sup>2</sup> This followed a period of very severe storms from 4/06/91 – 17/06/91 (see appendix C).

These incidents provide circumstantial evidence that GICs might exist in the Eskom MTS. From this data it appears that the Hydra and Beta substations may be susceptible to GICs. It is also interesting to note that the Poseidon-Neptune reactor that failed was commissioned less than one year before it failed and was removed [87]. Unfortunately the only investigation report available for the above incidents is the failure of the two 765 kV shunt reactors at Beta. An extract from this report by Eskom Transmission Group is available in appendix D. The observations made at Rotek correspond exactly to the damage that would be caused by GICs. The following quotes highlight some of these observations:

*“3.3 The upper shunts controlling the leakage flux from the winding returning to the yokes showed signs of overheating. The shunt insulation had also deteriorated.*

*3.4 At the tips of three upper magnetic shunts on the line side, a number of laminations had spread open and bent towards the yoke. They had penetrated the insulation causing electrical contact. The yoke laminations had melted at these points.*

*3.5 Molten metal particles from the yoke laminations were found between some of the winding conductors.”*

*“The shunts collecting the stray flux from the winding situated at the top neutral end of the winding overheated due to high flux density.”*

The estimated costs only for repairs at Beta alone was R 4 892 000 in 1991.

Note that it is rarely the case that transformer or reactor failure occurs at the exact same time as a geomagnetic storm [84]. Normally the overheating or hot spots will cause insulation breakdown, which will effectively decrease the expected life span of the equipment. At times the overheating may become so severe that part of the magnetic circuit, such as the leakage flux shunts, may melt and short out windings below as in the case of the Beta reactors.

# Chapter 4

## Modelling and Predicting GICs

### 4.1 Introduction

The theoretical evaluation of GICs in power networks can be divided into two parts:

- Network calculation: to calculate the GICs produced by this electric field in the different parts of the system. This is done by using Ohm and Kirchhoff's laws as well as Thevenin's theorem
- Geophysical calculation: to calculate the earth surface potential (ESP) from Maxwell's equations.

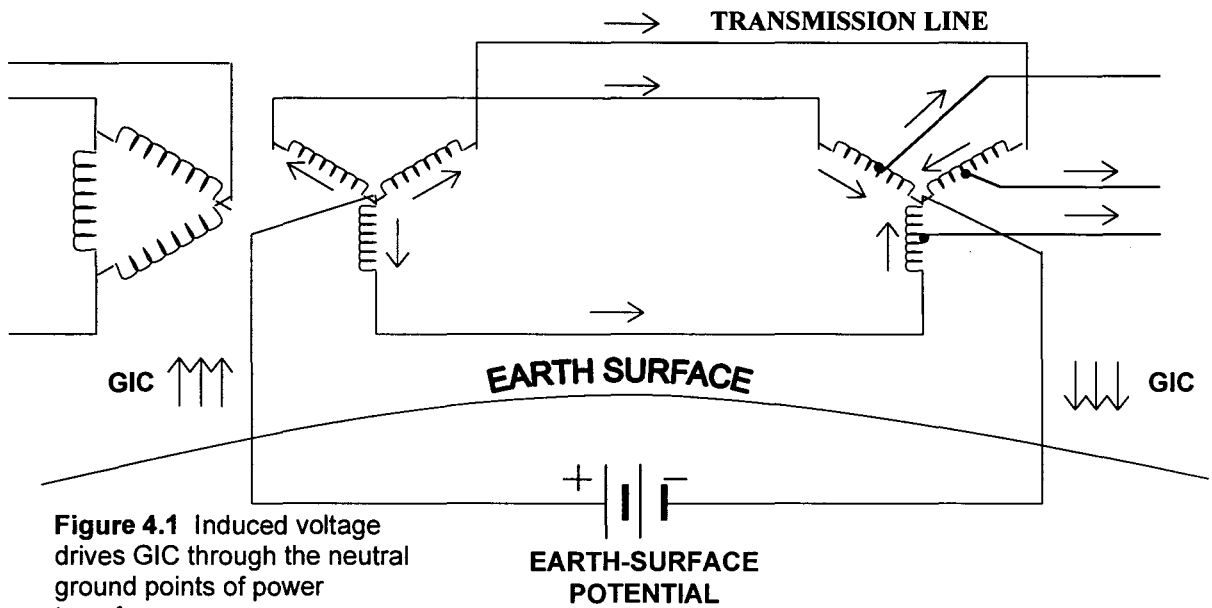
By combining these two steps the GIC at every substation can then be calculated. This chapter will address these two steps and describe how they are combined to predict the GIC at different substations during a geomagnetic storm.

### 4.2 Network Calculation

#### 4.2.1 Model Description

Figure 4.1 illustrates how the ESP caused by geomagnetic fluctuations will cause the GIC to flow into the power system. After entering the transformer through the neutral, it will split equally among the three phases of the transformer into the transmission line. From there it will terminate at the star point of the next transformer. In the case of an autotransformer, this current does not need to terminate at the earth point, and may flow via the series winding to the next transformer.





Since it is quasi-dc current, network equipment and transmission lines will be represented by only their dc-resistances and the three phases are considered to be in parallel. The source is represented by an idealised voltage source and exists between the grounded neutrals or ground mats (see fig. 4.2b) with a finite resistance to remote earth. Since an accurate value of this resistance is not available for all substations, it can be assumed to be  $0.1\Omega$  at the coast and  $0.5\Omega$  inland [43, 44, and 49]. Transformers are represented by their winding resistance values in parallel as shown in figure 4.2.

Symbols used in figure 4.2 are:

$R_L$  = line resistance per phase.

$R_Y$  = resistance of grounded star-connected winding per phase.

$R_S$  = autotransformer series winding resistance per phase.

$R_C$  = autotransformer common winding resistance per phase.

$R_{gi}$  = grounding resistance of bus i.

$I_{ni}$  = neutral GIC at bus i.

$V_{espi}$  = earth surface potential at bus i.

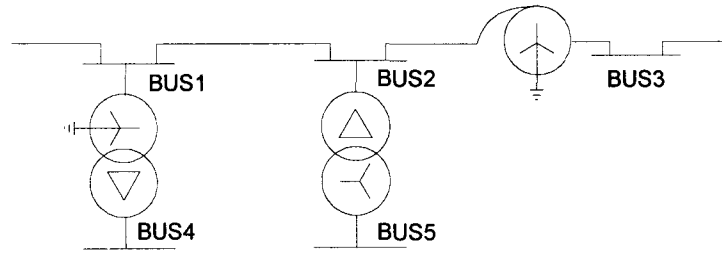


**Figure 4.2a** Sample network to illustrate modelling procedure

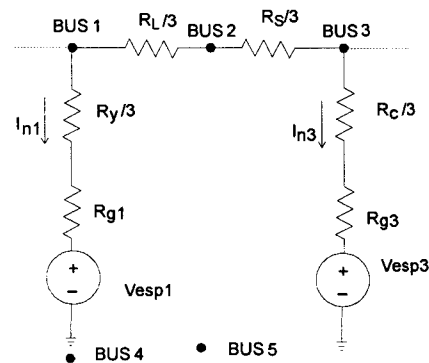


**Figure 4.2b** DC model of sample network

At some sites there is more than one transformer in parallel (as well as shunt reactors) which will correspondingly change the value of the transformer resistance.

The ac resistance of overhead transmission lines is normally reduced by 5% (skin effect factor) to give dc resistance. The effect of shield wires can be neglected since their high resistance as well as tower footing resistance limits currents through it, also since the concern lies with the GICs in the phase lines [47, 50].

### 4.2.2 Network Configuration

The following procedure to calculate the contribution of the network configuration to determine GICs has been derived by Lehtinen & Pirjola [42]. Note that bold letters will be used to represent vectors.

The earthing points of the network are defined by  $p_1, \dots, p_m$  (fig. 4.3). All these points have earthing resistances  $R_1 \dots R_m$ , which are the sum of the dc resistance of the transformer and the resistance of the transformer earth to true earth. Each pair of points  $(p_i, p_j)$  is interconnected by a transmission line with resistance  $R_{ij}$ . This value will be infinite should a pair of points not be connected. Current flowing in between nodal point  $p_i$  and  $p_j$  is denoted  $I_{ij}$  and the earthing current at a node  $p_j$  is denoted by  $I_j$  with the positive direction into earth.

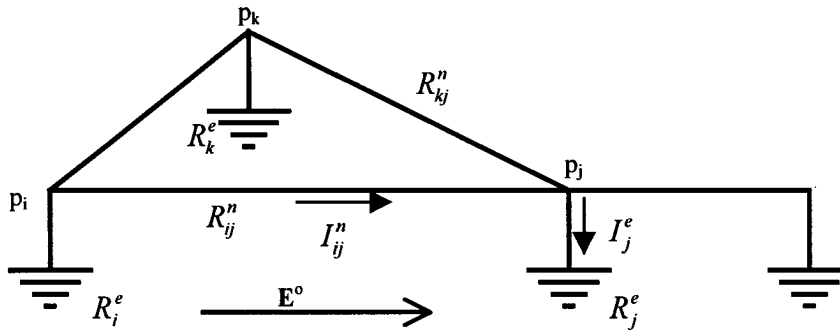


**Figure 4.3** Definition of symbols used for a transmission network

The earthing resistance is described by the earthing impedance matrix  $\mathbf{Z}$ . Since no time dependence exists for the quasi-dc GIC, all the elements of the matrix will be real. The earthing point is assumed to be far enough from each another so that the earthing current at one point does not affect the potential at another point. This assumption will imply that the earthing impedance matrix is simply a diagonal matrix with diagonal elements equal to the earthing resistances  $R_i$ . The values of these elements are the sums of the resistances of the transformers, with all three phases in parallel, and the actual earthing resistances.

The electric field at the earth's surface without the conductor network is denoted  $\mathbf{E}^o(\mathbf{r}, t)$  and is called the open-circuit electric field. Let  $s_{ij}$  denote the path of the line between a pair of nodal points  $p_i$  and  $p_j$ . The open-circuit electromotive force between these points can thus be defined as the path integral of the open-circuit electric field  $\mathbf{E}^o$  along the path  $s_{ij}$ :

$$V_{ij}^o = \int_{s_{ij}} \mathbf{E}^o \cdot d\mathbf{l} \quad (4.1)$$

When the conducting circuit is included in the calculation it will introduce two fields  $\mathbf{E}^{cur}$  and  $\mathbf{E}^{ind}$ . The latter is due to time variations of the currents in the conductors. The former arises due to the flow of GIC current in the earthing resistance  $R_j$  and line resistance  $R_{ij}$ . Therefore, the closed circuit field  $\mathbf{E}^e$  and corresponding electromotive force can be found as follow:

$$\mathbf{E}^e = \mathbf{E}^o + \mathbf{E}^{cur} + \mathbf{E}^{ind} \quad (4.2)$$

and

$$V_{ij} = V_{ij}^o + V_{ij}^{cur} + V_{ij}^{ind} \quad (4.3)$$

Once again, because of the quasi-dc nature of GICs,  $\mathbf{E}^{ind}$  and thus  $V_{ij}^{ind}$  can be ignored. For the same reason the field  $\mathbf{E}^{cur}$  has a single-valued potential,  $U_j^{cur}$  with respect to true earth and can be calculated as follow:

$$U_j^{cur} = \sum_{i=1}^m Z_{ji}^e I_i^e, \text{ or as a matrix equation} \quad (4.4)$$

$$\mathbf{U}^{cur} = \mathbf{Z}^e \mathbf{I}^e \quad (4.5)$$

From Kirchoff's voltage law the potential inside the loop between a pair of point  $p_i$  and  $p_j$  will be (see fig 4.4)

$$V_{ij}^o - (U_j^{cur} - U_i^{cur}) - I_{ij}^n R_{ij}^n = 0 \quad (4.6)$$

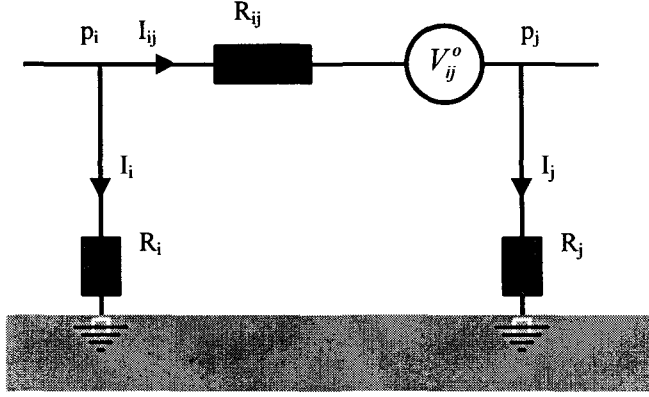


**Figure 4.4** The closed loop between two nodal points  $p_i$  and  $p_j$

And from Kirchoff's current law the currents at the nodal points will be defined by

$$I_i^e = \sum_{j \neq i} I_{ji}^n = - \sum_{j \neq i} I_{ij}^n \quad (4.7)$$

Solving for  $I_{ij}$  from equation (4.6) and substituting into (4.7) yields

$$I_i^e = - \sum_{j \neq i} (V_{ij}^o + U_i^{cur} - U_j^{cur}) / R_{ij}^n \quad (4.8)$$

which can also be written as

$$I_i^e = - \sum_{j \neq i} \frac{V_{ij}^o}{R_{ij}^n} - U_i^{cur} \sum_{j \neq i} \frac{1}{R_{ij}^n} + \sum_{j \neq i} \frac{U_j^{cur}}{R_{ij}^n} \quad (4.9)$$

The network admittance matrix is defined as

$$Y_{ij}^n = \begin{cases} -1/R_{ij}^n, & i \neq j \\ \sum_{k \neq i} 1/R_{ik}^n, & i = j \end{cases} \quad (4.10)$$

Once again because of the assumed time independence of GICs, the elements of the matrix are purely real.

Equation (4.9) can then be simplified to

$$I_i^e = -\sum_{j \neq i} \frac{V_{ij}^o}{R_{ij}^n} - U_i^{cur} Y_{ii}^n - \sum_{j \neq i} Y_{ij}^n U_j^{cur} \quad \text{and thus,}$$

$$I_i^e = -\sum_{j \neq i} \frac{V_{ij}^o}{R_{ij}^n} - \sum_j Y_{ij}^n U_j^{cur} \quad (4.11)$$

A column vector  $\mathbf{J}^e$  is defined by

$$J_i^e = \sum_{j \neq i} J_{ji}^n \quad (4.12)$$

where

$$J_{ij}^n = V_{ij}^o / R_{ij}^n \quad (4.13)$$

Therefore equation (4.11) can be written as

$$I_i^e = \sum_{j \neq i} J_{ji}^n - \sum_j Y_{ij}^n U_j^{cur} \quad (4.14)$$

and thus

$$I_i^e = J_i^e - (\mathbf{Y}^n \mathbf{U}^{cur})_i \quad (4.15)$$

which from equation (4.5) can be written as

$$I_i^e = J_i^e - (\mathbf{Y}^n \mathbf{Z}^e \mathbf{I}^e)_i \quad (4.16)$$

Equation (4.16) can be expressed as a complete matrix equation

$$\mathbf{I}^e = \mathbf{J}^e - \mathbf{Y}^n \mathbf{Z}^e \mathbf{I}^e \quad (4.17)$$

and therefore to calculate the earthing currents

$$\mathbf{I}^e = (\mathbf{I} + \mathbf{Y}^n \mathbf{Z}^e)^{-1} \mathbf{J}^e \quad (4.18)$$

where  $\mathbf{Y}$  is the network admittance matrix and  $\mathbf{Z}$  the earthing impedance matrix. The elements of this column vector  $\mathbf{I}^e$  depend only on the resistance and structure of the power system. They are therefore not the GIC value at the nodal points but a representation of the network and called “Network Constants”.



These network constants must be calculated respectively for an eastern and northern electric field of 1V/km, i.e. by changing the elements of column matrix  $\mathbf{J}^e$ . If the electric field is known the constants are used to calculate the GIC as follow:

$$I_{GIC} = aE_x + bE_y \quad (4.19)$$

where "a" is the GIC for the eastward surface potential of 1V/km and "b" the GIC for a northern surface potential of 1V/km. These surface potentials of 1V/km are constant and independent of the geology. The actual or theoretical electric field is represented by  $E_x$  and  $E_y$  which will determine the magnitude of the GIC at the site.  $E_x$  represents the electric field in the northern direction and  $E_y$  the eastern electric field.

Section 4.2 will elaborate on the calculation of the electric field and section 4.3 will show by means of an example how these calculations are applied.

### 4.3 Geophysical Calculation

Countries located at high latitudes beneath the auroral zone will generally use a three dimensional model to calculate local earth surface potentials (ESP). The ionospheric current is assumed to be one million amperes, about 600 km long, 450 km thick, and located at about 120 km above the earth surface [35]. This detail is not necessary for countries at mid-latitude such as South Africa where it is sufficient to assume an infinite current sheet with a spatially constant current density [50, 66]. The primary field is thus a vertically propagating plane wave.

The model for regional geology depends on the conductivity, permeability and permittivity of the area considered. A uniform earth model can be assumed when using the plane wave method.

The procedure to calculate the electric field has been derived by Viljanen and Pirjola [68]. The earth is described as a half-space with a constant conductivity of  $\sigma$  and the geomagnetic field propagates as a vertical plane wave in the earth. Using Cartesian coordinates, the x-axis is directed to the magnetic north, y to the magnetic east and z downwards. The electric field is then obtained by

$$E(T_N) = \frac{2}{\sqrt{\pi \mu_0 \sigma \Delta}} (R_{N-1} - R_N - \sqrt{M} b_{N-M}) \quad (4.20)$$

where  $\Delta$  is the sampling interval,  $N$  is the sample number,  $M = 10$  [66] and

$$R_N = \sum_{n=N-M+1}^N b_n \sqrt{N-n+1} \quad (4.21)$$

where  $b_n = B_n - B_{n-1}$  ( $B$  being the magnetic component).

Since magnetic and electric fields are perpendicular,  $E_x$  will be calculated from  $B_y$  and  $E_y$  from  $B_x$ . A simplified example has been included in appendix E to illustrate step by step how the electric field will be calculated from equations 4.20 and 4.21 in section 4.2.1.

### 4.4 Example Of Calculating GICs

The following example will illustrate how GIC can be calculated at various substations of an interconnected transmission network. The model will consist of six 400 kV substations numbered 1 through 6 as shown in fig 4.5.

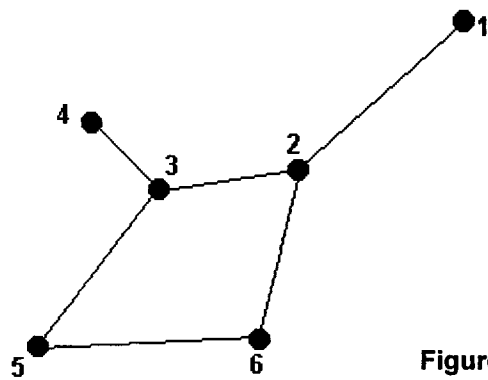


Figure 4.5 Single line diagram of model

#### 4.4.1 Network Constants

The line data necessary to calculate the admittance matrix (equation 4.10) is shown in the table below.

Table 4.1 Line resistances between any pair of connected substations (see comments at end of table)

Station Numbers		No. of lines	Voltage	Line length	Line type	$R_{pu}/km$	Line resistance
i	j		[kV]	[km]			$R_{ij}^n [\Omega]$
1	2	2	400	320	Twin Dinosaur	0.000015	1.280
2	3	2	400	125	Twin Dinosaur	0.000015	0.500
2	6	1	400	215	Quad Wolf	0.000030	3.440
3	4	1	400	105	Quad Wolf	0.000030	1.680
3	5	2	400	257	Twin Dinosaur	0.000015	1.028
5	6	1	400	262	Quad Wolf	0.000030	4.192

Comments: To determine the actual line resistance  $R_{ij}^n$ , the following formula is used:

$$R_{act} = R_{pu} * (V_{line}) / (S_{base})$$

where  $R_{pu} = (R_{pu}/km) * (line\ length)$ ,  $V_{line} = 400\ kV$  and,  $S_{base} = 100\ MVA$

This value must then be divided by three to take into account that it is a three-phase conductor. That value must again be divided by the number of three phase lines in parallel (assuming parallel conductors are of the same type and length).

From table 4.1 and equation (4.10) the admittance matrix can be calculated:

$$\mathbf{Y}^n = \begin{bmatrix} 0.781 & -0.781 & 0 & 0 & 0 & 0 \\ -0.781 & 3.072 & -2.000 & 0 & 0 & -0.291 \\ 0 & -2.000 & 3.568 & -0.595 & -0.973 & 0 \\ 0 & 0 & -0.595 & 0.595 & 0 & 0 \\ 0 & 0 & -0.973 & 0 & 1.212 & -0.239 \\ 0 & -0.291 & 0 & 0 & -0.239 & 0.530 \end{bmatrix}$$

As mentioned in section 4.1.2 the earthing impedance matrix is a diagonal matrix with real elements. These values are the sum of the resistances of the transformers with all three phases in parallel, and the actual earthing resistances. As mentioned in section 4.1.1 the latter is generally assumed to be  $0.1\Omega$  at the coast and  $0.5\Omega$  inland [43, 44, and 49]. For the model the transformer and reactor resistances will be assumed to be equal for all substations with a value of  $0.3\Omega$  ( $\frac{0.9}{3}\Omega = 0.3\Omega$ ). If there are more than one transformer or reactor at a site in parallel the value have to be changed correspondingly. However, this has been shown to be insignificant at times since, depending on the model, the line resistances are dominating and therefore changing the earthing resistance had almost no effect on the calculated value [43]. The necessary data to calculate the earthing impedance matrix is shown in table 4.2.

**Table 4.2** Data necessary to calculate the earthing impedance matrix. The diagonal elements of the  $\mathbf{Z}^e$  are those shown in the last column.

Substation No	Actual earthing resistance $[\Omega]$	No of transformers at substation	No of reactors at substation	Calculated earthing resistance $R_i^e [\Omega]$
1	0.1	2	1	0.13
2	0.5	2	0	0.40
3	0.5	2	0	0.40
4	0.5	2	0	0.40
5	0.1	2	1	0.13
6	0.1	1	0	0.40

The final values to be calculated are those of the column matrix  $\mathbf{J}^e$  (see equation 4.12 & 4.13). This matrix must be calculated twice, once for an eastern and once for a northern electric field of 1V/km. The following table lists these values.

**Table 4.3** Calculating the column vector  $\mathbf{J}^e$ . For calculating the horizontal and vertical distances, substation 1 was used as a reference point. As mentioned in section 4.1.2, positive direction is assumed to be into earth, therefore the values for substations to the east and north are assumed negative and visa versa.

Substation No	Connected to	Line resistance [ $\Omega$ ]	Horizontal surface potential [V]	Vertical surface potential [V]	$\mathbf{J}_{ij}^n$ Horizontal	$\mathbf{J}_{ij}^n$ Vertical
1	2	1.280	250	175	195.31	136.72
2	1	1.280	-250	-175	79.22	-28.58
	3	0.500	130	25		
	6	3.440	50	200		
3	2	0.500	-130	-25	-41.06	108.84
	4	1.680	90	-60		
	5	1.028	170	200		
4	3	1.680	-90	60	-53.57	35.71
5	3	1.028	-170	-200	-225.01	-200.52
	6	4.192	-250	-25		
6	2	3.440	-50	-200	45.10	-52.18
	5	4.192	250	25		

Combining these values through equation (4.18) the network constants (or GIC values for a constant field of 1 V/km) can be determined:  $\mathbf{I}^e = (\mathbf{1} + \mathbf{Y}^n \mathbf{Z}^e)^{-1} \mathbf{J}^e$

**Table 4.4** The network constant value “a” is the value for an eastward surface potential of 1V/km and “b” that for a northern surface potential of 1V/km.

Substation No	a	b
1	126	188
2	5	39
3	42	-19
4	37	-47
5	-163	-198
6	-47	36

Once the actual electric field is known the GIC can be calculated for each substation individually, from equation (4.19):  $I_{GIC} = aE_x + bE_y$ . The electric field will be calculated in the next section.



## 4.4.2 Magnetic Data and GIC

An example of the results during a very severe storm is given in figure 4.6 where the predicted GIC at substation 5 of the model is compared to the magnetic field (X and Y), as well as the magnetic field variation ( $dX/dt$  and  $dY/dt$ ). The magnetic data used for the graph were sampled over a 120 second interval for a period of 180 minutes during a very severe storm ( $K = 9$ ). The detailed magnetic data and corresponding electric field is available in appendix F.

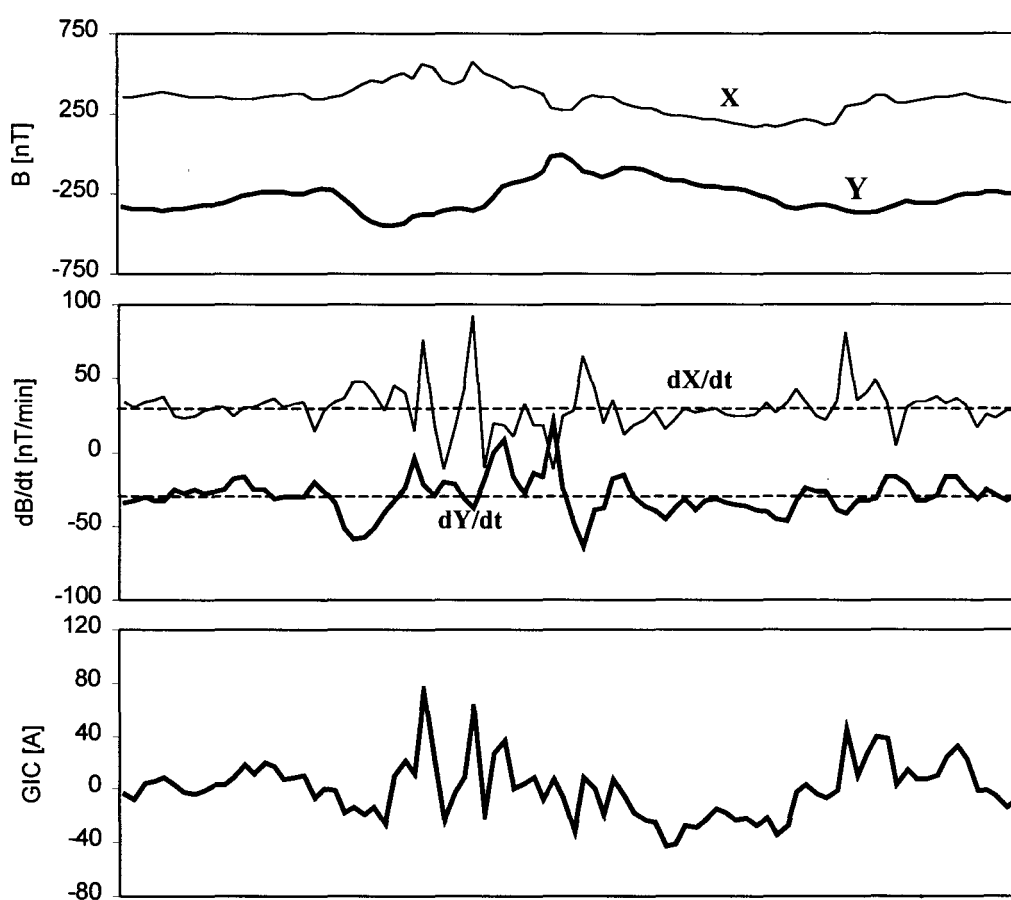


**Figure 4.6** Top panel: X (thin line) and Y (thick line) at substation 5 during very severe storm of 13 March 1989. Note that X is normalised around 9500 nT and Y around -4000 nT.  
Middle panel:  $dX/dt$  (thin line) and  $dY/dt$  (thick line). Zero levels are plotted with dashed lines.  
Bottom panel: Predicted GICs at substation 5. Positive current flows into the earth.

### 4.4.3 Interpretation of Results

From table 4.4 it is evident that the most susceptible substations are 1 and 5. The main reason for this is the fact that they are at the ends of the longest effective span of the network. Distance plays a major role since the earth surface potential will increase linearly with the distance between the nodes. Another contributing factor is the fact that both these substations have very little earthing resistance (see table 4.2), however this will not dominate the GIC value since the line resistance is higher and therefore of more significance. In fact, it was shown that on some networks the value of the earthing resistances have almost no effect [43].

Table 4.6 shows how different values of the earthing resistance influence the GIC. From the table it is evident that substations 1 and 5 will be the most susceptible even when all substations are allocated the same earthing resistance value. Combined with the fact that the magnitude does not change drastically it shows that the line length and also the fact that GICs have to terminate at these end points play a more significant role than the earthing resistance.

**Table 4.6** The influence of earthing resistance value on the GIC

	$R_{1,5}^e = 0.13\Omega$ $R_{2,3,4,6}^e = 0.40\Omega$		$R_5^e = 0.13\Omega$ $R_{1,2,3,4,6}^e = 0.40\Omega$		$R_1^e = 0.13\Omega$ $R_{2,3,4,5,6}^e = 0.40\Omega$		<b>All substations:</b> $R_i^e = 0.40\Omega$	
<b>Substation No</b>	a	b	a	b	a	b	a	b
<b>1</b>	126	188	108	162	124	186	107	160
<b>2</b>	5	39	16	55	0	32	10	48
<b>3</b>	42	-19	45	-13	27	-37	31	-31
<b>4</b>	37	-47	38	-46	34	-50	35	-49
<b>5</b>	-163	-198	-162	-196	-131	-159	-130	-158
<b>6</b>	-47	36	-46	38	-53	28	-52	29

This table also shows that substation 4 is least affected by changing the earthing resistance at 1 and 5. This is since substation 4 is remote from the mesh network and therefore not significantly influenced by the “line” of current between 1 and 5 (see fig 4.5). The line connecting 3 to 4 is also much higher than that connecting 3 to 5.

It was also found that changing the value of the earthing resistance at substation 6 had almost no influence on its GIC magnitude. This is since the lines connecting it with 2 and 5 has very high resistance compared to the earthing resistance at 6 and are therefore dominant on the GIC magnitude.

Figure 4.6 comparing the predicted GIC at substation 5 to the magnetic field (X and Y), as well as the magnetic field variation ( $dX/dt$  and  $dY/dt$ ) shows clearly that the GIC is more dependant on the rate of change of the magnetic field rather than its magnitude. This is as expected since from Faraday’s law it is known that the magnitude of the electric field is related to the rate of change of the magnetic field. There is no simple relation between the GIC and  $dB/dt$  but it is without doubt more related than the GIC with B.

# **Chapter 5**

## **Measurements and Mitigation**

### **5.1 Introduction**

GIC interaction with a power system is a non-linear phenomenon (due to the presence of the magnetic core) and requires direct measurement to accurately determine its magnitude and effects. Parameters of importance will be the variation of the magnetic field, the magnitude of the GIC in the transformer neutral and the level of the saturation caused by it. The latter will be evident through measurements such as harmonic distortion, reactive power demand, transformer noise and transformer heating. Section 5.1 will elaborate more on the measurements as proposed here.

Through mitigation the detrimental effects of GICs can be limited and even avoided. Both passive and active devices have been developed for this purpose. Another popular alternative is through system operations i.e., changing the network during the event of a storm to reduce GICs. These methods will be discussed in section 5.2.

## 5.2 Measurements

There are three main methods to monitor GICs [2]:

- Measure perturbations of the earth's magnetic field in terms of its variation with time  $dB/dt$
- Measure the GIC in the transformer neutrals or transmission lines
- Measure the adverse effects on the network such as transformer saturation; this is done through parameters such as harmonic distortion, reactive power demand etc.

Magnetic data such as  $dB/dt$  and values of the K-index is available from magnetic observatories. Once such an institution in South Africa is that of the CSIR in Hermanus. If this data is available on a real time basis it can be used to warn network controllers of a magnetic storm to which they can react and effectively minimise the GIC. This will be discussed in section 5.2.

The GIC is usually measured in the transformer neutral since it is easier and more practical compared to installing a dc transformer on a transmission line. The problems with the latter are that dc transformers for transmission line voltages are quite limited and it is more difficult to install. A method adopted in Finland to measure GICs in the transmission lines was by using a magnetometer near a 400 kV line in Porvoo [36]. This can be done in very isolated areas since this instrument is very sensitive to other disturbances.

The half-cycle saturation of the transformer not only depends on the GIC in the neutral but also on its load which will push it beyond the knee-point of the saturation curve. Monitoring methods that can indicate this level are the following:

- Harmonic distortion
- Reactive power demand
- Noise level of transformer
- Heating of transformer

The EPRI SUNBURST program is a global monitoring network used by participating utilities. Its purpose is to provide a database for multiple sites regarding the effects of similar disturbances on different network configurations as well as various transformer types and designs. The harmonic components measured by this system are those of the second to the eighth. The reactive power demand at a site can also be calculated from this system since it measures the current and voltage on each side and determines the phase angle relationship. The increase in reactive power demand of the system instead of individual equipment can also be measured at various generators and reactive power compensators who will attempt to provide this extra demand.

Transformer noise will occur because the ferromagnetic material changes size slightly when magnetised causing the vibration of the lamella of the core. This level increases drastically during half-cycle saturation due to the increased magnetisation and presence of harmonics. This indicates undesired mechanical strain of the transformer and will also be a psychological problem in power transformers operate near human activity [54].

Transformer heating takes place when the leakage flux from the saturated core causes hot spots. This heating can be quite dramatic and cause the failure of transformers such as the GSU transformer (as mentioned in section 3.2.1) that was damaged beyond repair. Another well-monitored transformer had a rapid rise in internal heating due to GIC when the temperature of a hot spot on the tank increased from 60°C to over 175°C in as few as 10 minutes.

Since measuring equipment is very expensive to buy, install and maintain it should only be installed at sites most susceptible. These sites can be identified through the modelling of the network. Generally the sampling interval to measure GICs are 10 s with an average value determined every minute [36].

## **5.3 Mitigation**

### **5.3.1 Passive Devices**

Due to the quasi-dc nature of GICs devices such as Transmission Line Series Capacitors can block their flow. Although such devices will provide additional line impedance compensation and increase the power flow transfer limit, they are not feasible for the sole purpose of blocking GICs. Very low impedance capacitors make this method more cost effective. These devices offer almost no compensation, and hence have very little voltage across them [35].

Another method that is under investigation is the installation of a series capacitor in the transformer neutral. This device has a by-pass circuit in parallel with it for the purpose of shunting fault currents. This method might however interfere with the safe operation of the ac system [62].

### **5.3.2 Active Devices**

Research was done to investigate the possibility of a controlled dc circuit in a special purpose winding on the transformer core [35]. This dc current tertiary winding would produce a counter MMF to that of the GIC. This method was however deemed non-successful by the investigators.

### **5.3.3 Operational Mitigation**

Breaking the network into smaller sections can drastically reduce the flow of GICs, especially in a long interconnected network such as the Eskom MTS. However care has to be taken when using this method since blindly breaking the network could actually increase the GIC at certain substations due to the reduction of GIC terminating nodes.

The method is especially attractive for networks with series compensated lines. This is since taking out non-compensated lines can reduce the flow of GICs while still supplying sufficient power flow through series compensated lines. It is also the most cost- and time-effective method.

Operational mitigation is even more effective when the operators are given a lead-time to a geomagnetic storm. This is now possible through a company that predicts storm onset through observations from space (utilising the ACE satellite) of the formation of the Aurora Borealis. This service provides a lead-time of 30 to 45 minutes.



## Chapter 6

### Conclusions and Recommendations

Geomagnetic storms occur when the charged particles of the solar wind caused by a Coronal Mass Ejection on the sun are captured by the earth's dipole magnetic field. The perturbation of this magnetic field will cause an electric field on the earth's surface. This field is the source of GICs through the earthed transformer neutral. These storms are of a cyclic nature and peak every eleventh year.

The quasi dc GIC will cause an offset of the core magnetisation which could lead to half cycle saturation of a transformer if it supplies a big enough load. This could lead to all kinds of detrimental effects such as harmonics, reactive power swings, transformer overheating etc. This has happened in many countries at high latitude since they experience a more severe perturbation of the magnetic field than countries at mid latitude such as South Africa. However, the modelling does implicate that network configuration is as important factor as the induced electric field. Therefore utilities at mid-latitude such as Eskom could experience harmful GICs due to factors such as long-interconnected lines. The techniques to determine the effect of the network configuration and electric field were provided.

Eskom has been aware since about 1990, that occasional severe geomagnetic storms in the Southern Cape might disrupt the MTS in that area. At that time no correlation was observed between disruptions at selected sites of the Eskom MTS and geomagnetic activity. (The sites selected were based on the knowledge at that time.) However, an investigation into the past events on the Eskom MTS and correlation with geomagnetic storms have indicated that GICs may have caused damage to the extent of millions of

rands. Since this has happened during the previous solar peak (1991) to much time has passed and therefore detailed information was unavailable. This evidence suggests that the sites most susceptible are not at the conventionally accepted locations, and that damage and disruption may have occurred where it was not expected. Circumstantial evidence such as the failure of a reactor at Poseidon and Beta substations has been provided. The damage caused at these sites correlated very closely with geomagnetic storms and the extend of the damage is what is expected from GICs. It was also found that the core types of the power transformers generally used by Eskom are susceptible to GICs. Measurement techniques and mitigation methods were also provided, this could be applied to the Eskom MTS.

In light of the findings the following recommendations are made:

- Develop a complete network model and identify all the most sensitive locations
- Investigate for a correlation (if any) between the sites most susceptible from the theoretical modelling and past system events seemed to be caused by GICs
- Installation of monitors and sensors at most susceptible sites
- Train system controllers and develop a pro-active response so mitigation plans can be prepared as an operational mitigation technique
- Train network planners to apply mitigation techniques for future planning
- Review existing project implementation plans for installation of series capacitors to reduce the sensitivity of the network to GICs

This project provides information on the mechanism, impact and influencing factors of geomagnetically induced currents. The report also suggests that the Eskom MTS may be susceptible to it. Future research could establish the severity of GICs in the Eskom MTS and methods to reduce and even completely avoid its detrimental effects.

## References

1. Kappenman, J.G., Albertson, V.D., "Bracing for the Geomagnetic Storms", IEEE Spectrum Magazine, pp. 27-33, March 1990.
2. Molinski, T.S., "Why Utilities Respect GICs", XXVIth General Assembly International Union of Radio Science, August 1999.
3. Kappenman, J.G., "Geomagnetic Storms and Impacts on Power Systems: Lessons Learned from Solar Cycle 22 and Outlook for Solar Cycle 23", IEEE Power Engineering Review, May 1996
4. Eather, "Majestic Lights," American Geophysical Union, Washington D.C., 1980.
5. Towle, F.S. Prabhakara and J.Z. Ponder, "Geomagnetic Effects Modelling for the PJM Interconnection System Part I - Earth Surface Potentials Computation," IEEE Transactions on Power Systems, Vol. 7, No. 3, pp. 949-955, August 1992.
6. K. Hufbauer, "Exploring the Sun," John Hopkins University Press, 1991.
7. B.W. Carroll and D.A. Ostlie, "Modern Astrophysics," Addison-Wesley Publishing Company, 1996.
8. P.R. Sutcliffe and P.B. Kotzé, "Proceedings of the workshop on the Hermanus Magnetic Observatory's Geophysical Services," no publisher, February 1992.
9. J.S. Lewis, "Physics and Chemistry of the Solar System," Academic Press, 1995.
10. Private communications to Dr P. Sutcliffe, Hermanus Magnetic Observatory, CSIR, March 1999.
11. [http://science.nasa.gov/newhome/headlines/ast09mar99\\_2.htm](http://science.nasa.gov/newhome/headlines/ast09mar99_2.htm)
12. <http://www.sunspotcycle.com/#aurora>
13. <http://solar.physics.montana.edu/YPOP/Classroom/Lessons/Rotation/>
14. [http://www.oma.be/KSB-ORB/SIDC/sidc\\_graphics.html](http://www.oma.be/KSB-ORB/SIDC/sidc_graphics.html)
15. [http://pss.fit.edu/Space\\_Physics/workshop/structure.html](http://pss.fit.edu/Space_Physics/workshop/structure.html)
16. <http://zebu.uoregon.edu/~mbartels/eclipse98/part3.html>

17. <http://umbra.nascom.nasa.gov/images/latest.html>
18. <http://dac3.pfrr.alaska.edu/~ddr/ASGP/ELEMPART/AURORA/6.HTM>
19. <http://solar.physics.montana.edu/YPOP/Classroom/Lessons/Sunspots/>
20. <http://umbra.nascom.nasa.gov/sdac.html>
21. <http://science.msfc.nasa.gov/ssl/pad/solar/feature2.htm>
22. <http://athena.wednet.edu/curric/space/solterr/sunaur.html>
23. <http://www-spof.gsfc.nasa.gov/Education/wfldline.html>
24. [http://blackbird.eps.pitt.edu/pe\\_book/c\\_xiv/chap14.html](http://blackbird.eps.pitt.edu/pe_book/c_xiv/chap14.html)
25. <http://www-spof.gsfc.nasa.gov/Education/lexplore.html>
26. <http://vestige.lmsal.com/TRACE/Public/magnetic.htm>
27. <http://science.msfc.nasa.gov/ssl/pad/solar/images/grandad.jpg>
28. <http://www-spof.gsfc.nasa.gov/Education/waurora1.html>
29. [http://www.ips.gov.au/papers/richard/aurora\\_pictures\\_03.html](http://www.ips.gov.au/papers/richard/aurora_pictures_03.html)
30. [http://gate.dmi.dk/fsweb/solar-terrestrial/images/solar\\_terrestrial\\_sys.gif](http://gate.dmi.dk/fsweb/solar-terrestrial/images/solar_terrestrial_sys.gif)
31. Viljanen, A., "Geomagnetic induction in a one- or two- dimensional earth due to horizontal ionospheric currents", Finnish Meteorological Institute Contributions, Helsinki, 1992.
32. Pirjola, R., and Viljanen, A., "On Geomagnetically Induced Currents in the Finnish 400kV Power System by an Auroral Electrojet Current", IEEE Transactions on Power Delivery, Vol. 4, No.2, pp. 1239 – 1245, April 1989.
33. Kappenman, J.G., et al., "Geomagnetic Storms can Threaten Electric Power Grid", Earth in Space, Vol. 9, No. 7, pp. 9-11, March 1997.
34. Albertson, V., D., et al., "Load-Flow Studies in the Presence of Geomagnetically Induced Currents", IEEE Transactions on Power Apparatus and Systems, Vol. PAS-100, No. 2, pp. 594-607, February 1981.
35. Transmission and Distribution Committee Working Group on Geomagnetic Disturbances and Power System Effects, "Geomagnetic Disturbance Effects on Power Systems", IEEE Transactions on Power Delivery, Vol. 8, No. 3, pp. 1206-1215, July 1993

36. Viljanen, A., and Pirjola, R., "Geomagnetically Induced Currents in the Finnish High Voltage Power System", *Surveys in Geophysics*, Vol. 15, pp. 383 – 408, 1994.  
Detailed discussion of the ESP as calculated and measured in Finland.
37. Sutcliffe, P.R., Kotze, P.B., "Proceedings of the Workshop on the Hermanus Magnetic Observatory's Geophysical Services", Hermanus Magnetic Observatory, pp. 1-61, February 1992.
38. Private communications with Dr Peter Sutcliffe, Hermanus Magnetic Observatory, CSIR, Hermanus, 1999.
39. Hruska, J., et al., "The major storm of 13-14 March 1989: Its character in Canada and some effects", *STPW Proceedings*, October 1989.
40. Viljanen, A., "The relation between geomagnetic variations and their time derivatives and implications for estimation of induction risks", *Geophysical Research Letters*, Vol. 24, No. 6, pp 631-634, March 15, 1997.
41. Viljanen, A., "Relation of Geomagnetically Induced Currents and Local Geomagnetic Variations", *IEEE Transactions on Power Delivery*, Vol. 13, No. 4, pp. 1285-1290, October 1998.
42. Lehtinen, M., Pirjola, R., "Currents produced in earthed conductor networks by geomagnetically-induced electric fields", *Annalas Geophysicae*, Vol. 3, No. 4, pp. 479-484, 1985.
43. Pirjola, R., Lehtinen, M., "Currents produced in the Finnish 400kV power transmission grid and in the Finnish natural gas pipeline by geomagnetically-induced electric fields", *Annalas Geophysicae*, Vol. 3, No. 4, pp. 485-491, 1985.
44. Elovaara, J., et al., "Geomagnetically Induced Currents in the Nordic Power System and their effects on Equipment, Control, Protection and Operation", *Cigre*, 1992.
45. Boteler, D.H., Bui-Van, Q., Lemay, J., "Directional sensitivity to geomagnetically induced currents of the Hydro-Quebec 735kV power system", *IEEE Transactions on Power Delivery*, Vol. 9, No. 4, October 1994.
46. Towle, J.N., Prabhakara, F.S., Ponder, J.Z., "Geomagnetic effects modelling for the PJM interconnection system; Part I – Earth surface potentials computation", *IEEE Transactions on Power Systems*, Vol. 7, No. 3, August 1992.

47. Prabhakara, F.S., et al., "Geomagnetic effects modelling for the PJM interconnection system; Part II – Geomagnetically induced current study results", IEEE Transactions on Power Systems, Vol. 7, No. 2, May 1992.
48. Private communications with Dr Johan de Beer, CSIR Enviromentek, Stellenbosch, 1999.
49. Rackliffe, G.B., et al., "Simulation of Geomagnetic currents induced in a power system by magnetohydrodynamic eletromagnetic pulses", IEEE Transactions on Power Delivery, Vol. 3, No. 1, pp392-397, January 1988.
50. Private communications with Prof. Risto Pirjola, Finnish Meteorological Institute, Helsinki, Finland, 1999.
51. Private communications with Mr. Jarmo Elovaara, Fingrid Power Company, Helsinki, Finland, 1999.
52. Takasu, N., et al., "An experimental analysis if dc excitation of transformers by geomagnetically induced currents", IEEE Transactions on Power Delivery, Vol. 9, No. 2, April 1994.
53. Lu, S., Liu, Y., "FEM analysis of dc saturation to assess transformer susceptibility to geomagnetically induced currents", IEEE Transactions on Power Delivery, Vol. 8, No. 3, July 1993.
54. Aspnes, J.D., Merritt, R.P., Akasofu, S.I., "Harmonic generation in transformers related to dc excitation and system loading", IEEE Transactions on Power Apparatus and Systems, Vol. PAS-100, No. 4, April 1981. A series of tests were run with small transformers to determine the harmonic generation from saturation.
55. Aspnes, J.D., Merritt, R.P, and Spell, B.D. Geomagnetic Disturbances and Their Effect on Electric Power Systems. IEEE Power Engineering Review, Vol. 9, No. 7, pp 10-14, July 1989. The discussion is on an Alaskan three-legged transformer and the reaction of the tertiary current to the neutral DC current. The protection of the transformer is also discussed.

56. Douglas, D.A., "Current Transformer Accuracy with Asymmetric and High Frequency Fault Currents", IEEE Transactions on Power Apparatus and Systems, Vol. PAS-100, No. 3, pp 1006-1012, March 1981. -----Extensive discussion of CT modelling with some detail about saturation due to inrush which may be related to GIC.
57. IEEE Communications Committee Working Group on Solar Effects, "Solar Effects on Communications", IEEE Transactions on Power Delivery, Vol. 7, No. 2, pp 460-467, April 1992.
58. Boteler, D.H., "Geomagnetically Induced Currents: Present Knowledge and Future Research", IEEE Transactions on Power Delivery, Vol. 9, No. 1, pp. 50–58, January 1994.
59. Pirjola, R., "Induction in Power Transmission Lines During Geomagnetic Disturbances", Space Science Review, No. 35, pp 185-193, 1983.
60. Kappenman, J.G., Albertson, V.D., and Mohan, N., "Current Transformer and Relay Performance in the Presence of Geomagnetically-Induced Currents", IEEE Transactions on Power Apparatus and Systems, Vol. PAS-100, No. 3, pp. 1078-1088, March 1981. -----Extensive discussion of CT modelling and simulations including saturation characteristics.
61. Albertson, V.D., "Electric and Magnetic Field at the Earth's Surface Due to Auroral Currents", IEEE Transactions on Power Apparatus and Systems, Vol. PAS-89, No. 4, pp. 578-584, April 1970.
62. Kappenman, J.G., et al., "GIC Mitigation: A Neutral Blocking / Bypass Device to prevent the flow of GIC in Power Systems", IEEE Transactions on Power Delivery, Vol. 6, No. 3, pp. 1271–1281, July 1991.
63. Boteler, D.H., Pirjola, R.J., Nevanlinna, H., "The Effects of Geomagnetic Disturbances on Electrical Systems at the Earth's Surface", Adv. Space Res., Vol. 22, No. 1, pp 17-27, 1998.
64. Mäkinen, T., "Geomagnetically Induced Currents in the Finnish Power Transmission System", Finnish Meteorological Institute, No. 32, p26, 1993.
65. Cigre, "Guide on EMC in Power Plants and Substations", Working Group 36.04, pp. 40–42, December 1997.

66. Private communications with Dr Ari Viljanen, Finnish Meteorological Institute, Helsinki, Finland, 1999.
67. Technology Group Research Proposal, "Eskom/EPRI Sunburst 200 Collaboration: Geomagnetic Currents in Eskom's Southern Cape 400kV Network", Eskom, Report No TRR/CONS9/1998, 1998.
68. Viljanen, A., Pirjola, R., "Statistics on Geomagnetically-Induced Currents in the Finnish 400kV Power System Based on Recordings of Geomagnetic Variations", *Journal on Geomagnetism and Geoelectricity*, Vol. 41, pp 411-420, 1989.
69. Girgis, R.S., Ko, C., "Calculation techniques and Results of GIC Currents as Applied to Two Large Power Transformers", *IEEE Transactions on Power Delivery*, Vol. 7, No.2, pp. 669–705, April 1992.
70. Electric Research and Management, Inc., "SUNBURST GIC Network – Phase II Progress Report", Prepared for Electric Power Research Institute, February 1997.
71. Calabrò, S., Coppadoro, F., Crepaz, S., "The measurement of the magnetisation characteristics of large power transformers and reactors through D.C. excitation", *IEEE Transactions on Power Delivery*, Vol. 1, No.4, pp. 224– 234, October 1986.
72. Aspnes, J.D., Merritt R.P., Spell, B.D., "Instrumentation Systems to Measure geomagnetically Induced Current Effect" *IEEE Transactions on Power Delivery*, Vol. 2, No.4, pp. 1031 – 1036, April 1989.
73. Pirjola, R., "On Currents Induced in Power Transmission Systems During Geomagnetic Variations", *IEEE Transactions on Power Apparatus and Systems*, Vol. PAS-104, No. 10, pp. 2825-2831, October 1985.
74. Pirjola, R., "Modelling the electric and magnetic fields at the Earth's surface due to an auroral electrojet", *Journal of Atmospheric and Solar-Terrestrial Physics*, No. 60, pp 1139-1148, 1998.
75. Petschek, H., Feero, W., "Electric Power and Space Weather", *Geomagnetic Applications Bulletin*, pp 5 & 7, January 1997.
76. Appell, D., "Fire in the Sky", *New Scientist*, pp 29-32, 27 February 1999.
77. Leshner, R.L., Porter, J.W., Byerly, R.T., "SUNBURST – A Network of Monitoring Systems", *IEEE Transactions on Power Delivery*, Vol. 9, No.1, pp. 128–137, January 1994.



78. Albertson, V.D., et al, "Solar-Induced-Currents in Power Systems: Cause and Effects", IEEE PES Summer Meeting, San Francisco, California, July 1972.
79. Kappenman, J.G., "Geomagnetic Storm Forecasting Mitigates Power System Impacts", IEEE Power Engineering Review, pp 4-7, November 1998.
80. Albertson, V.D., Thorson, J.M., Miske, S.A., "The Effects of Geomagnetic Storms on Electrical Power Systems, IEEE PAS-93, No. 4, pp 1031-1044, July/August 1974.
81. Pirjola, R., Viljanen, A., "Complex image method for calculating electric and magnetic fields produced by an auroral electrojet of finite length", *Annalas Geophysicae*, No. 16, pp. 1434-1444, 1998.
82. De Beer, J.H., "Magnetometer Array Studies and Electrical Conductivity in Southern Africa", PhD Theses, University of Alberta, 1976.
83. Working Group K-11 of the Substation Protection Subcommittee of the Power System Relaying Committee, "The Effects of GIC on Protective Relaying", IEEE PAS-11, No. 2, pp 725-739, April 1996.
84. Private communications with Mr. John Kappenman, Metatech Company, Sunburst Annual Meeting, Washington DC, USA, 1999.
85. Private communications with Dr Arslan Erinmez, National Grid Company, Sunburst Annual Meeting, Washington DC, USA, 1999.
86. Private communications with Mr Edmund Stokes-Waller, Eskom Power Pool and System Operations, Eskom, South Africa, 1999.
87. Private communications with Mr Pieter Olivier, Eskom Transmission, Eskom, South Africa, 1999.

# Appendix A

## GEOMAGNETICALLY INDUCED CURRENTS IN ESKOM'S MTS LITERATURE REVIEW

18 November 1999

### Introduction

This report has been prepared for Eskom Technology Group to serve as feedback on the literature review done by J Koen as part of the above-mentioned project, which commenced in January 1999. The review covered all three aspects of the project namely, astrophysics, geophysics and engineering.

This report is submitted through the Department of Electrical Engineering at the University of Cape Town and presents a bibliography of GIC literature relevant to the project.

### GIC Related Literature

This section lists the sources obtained to review the present understanding of mechanism of GICs and effects on power network equipment. The sources were mostly from journals. Other sources included theses, the Internet and reports.

A complete reference of a source is given in the list below, each followed by a short description of the information obtained or available through that source.

1. Viljanen, A., "Geomagnetic induction in a one- or two- dimensional earth due to horizontal ionospheric currents", Finnish Meteorological Institute Contributions, Helsinki, 1992.

*The thesis discusses the various methods available to calculate the secondary electric field due to geomagnetic induction.*

2. Kappenman, J.G., Albertson, V.D., "Bracing for the Geomagnetic Storms", IEEE Spectrum Magazine, pp. 27-33, March 1990.

*A good general introduction to GICs discussing the sun as source, why and how it effects power systems, and a description of the Hydro-Quebec blackout in March 1989.*

3. Pirjola, R., and Viljanen, A., "On Geomagnetically Induced Currents in the Finnish 400kV Power System by an Auroral Electrojet Current", IEEE Transactions on Power Delivery, Vol. 4, No.2, pp. 1239 – 1245, April 1989.

*The paper derives gives an expression to determine the earth surface electric field assuming a two-layered earth model.*

4. Kappenman, J.G., et al., "Geomagnetic Storms can Threaten Electric Power Grid", Earth in Space, Vol. 9, No. 7, pp. 9-11, March 1997.

*A good informative paper which discusses the potential disruption due to GICs as well as financial implications and forecasting methods for mitigation.*

5. Albertson, V., D., et al., "Load-Flow Studies in the Presence of Geomagnetically Induced Currents", IEEE Transactions on Power Apparatus and Systems, Vol. PAS-100, No. 2, pp. 594-607, February 1981.

*One of the first papers to discuss the modelling of a network to determine expected GIC magnitude. It presents the results of load flow analysis beginning with earth-surface potential and the modelling of the power system and transformers in a load flow program. The paper also elaborates on the implications of GICs on a network.*

6. Transmission and Distribution Committee Working Group on Geomagnetic Disturbances and Power System Effects, "Geomagnetic Disturbance Effects on Power Systems", IEEE Transactions on Power Delivery, Vol. 8, No. 3, pp. 1206-1215, July 1993

*The paper briefly discusses almost every single aspect of GICs. It is a very good summary of the source, effect and mitigation of GICs.*

7. Viljanen, A., and Pirjola, R., "Geomagnetically Induced Currents in the Finnish High Voltage Power System", Surveys in Geophysics, Vol. 15, pp. 383 – 408, 1994.

*Detailed discussion of the earth surface potential as calculated and measured in Finland.*

8. Sutcliffe, P.R., Kotze, P.B., "Proceedings of the Workshop on the Hermanus Magnetic Observatory's Geophysical Services", Hermanus Magnetic Observatory, pp. 1-61, February 1992.

*The notes describe the physics of geomagnetic storms and GICs. It also covers the severity of geomagnetic field variations in South Africa.*

9. Hruska, J., et al., "The major storm of 13-14 March 1989: Its character in Canada and some effects", STPW Proceedings, October 1989.

*A detailed description of the magnetic storm that led to the collapse of the Hydro-Quebec power system in March 1989.*

10. Viljanen, A., "The relation between geomagnetic variations and their time derivatives and implications for estimation of induction risks", *Geophysical Research Letters*, Vol. 24, No. 6, pp 631-634, March 15, 1997.

*The paper shows that the main concern during a geomagnetic storm is the rate of change of the magnetic field instead of the amplitude of the variation. It concludes that the geoelectric field can have large values in any direction, not only parallel to the electrojet.*

11. Viljanen, A., "Relation of Geomagnetically Induced Currents and Local Geomagnetic Variations", *IEEE Transactions on Power Delivery*, Vol. 13, No. 4, pp. 1285-1290, October 1998.

*A comparison of two models to calculate GICs from the time derivative of the magnetic field. The first model is a plane wave with homogenous earth and the second is an impulse response between the GIC and time derivative of the magnetic field. From this paper one can conclude that the former method should be an accurate way to model the Eskom MTS.*

12. Lehtinen, M., Pirjola, R., "Currents produced in earthed conductor networks by geomagnetically-induced electric fields", *Annalas Geophysicae*, Vol. 3, No. 4, pp. 479-484, 1985.

*A very good paper explaining the derivation of the matrix method necessary to complete the engineering step.*

13. Pirjola, R., Lehtinen, M., "Currents produced in the Finnish 400kV power transmission grid and in the Finnish natural gas pipeline by geomagnetically-induced electric fields", *Annalas Geophysicae*, Vol. 3, No. 4, pp. 485-491, 1985.

*This paper is a follow up of the previous mentioned paper. It describes the application of the matrix derived to determine GICs in the Finnish 400kV network.*

14. Elovaara, J., et al., "Geomagnetically Induced Currents in the Nordic Power System and their effects on Equipment, Control, Protection and Operation", *Cigre*, 1992.

*The paper compares the Finnish and Swedish Power Systems. The comparison was done since the Swedish grid have experienced may more disruption than in Finland although the countries are located next to each other. It is interesting to note that the Eskom network may be more similar to that of Sweden than Finland.*

15. Boteler, D.H., Bui-Van, Q., Lemay, J., "Directional sensitivity to geomagnetically induced currents of the Hydro-Quebec 735kV power system", *IEEE Transactions on Power Delivery*, Vol. 9, No. 4, October 1994.

*A description of a model used to calculate GICs. The model is then used to compare GIC magnitudes while varying the direction of the magnetic field. The results serve to indicate a possible worst case scenario.*

16. Towle, J.N., Prabhakara, F.S., Ponder, J.Z., “Geomagnetic effects modelling for the PJM interconnection system; Part I – Earth surface potentials computation”, IEEE Transactions on Power Systems, Vol. 7, No. 3, August 1992.

*A description of the modelling of the Pennsylvania – New Jersey – Maryland (PJM) Interconnection to calculate GICs. This model is very complex since it consists of 11 different earth resistivity regions and a three dimensional ionospheric source.*

17. Prabhakara, F.S., et al., “Geomagnetic effects modelling for the PJM interconnection system; Part II – Geomagnetically induced current study results”, IEEE Transactions on Power Systems, Vol. 7, No. 2, May 1992<sup>1</sup>

*This paper follows on the Towle et al one describing a method to calculate GICs. This was done for different ionospheric sources and used to compare different mitigation methods.*

18. Rackliffe, G.B., et al., “Simulation of Geomagnetic currents induced in a power system by magnetohydrodynamic electromagnetic pulses”, IEEE Transactions on Power Delivery, Vol. 3, No. 1, pp 392-397, January 1988.

*The paper discusses the effect of a magnetohydrodynamic-electromagnetic pulse (MHD-EMP) on a power system. This is of importance since it will produce quasi-dc currents in a power system, similar to a geomagnetic storm.*

19. Kappenman, J.G., “Geomagnetic Storms and Impacts on Power Systems: Lessons Learned from Solar Cycle 22 and Outlook for Solar Cycle 23”, IEEE Power Engineering Review, May 1996

*This paper discusses the threat to power systems as well as the improvements in geomagnetic storm forecasting.*

20. Takasu, N., et al., “An experimental analysis if dc excitation of transformers by geomagnetically induced currents”, IEEE Transactions on Power Delivery, Vol. 9, No. 2, April 1994.

*The paper discusses the results of excitation tests done on various small-scale transformer models. This was done by analysing the excitation current.*

21. Lu, S., Liu, Y., “FEM analysis of dc saturation to assess transformer susceptibility to geomagnetically induced currents”, IEEE Transactions on Power Delivery, Vol. 8, No. 3, July 1993.

*The paper presents the result of a systematic finite element simulation of transformer susceptibility to GIC. It contributes to the understanding of transformer magnetisation due to GICs and the analysis is done on 5 different transformers.*

---

<sup>1</sup> although this is the second of the two papers it was published before part 1

22. Aspnes, J.D., Merritt, R.P., Akasofu, S.I., "Harmonic generation in transformers related to dc excitation and system loading", IEEE Transactions on Power Apparatus and Systems, Vol. PAS-100, No. 4, April 1981.

*A series of tests were run with small transformers to determine the harmonic generation from saturation.*

23. Aspnes, J.D., Akasofu, S.I., "Effect of Solar Induced Current on Autotransformer Tertiary Windings", IEEE Transactions on Power Apparatus and Systems, Vol. PAS-101, No. 3, March 1982.

*The discussion is on an Alaskan three-legged transformer and the reaction of the tertiary current to the neutral DC current. The protection of the transformer is also discussed.*

24. Douglas, D.A., "Current Transformer Accuracy with Asymmetric and High Frequency Fault Currents", IEEE Transactions on Power Apparatus and Systems, Vol. PAS-100, No. 3, pp 1006-1012, March 1981.

*Extensive discussion of CT modelling with some detail about saturation due to inrush which may be related to GIC.*

25. IEEE Communications Committee Working Group on Solar Effects, "Solar Effects on Communications", IEEE Transactions on Power Delivery, Vol. 7, No. 2, pp 460-467, April 1992.

*The paper considers the effect of geomagnetic storms on a different technology, communications. It also gives a good explanation of the cause of geomagnetic storms.*

26. Boteler, D.H., "Geomagnetically Induced Currents: Present Knowledge and Future Research", IEEE Transactions on Power Delivery, Vol. 9, No. 1, pp. 50-58, January 1994.

*The paper that provides a review of GICs in power systems. It then calculates the electric and magnetic field in a layered earth for Quebec during the March 1989, magnetic disturbance.*

27. Pirjola, R., "Induction in Power Transmission Lines During Geomagnetic Disturbances", Space Science Review, No. 35, pp 185-193, 1983.

*The paper elaborates about the calculation of the electric field. It also considers measurements of GICs at 4 different substations.*

28. Kappenman, J.G., Albertson, V.D., and Mohan, N., "Current Transformer and Relay Performance in the Presence of Geomagnetically-Induced Currents", IEEE Transactions on Power Apparatus and Systems, Vol. PAS-100, No. 3, pp. 1078-1088, March 1981.

*Extensive discussion of CT modelling and simulations including saturation characteristics.*

29. Albertson, V.D., "Electric and Magnetic Field at the Earth's Surface Due to Auroral Currents", IEEE Transactions on Power Apparatus and Systems, Vol. PAS-89, No. 4, pp. 578-584, April 1970.

*The paper considers the calculation of the electric and magnetic field at the surface of the earth.*

30. Kappenman, J.G., et al., "GIC Mitigation: A Neutral Blocking / Bypass Device to prevent the flow of GIC in Power Systems", IEEE Transactions on Power Delivery, Vol. 6, No. 3, pp. 1271-1281, July 1991.

*The paper discusses the possibility and performance of a capacitor in a transformer neutral as a blocking device for GIC.*

31. Boteler, D.H., Pirjola, R.J., Nevanlinna, H., "The Effects of Geomagnetic Disturbances on Electrical Systems at the Earth's Surface", Adv. Space Res., Vol. 22, No. 1, pp 17-27, 1998.

*The paper discusses the occurrence of geomagnetic storms, which is followed by an explanation of the susceptibility of a power system to the effects of such a storm.*

32. Mäkinen, T., "Geomagnetically Induced Currents in the Finnish Power Transmission System", Finnish Meteorological Institute, No. 32, p26, 1993.

*A very good paper on the prediction of GICs in the Finnish Power Grid based on measurements and theoretical models.*

33. Cigre, "Guide on EMC in Power Plants and Substations", Working Group 36.04, pp. 40-42, December 1997.

*A short general overview of GICs and their effects.*

34. Molinski, T.S., "Why Utilities Respect GICs", XXVIth General Assembly International Union of Radio Science, August 1999.

*A very good paper giving a general overview and covering almost all aspects of GICs.*

35. Technology Group Research Proposal, "Eskom/EPRI Sunburst 200 Collaboration: Geomagnetic Currents in Eskom's Southern Cape 400kV Network", Eskom, Report No TRR/CONS9/1998, 1998.

*The initial research proposal by Eskom used to approve the project. The proposal outlines the ultimate objectives of the research.*

36. Viljanen, A., Pirjola, R., "Statistics on Geomagnetically-Induced Currents in the Finnish 400kV Power System Based on Recordings of Geomagnetic Variations", Journal on Geomagnetism and Geoelectricity, Vol. 41, pp 411-420, 1989.

*A description of the Finnish system and the development of the earth surface potential.*

37. Girgis, R.S., Ko, C., "Calculation techniques and Results of GIC Currents as Applied to Two Large Power Transformers", IEEE Transactions on Power Delivery, Vol. 7, No.2, pp. 669–705, April 1992.

*A good description and analysis on the effect and mechanism of GICs inside transformers.*

38. Electric Research and Management, Inc., "SUNBURST GIC Network – Phase II Progress Report", Prepared for Electric Power Research Institute, February 1997.

*The report presents the progress of the Sunburst Network as well as technical discussions on the effect of GICs.*

39. Calabrò, S., Coppadoro, F., Crepaz, S., "The measurement of the magnetisation characteristics of large power transformers and reactors through D.C. excitation", IEEE Transactions on Power Delivery, Vol. 1, No.4, pp. 224–234, October 1986.

*The paper discusses the non-linear magnetisation characteristics through dc excitation of both transformers and reactors.*

40. Aspnès, J.D., Merritt R.P., Spell, B.D., "Instrumentation Systems to Measure geomagnetically Induced Current Effect" IEEE Transactions on Power Delivery, Vol. 2, No.4, pp. 1031 – 1036, April 1989.

*The paper describes an instrumentation system that was used to measure the effects of GIC to the Alaska intertie.*

41. Pirjola, R., "On Currents Induced in Power Transmission Systems During Geomagnetic Variations", IEEE Transactions on Power Apparatus and Systems, Vol. PAS-104, No. 10, pp. 2825-2831, October 1985.

*The discussion concerns the calculation of the horizontal electric field and earth surface potential linking it to the varying geomagnetic fields from the electrojet.*

42. Pirjola, R., "Modelling the electric and magnetic fields at the Earth's surface due to an auroral electrojet", Journal of Atmospheric and Solar-Terrestrial Physics, No. 60, pp 1139-1148, 1998.

*The paper compares two models to calculate the electric and magnetic fields from the electrojet. The one model concerns the electrojet to be of infinite length and for the other model it has a finite length.*

43. Petschek, H., Feero, W., "Electric Power and Space Weather", Geomagnetic Applications Bulletin, pp 5 & 7, January 1997.

*A short article that serves to inform the reader of GICs, its effects and preventative steps.*

44. Appell, D., "Fire in the Sky", New Scientist, pp 29-32, 27 February 1999.

*A scientific report informing the reader of the source of GICs, its effects and modelling of the currents and electrojets.*



# Appendix B

## TRIP TO UNITED STATES AND SCANDINAVIA BY JACKO KOEN

27 September 1999 to 19 October 1999

---

### 1 Introduction

The purpose of the visit was to hold technical discussions and undertake work with various researchers and Power Company Authorities on Geomagnetically Induced Currents (GICs) in power systems. The phenomenon and its possible effects on the Eskom MTS is not well understood and it was necessary to visit other researchers and utilities to strengthen the research being done by Eskom.

### 2 Itinerary

Date	Location	Reason
Travel to Washington DC from Cape Town		
29/09/99	Washington DC, USA	Attend Sunburst 2000 annual meeting
30/09/99	Washington DC, USA	Attend Sunburst 2000 annual meeting
Travel to Pittsburgh from Washington DC		
4/10/99	Pittsburgh, USA	Attend Sunburst Workshop
5/10/99	Pittsburgh, USA	Attend Sunburst Workshop
Travel back to Washington DC and from there to Helsinki		
11/10/99	Helsinki, Finland	Visit Finnish Meteorological Institute
12/10/99	Helsinki, Finland	Visit Finnish Meteorological Institute
13/10/99	Helsinki, Finland	Visit Finnish Meteorological Institute
14/10/99	Helsinki, Finland	Visit Fingrid Company
15/10/99	Helsinki, Finland	Visit Finnish Meteorological Institute
Travel to Stockholm from Helsinki		
18/10/99	Stockholm, Sweden	Visit to Swedish National Grid
Travel from Stockholm to Helsinki and from there back to Cape Town		

### **3 United States.**

#### **3.1 Washington D.C.: Attending the Sunburst 2000 Annual Meeting**

The purpose of this trip was as follows :

To attend the EPRI Sunburst 2000 Review Meeting in Washington, DC. As part of the approved TRI research project it was anticipated to take part in the EPRI Sunburst 2000 survey of GICs in large transmission systems world-wide. Since this participation is currently being reassessed, it served to investigate the technical and financial benefits of the proposed collaboration.

A major part of the meeting was a presentation and discussion of the SUNBURST-2000 project including progress made as well as a practical demonstration to illustrate the effectiveness of the hardware and software.

Some presentations at the meeting included:

- Strategy for Managing the Impact of GIC on the NGC Transmission System – Arslan Erinmez, NGC
- SpaceCast / PowerCast (a proposed mitigation technique by a warning in advance of a storm) – John Kappenman, Metatech
- Fingrid Transformer Test Plans and Update on the Complex Image Method – Risto Pirjola, Finnish Meteorological Institute (FMI)
- Space Weather Predictions / Forecasting – Brian Anderson and Dimitris Vassiliadis, NASA

#### **3.2 Pittsburgh: Attending the Sunburst 2000 Workshop**

The 2 day workshop served as an introduction to the Sunburst-2000 hardware and software. The workshop was presented by George Batrus of Electric Research. This company supplies and calibrates all the equipment needed to effectively measure GICs and its effects. Attending the workshop was successful from a financial perspective since the installation of the measuring equipment can now be done by the author, saving the costs of it being done by Electric Research.

#### **3.3 Summary of visit to the USA**

The trip was very successful in giving an insight into the progress and to receive up to date information as preparation for the occurrence of GICs. I found it surprising that many utilities who are very familiar with the effects of GICs are unprepared and ignoring the problem. I can only attribute this attitude to the fact that GICs occur mainly in 11 year cycles, causing a false comfort.

Although participating in the Sunburst 2000 program is quite costly this amount is minute compared to the possible financial implications due to GICs. Through participation one can accurately assess possible perturbations and then decide whether it is feasible to continue.

## **4 Scandinavia**

### **4.1 Finland**

#### **4.1.1 Helsinki: Visit to the Finnish Meteorological Institute (FMI)**

The purpose of this visit was to develop and test geomagnetic and engineering models of the Eskom grid. The author met with Prof. Risto Pirjola and Dr Ari Viljanen of the FMI. The FMI has been carrying out research of GICs, including their effects on power network equipment as well as measurements in transformer neutrals for more than 20 years. The FMI has also been participating in the EPRI SUNBURST project since 1994.

Geological, geomagnetic and engineering data from South Africa was discussed. It was decided to use the plane wave method assuming a homogenous earth to model the geoelectric field. A method to model autotransformers in the engineering step was also discussed. Two software programs for the geomagnetic and engineering models, based on the FMI models, were developed by the author and will be used for the Eskom grid.

#### **4.1.2 Helsinki: Visit to the Fingrid Power Company**

The author met with Mr Jarmo Elovaara of the Fingrid company. The company is responsible for the Finnish Transmission Lines. Their small personnel of 270 are responsible to manage the grid comprising of 100 substations and 14'000 km of transmission lines. They have experienced large GICs in their power network equipment and work closely with the FMI. One of their current projects is to assess the performance of a 3 phase, 5 limb transformer in the presence of GICs by injecting dc current into the neutral.

Although the company has measured very large GICs in the transformer neutrals they have not had severe incidents due to GICs. It has not caused any power system disturbances nor any equipment failure. However, there is clear evidence of transformer saturation due to GICs because of the increase in harmonic content in line currents as well as irregular fluctuations of reactive power. They believe that the excellent behaviour of the system during a geomagnetic storm is due to their transformer design where a lot of emphasis is put on the prevention of leakage flux. Another contributing factor is that almost all their transformers are used at less than 50% of rated load. They have identified the "hot spots" on their network and measurements are done at these sites on a full time basis to maintain the integrity of the network.

## **4.2 Sweden**

### **4.2.1 Stockholm: Visit to the Svenska Kraftnät**

The author met with Mr Bertil Kielen and Mr Lars Wallin of the Swedish National Grid. The company, who employs a staff of 235 people, is responsible for the transmission grid in Sweden. They have in the past experienced relay trips due to GICs; most of this is blamed on the old electromechanical overcurrent relays used at that time. These relays did not have any stabilisation against the 100Hz harmonic. Another factor which decreased the networks susceptibility to GICs is that they use series capacitors in most of their longer lines, effectively blocking the quasi-dc GICs.

At this time only one site is being monitored. It is a generator step-up transformer at a nuclear power station. Through past events it seems that this site experience the highest magnitude of GICs. When the measured value at this site exceeds a certain threshold it will set an alarm at the Swedish National Control to make the operators aware of a possible problem. They will then be conscious of a possible problem (such as increase in MVAR demand, voltage or frequency swing, etc.) and if required disconnect the transformer. This system has been in operation following the previous cycle and to date such an action has not been necessary, taking in mind that this was during a solar minimum period.

## **4.3 Summary of visit to Scandinavia**

The visit to the FMI was very successful in understanding the modelling of a power grid and to calculate the flow of GICs. Other benefits were the exposure to their established experience and guidance concerning the measurement of currents and the effect of the currents on the high voltage equipment.

The researchers at the FMI have been very helpful since the start of this project. Once again they went through a lot of trouble to help and give guidance. The visit to the FMI has helped to understand and apply some of the essential steps to complete both the engineering and geophysical step.

The Fingrid company is very aware of GICs and have measured them for more than 20 years. However, they have not incorporated any mitigation techniques to date since they have not experienced any major disturbances such as the blackout in Canada during March 1989. They do not anticipate any problems due to overheating of transformers but are aware that the saturation of more than one transformer could cause the reactive power demand to cause problems.

The Swedish National Grid does not seem to be too concerned with GICs. Apart from the measurements at a selected site they do not have any other formal mitigation techniques. They are satisfied through past experience that it is only necessary to monitor GICs at a selected site and react if necessary.

# Appendix C

## Data of Geomagnetic Activity (K-index) for Period 1/01/89 – 31/12/92

Major to severe storms (i.e.  $K \geq 6$ ) are indicated in bold

Year	Date		K-index	
1989	1	January	3122	2132
	2	January	1122	2221
	3	January	22	1122
	4	January	1033	2234
	5	January	4443	4552
	6	January	2223	1123
	7	January	4233	2321
	8	January	1133	3333
	9	January	2222	4333
	10	January	2231	3321
	11	January	1121	<b>4666</b>
	12	January	4322	2121
	13	January	2	4433
	14	January	3311	2234
	15	January	3434	4455
	16	January	3334	3535
	17	January	3334	5342
	18	January	4233	3211
	19	January	2120	122
	20	January	2134	<b>7754</b>
	21	January	3233	3444
	22	January	4333	4323
	23	January	2243	4323
	24	January	1122	2332
	25	January	1023	3232
	26	January	2223	2211
	27	January	2123	3211
	28	January	1212	2232
	29	January	2122	3321
	30	January	1212	2222
	31	January	2122	<b>2366</b>
	1	February	4324	4235
	2	February	4320	3344
	3	February	4534	4454
	4	February	4322	4244
	5	February	3223	2334
	6	February	3232	3332
	7	February	3224	3233
	8	February	3222	2223
	9	February	3322	3233
	10	February	3212	2010
	11	February	1023	2342
	12	February	2112	2343
	13	February	3344	3442
	14	February	2232	3310
	15	February	1111	1244

	16	February	4423	3123
	17	February	2222	2011
	18	February	1210	3431
	19	February	122	2323
	20	February	2343	3331
	21	February	2133	2311
	22	February	1133	2222
	23	February	1122	2
	24	February	2223	2111
	25	February	22	1011
	26	February	1011	1001
	27	February	1112	2201
	28	February	233	3334
	1	March	3223	3222
	2	March	3534	4232
	3	March	2344	3442
	4	March	3113	3300
	5	March	3345	4333
	6	March	3234	<b>6533</b>
	7	March	3323	2212
	8	March	2110	<b>465</b>
	9	March	4422	3334
	10	March	3332	2222
	11	March	2233	2234
	12	March	4223	4543
	13	March	<b>5679</b>	<b>7889</b>
	14	March	<b>9765</b>	<b>3466</b>
	15	March	<b>6443</b>	3332
	16	March	1445	5343
	17	March	4343	3322
	18	March	222	3301
	19	March	<b>1264</b>	5333
	20	March	1322	3323
	21	March	4243	2133
	22	March	3233	4555
	23	March	3224	3434
	24	March	4332	1101
	25	March	1122	233
	26	March	2213	3224
	27	March	3253	<b>5634</b>
	28	March	<b>5336</b>	5434
	29	March	5444	<b>4366</b>
	30	March	4553	2244
	31	March	4543	4444
	1	April	5333	3454
	2	April	3333	3422

	3	April	4323	2234
	4	April	4345	5445
	5	April	5334	3354
	6	April	4322	2232
	7	April	1143	4334
	8	April	4323	3432
	9	April	4223	2342
	10	April	3011	2132
	11	April	1222	4432
	12	April	2121	1112
	13	April	1243	2223
	14	April	3132	2455
	15	April	4533	2221
	16	April	1120	3354
	17	April	4012	1211
	18	April	3313	1000
	19	April	1022	2211
	20	April	2222	1222
	21	April	2232	2210
	22	April	3101	2112
	23	April	2122	2442
	24	April	3103	3213
	25	April	2234	3555
	26	April	5554	4454
	27	April	<b>6544</b>	2444
	28	April	4333	3344
	29	April	2344	3344
	30	April	3232	2232
	1	May	3112	1223
	2	May	3333	2243
	3	May	3222	2123
	4	May	4321	2334
	5	May	5544	1143
	6	May	2323	1133
	7	May	444	4345
	8	May	2011	13
	9	May	1010	2100
	10	May	1000	2
	11	May	11	122
	12	May	2232	1221
	13	May	113	4310
	14	May	1322	1211
	15	May	1132	1232
	16	May	1222	1211
	17	May	1222	1111
	18	May	1222	2210
	19	May	12	1211
	20	May	1015	4220
	21	May	1122	2111
	22	May	2122	3223
	23	May	2212	<b>5646</b>
	24	May	5454	5544
	25	May	4232	2233
	26	May	2113	3334

	27	May	3333	2233
	28	May	2312	3332
	29	May	4233	3322
	30	May	3221	1022
	31	May	3122	2123
	1	June	3212	2122
	2	June	1123	4133
	3	June	3311	3323
	4	June	4401	1001
	5	June	1021	112
	6	June	2222	2104
	7	June	5445	4023
	8	June	3222	2044
	9	June	5423	2255
	10	June	4444	4544
	11	June	4333	2222
	12	June	3232	2110
	13	June	1022	1333
	14	June	2345	4344
	15	June	5443	3433
	16	June	3322	1000
	17	June	2	111
	18	June	1	1110
	19	June	22	1122
	20	June	2223	3343
	21	June	11	1
	22	June	10	1011
	23	June	1012	1111
	24	June	1123	3102
	25	June	1212	1101
	26	June	22	2222
	27	June	2101	1002
	28	June	2112	1101
	29	June	3322	1222
	30	June	3322	11
	1	July	1032	<b>1643</b>
	2	July	3120	0
	3	July	11	0
	4	July	11	1000
	5	July	1002	1233
	6	July	2212	2221
	7	July	1121	1010
	8	July	10	0
	9	July	2100	1011
	10	July	1223	1223
	11	July	1001	0
	12	July	1	1
	13	July	30	110
	14	July	0	121
	15	July	12	1110
	16	July	0	0
	17	July	3232	2331
	18	July	3322	1222

	19	July	1100	0
	20	July	12	102
	21	July	1112	1
	22	July	1001	2002
	23	July	1312	3311
	24	July	2013	2211
	25	July	1132	2103
	26	July	1122	2222
	27	July	2221	213
	28	July	2112	1123
	29	July	3123	1223
	30	July	1021	112
	31	July	1011	1001
	1	August	1010	1112
	2	August	3110	1
	3	August	2222	1000
	4	August	12	2122
	5	August	1000	1
	6	August	1001	1222
	7	August	1122	3222
	8	August	2222	12
	9	August	2012	1143
	10	August	3355	3344
	11	August	4424	3312
	12	August	3122	3102
	13	August	3321	2111
	14	August	<b>3366</b>	5335
	15	August	5543	<b>5336</b>
	16	August	5522	2123
	17	August	3222	3544
	18	August	5444	3343
	19	August	3411	1120
	20	August	1244	5411
	21	August	2111	2445
	22	August	4332	11
	23	August	2323	4544
	24	August	3021	1001
	25	August	11	1212
	26	August	122	0
	27	August	2433	<b>4364</b>
	28	August	2012	1245
	29	August	<b>6642</b>	3331
	30	August	2323	3333
	31	August	2010	1222
	1	September	2220	1000
	2	September	2222	1210
	3	September	1321	2012
	4	September	5444	2003
	5	September	3353	1021
	6	September	2222	2321
	7	September	2023	3533
	8	September	4432	1212
	9	September	2113	3233

	10	September	2222	2321
	11	September	2	2
	12	September	2233	2101
	13	September	1122	2223
	14	September	1123	2000
	15	September	3423	<b>4466</b>
	16	September	4331	2222
	17	September	2010	1023
	18	September	3234	<b>3466</b>
	19	September	<b>5653</b>	3230
	20	September	101	1111
	21	September	2221	1001
	22	September	245	4333
	23	September	2010	102
	24	September	22	2122
	25	September	1100	1111
	26	September	135	<b>4666</b>
	27	September	3022	2000
	28	September	2100	1222
	29	September	2112	1322
	30	September	2202	1354
	1	October	2222	2212
	2	October	1433	3210
	3	October	1134	3432
	4	October	2111	1122
	5	October	2101	1111
	6	October	1034	2213
	7	October	3222	2222
	8	October	2223	1003
	9	October	3322	2113
	10	October	3322	2311
	11	October	2233	2211
	12	October	1233	2112
	13	October	1100	0
	14	October	0	1000
	15	October	201	2130
	16	October	1123	3121
	17	October	2223	1021
	18	October	4324	3333
	19	October	5444	4120
	20	October	2335	<b>7775</b>
	21	October	<b>4567</b>	<b>6566</b>
	22	October	4423	3444
	23	October	3431	2343
	24	October	2243	2333
	25	October	3332	1102
	26	October	2322	4454
	27	October	4234	3232
	28	October	1122	1432
	29	October	1222	2234
	30	October	3233	2233
	31	October	3222	4131
	1	November	1112	1223

	2	November	4332	2343
	3	November	4244	4232
	4	November	2134	4335
	5	November	5233	1144
	6	November	2112	3231
	7	November	3334	5223
	8	November	2224	3430
	9	November	4444	3541
	10	November	2343	2322
	11	November	4344	4354
	12	November	3332	2123
	13	November	3444	4554
	14	November	3333	2223
	15	November	2032	2211
	16	November	1012	3221
	17	November	2337	<b>6767</b>
	18	November	<b>6443</b>	2122
	19	November	33	343
	20	November	1113	2232
	21	November	3144	3101
	22	November	111	2321
	23	November	3101	11
	24	November	231	1112
	25	November	2300	0
	26	November	1024	1333
	27	November	2222	3334
	28	November	4443	4435
	29	November	4334	3343
	30	November	3212	4244
	1	December	4323	<b>4565</b>
	2	December	4434	1223
	3	December	4335	3333
	4	December	4433	3335
	5	December	4210	121
	6	December	2100	2111
	7	December	2222	233
	8	December	1122	2012
	9	December	1112	1020
	10	December	10	10
	11	December	122	3211
	12	December	1121	2113
	13	December	2223	2120
	14	December	13	4332
	15	December	2123	2222
	16	December	1124	3323
	17	December	2224	3211
	18	December	1033	2133
	19	December	3212	3021
	20	December	1222	2222
	21	December	3222	2221
	22	December	3344	<b>5463</b>
	23	December	3434	3222
	24	December	2223	3443
	25	December	3232	2234

	26	December	2133	3354
	27	December	3323	4433
	28	December	3322	2213
	29	December	2244	4555
	30	December	4232	2334
	31	December	4334	3434



Year	Date		K-index	
1990	2	January	4124	3224
	3	January	3222	1331
	4	January	2013	2223
	5	January	3122	2343
	6	January	2111	2111
	7	January	2121	1001
	8	January	1112	4543
	9	January	3232	3212
	10	January	3233	2333
	11	January	2234	4343
	12	January	3224	3232
	13	January	2123	2101
	14	January	12	3211
	15	January	1111	2310
	16	January	1133	1233
	17	January	2221	1212
	18	January	2013	3112
	19	January	1001	1022
	20	January	3243	3332
	21	January	3334	4342
	22	January	3324	3233
	23	January	3423	3333
	24	January	3443	3344
	25	January	4333	2211
	26	January	2123	2330
	27	January	1110	210
	28	January	22	3334
	29	January	4342	4233
	30	January	4432	4443
	31	January	3333	3331
	1	February	2123	4453
	2	February	3333	4443
	3	February	2102	1332
	4	February	3323	<b>3663</b>
	5	February	3333	2331
	6	February	2221	1111
	7	February	223	3445
	8	February	2220	10
	9	February	22	3211
	10	February	1032	3211
	11	February	1232	3222
	12	February	3123	1000
	13	February	102	1313
	14	February	4445	3211
	15	February	2244	<b>4456</b>
	16	February	5533	2334
	17	February	5323	3334
	18	February	3234	3334
	19	February	4334	4445
	20	February	4443	5354
	21	February	2323	2232
	22	February	2223	3354
	23	February	3334	5434

	24	February	4223	3334
	25	February	3334	3343
	26	February	3223	2033
	27	February	4335	3232
	28	February	3433	4242
	1	March	4323	3334
	2	March	2233	2233
	3	March	2222	3232
	4	March	22	1012
	5	March	3212	1103
	6	March	4443	3211
	7	March	2223	3202
	8	March	2113	3211
	9	March	2124	2112
	10	March	1122	3121
	11	March	3233	2321
	12	March	2233	<b>3566</b>
	13	March	<b>6423</b>	2234
	14	March	5335	3321
	15	March	3112	1133
	16	March	3122	1022
	17	March	1021	0
	18	March	1134	4455
	19	March	5212	1112
	20	March	3223	<b>3336</b>
	21	March	<b>6345</b>	4453
	22	March	4233	3344
	23	March	3333	3343
	24	March	3323	3244
	25	March	3334	4344
	26	March	5333	3443
	27	March	4443	2355
	28	March	3323	3233
	29	March	3313	3325
	30	March	<b>3365</b>	4322
	31	March	2111	1012
	1	April	2000	1022
	2	April	223	3222
	3	April	1223	4333
	4	April	3123	3220
	5	April	23	4220
	6	April	123	2112
	7	April	1133	2211
	8	April	2102	2111
	9	April	1145	4432
	10	April	<b>3346</b>	<b>7675</b>
	11	April	5433	3442
	12	April	<b>3664</b>	5554
	13	April	5343	3444
	14	April	4444	3334
	15	April	3432	3231
	16	April	2121	2022
	17	April	4245	5344

	18	April	4433	3213
	19	April	2121	1233
	20	April	2123	2244
	21	April	4432	1001
	22	April	2332	1324
	23	April	3444	3433
	24	April	2243	3223
	25	April	3333	2223
	26	April	3421	1101
	27	April	2432	1224
	28	April	3233	3243
	29	April	3344	2234
	30	April	<b>6323</b>	1113
	1	May	2212	2120
	2	May	124	2112
	3	May	2214	3233
	4	May	3123	3322
	5	May	2123	1130
	6	May	121	1011
	7	May	1021	1200
	8	May	1222	2213
	9	May	2233	3134
	10	May	3444	3342
	11	May	4333	3223
	12	May	4101	1
	13	May	112	3322
	14	May	110	10
	15	May	1002	3010
	16	May	10	1000
	17	May	112	0
	18	May	2143	4434
	19	May	4422	4324
	20	May	2323	3343
	21	May	3203	4433
	22	May	3344	4333
	23	May	3122	212
	24	May	0	101
	25	May	3223	3323
	26	May	4313	<b>4346</b>
	27	May	3554	3422
	28	May	112	1211
	29	May	1022	2214
	30	May	3324	3243
	31	May	3212	1132
	1	June	1212	2121
	2	June	1011	1100
	3	June	1111	1011
	4	June	101	0
	5	June	1	1011
	6	June	2222	1223
	7	June	3333	2122
	8	June	2423	134
	9	June	3353	4322

	10	June	4222	3214
	11	June	3212	2123
	12	June	4335	<b>3566</b>
	13	June	<b>6554</b>	5432
	14	June	4535	<b>6433</b>
	15	June	2322	1113
	16	June	3000	0
	17	June	10	0
	18	June	23	2333
	19	June	2210	1000
	20	June	0	1
	21	June	1	21
	22	June	2210	1
	23	June	1011	1200
	24	June	12	1111
	25	June	1122	2011
	26	June	1112	1101
	27	June	1022	2113
	28	June	2122	1100
	29	June	121	2110
	30	June	1000	1
	1	July	1000	13
	2	July	3310	0
	3	July	1211	1000
	4	July	1022	322
	5	July	1202	1122
	6	July	1001	21
	7	July	10	13
	8	July	312	1213
	9	July	2111	2100
	10	July	323	3111
	11	July	120	1030
	12	July	1132	1003
	13	July	2333	123
	14	July	2021	2232
	15	July	2321	120
	16	July	3100	1021
	17	July	100	3
	18	July	2020	1120
	19	July	1223	3223
	20	July	2233	2222
	21	July	2010	21
	22	July	1110	1001
	23	July	1100	11
	24	July	102	0
	25	July	1012	1000
	26	July	11	1132
	27	July	1222	1021
	28	July	<b>2456</b>	<b>6566</b>
	29	July	5544	4324
	30	July	2222	123
	31	July	3021	0
	1	August	32	4343

	2	August	3221	2
	3	August	2122	2033
	4	August	3120	2010
	5	August	1001	1102
	6	August	2112	1232
	7	August	1112	1102
	8	August	1220	0
	9	August	2001	100
	10	August	111	111
	11	August	3132	2001
	12	August	2212	2
	13	August	2323	2221
	14	August	2244	2223
	15	August	2114	3334
	16	August	3244	3324
	17	August	4331	1332
	18	August	2322	2202
	19	August	4321	3113
	20	August	2432	2230
	21	August	2123	3354
	22	August	3443	3324
	23	August	4333	4543
	24	August	3443	3200
	25	August	1010	122
	26	August	2355	5433
	27	August	4332	4221
	28	August	2122	2100
	29	August	1123	2142
	30	August	3223	4433
	31	August	4223	2111
	1	September	2314	4431
	2	September	1	0
	3	September	11	10
	4	September	1012	1323
	5	September	4222	2112
	6	September	3143	2221
	7	September	3233	3211
	8	September	1122	133
	9	September	1212	1123
	10	September	3120	123
	11	September	2244	3345
	12	September	3333	2143
	13	September	4133	3323
	14	September	4334	3332
	15	September	3334	4331
	16	September	4345	4212
	17	September	2232	1123
	18	September	123	2243
	19	September	4223	1423
	20	September	4101	1345
	21	September	3123	2223
	22	September	3332	2233
	23	September	3333	1221
	24	September	1232	2222

	25	September	4322	43
	26	September	2123	2221
	27	September	3211	2111
	28	September	2212	2112
	29	September	2112	2012
	30	September	2101	1011
	1	October	1111	1
	2	October	1011	2221
	3	October	2222	2223
	4	October	1233	3332
	5	October	2233	3212
	6	October	2233	2222
	7	October	1122	2233
	8	October	11	2111
	9	October	1012	4543
	10	October	<b>5464</b>	4222
	11	October	5254	5345
	12	October	3433	2333
	13	October	3222	2233
	14	October	3232	2334
	15	October	3323	3343
	16	October	2122	1233
	17	October	1111	1001
	18	October	1	1121
	19	October	3223	1123
	20	October	1233	5534
	21	October	3232	2010
	22	October	3332	2111
	23	October	1122	2233
	24	October	4434	4131
	25	October	3212	2112
	26	October	2014	3432
	27	October	1202	1111
	28	October	1132	0
	29	October	103	3243
	30	October	5222	2233
	31	October	1232	3453
	1	November	1222	1213
	2	November	2321	1123
	3	November	1213	2111
	4	November	1011	0
	5	November	0	1
	6	November	113	11
	7	November	22	2221
	8	November	22	2222
	9	November	2232	2112
	10	November	2123	2122
	11	November	1133	3121
	12	November	2302	1112
	13	November	1121	110
	14	November	1	1000
	15	November	1012	121
	16	November	3132	3333

	17	November	1233	3432
	18	November	4302	3332
	19	November	3322	1212
	20	November	2212	2122
	21	November	2212	3121
	22	November	21	1020
	23	November	111	1101
	24	November	1000	1000
	25	November	1022	1111
	26	November	2132	3004
	27	November	4234	<b>5653</b>
	28	November	3322	2241
	29	November	1111	121
	30	November	1012	2421
	1	December	1100	1001
	2	December	112	2221
	3	December	11	1233
	4	December	3322	3323
	5	December	2122	2331
	6	December	1122	2111
	7	December	1111	1210
	8	December	12	3432
	9	December	2222	2220
	10	December	23	10
	11	December	11	200
	12	December	11	1233
	13	December	3334	2121
	14	December	2121	2110
	15	December	111	1111
	16	December	1012	2222
	17	December	2322	1120
	18	December	2002	1100
	19	December	10	1000
	20	December	1001	2231
	21	December	1	1111
	22	December	113	3003
	23	December	43	1213
	24	December	2233	3333
	25	December	2323	3221
	26	December	1022	2000
	27	December	2311	2110
	28	December	1211	1111
	29	December	1100	110
	30	December	1334	3332
	31	December	1113	3322

Year	Date		K-index	
1991	1	January	3112	1001
	2	January	1121	1011
	3	January	1212	3112
	4	January	2220	12
	5	January	2212	3121
	6	January	1112	1000
	7	January	1000	1
	8	January	2122	3221
	9	January	112	1022
	10	January	2122	2213
	11	January	22	2221
	12	January	4253	2422
	13	January	2211	2130
	14	January	1111	0
	15	January	2122	3133
	16	January	1022	3112
	17	January	2114	3322
	18	January	1221	2323
	19	January	101	10
	20	January	2	110
	21	January	111	2
	22	January	2211	1011
	23	January	122	1023
	24	January	3234	3443
	25	January	3333	3443
	26	January	2333	3113
	27	January	23	3223
	28	January	122	3111
	29	January	1112	1211
	30	January	100	1322
	31	January	3244	2333
	1	February	3233	2355
	2	February	5321	1001
	3	February	111	1101
	4	February	1	1013
	5	February	2132	2232
	6	February	122	1021
	7	February	1212	2223
	8	February	2223	2322
	9	February	4113	2443
	10	February	3112	1111
	11	February	3222	1323
	12	February	4333	3212
	13	February	2204	3222
	14	February	1102	2323
	15	February	3012	2022
	16	February	10	0
	17	February	10	1000
	18	February	11	11
	19	February	2	4420
	20	February	1011	1243
	21	February	2223	1210
	22	February	1334	3222

	23	February	2233	3432
	24	February	1210	21
	25	February	1123	2221
	26	February	1133	2201
	27	February	23	2122
	28	February	3233	3223
	1	March	3233	2134
	2	March	2223	2122
	3	March	2021	22
	4	March	1001	1332
	5	March	3244	3423
	6	March	2243	3354
	7	March	3323	3444
	8	March	3234	3324
	9	March	4434	4325
	10	March	4422	3010
	11	March	12	2001
	12	March	2233	3234
	13	March	<b>6443</b>	2310
	14	March	1033	1000
	15	March	1013	3100
	16	March	1	352
	17	March	2224	2133
	18	March	3333	0
	19	March	112	2333
	20	March	3333	2121
	21	March	1144	5432
	22	March	2343	3224
	23	March	4323	3211
	24	March	<b>2866</b>	<b>5378</b>
	25	March	<b>6643</b>	4555
	26	March	<b>6555</b>	<b>7443</b>
	27	March	4543	3444
	28	March	4323	2331
	29	March	121	102
	30	March	1332	3334
	31	March	3222	12
	1	April	4444	4334
	2	April	4334	2334
	3	April	4354	3344
	4	April	<b>3236</b>	<b>6443</b>
	5	April	3232	2111
	6	April	3323	1332
	7	April	2323	2122
	8	April	2011	1022
	9	April	3222	1232
	10	April	1122	2101
	11	April	1012	1110
	12	April	1233	3211
	13	April	122	1110
	14	April	1123	2121
	15	April	1023	2100
	16	April	2	1221

	17	April	1223	3331
	18	April	1134	2132
	19	April	1344	1011
	20	April	11	1000
	21	April	1113	2111
	22	April	1023	2110
	23	April	3	2322
	24	April	2122	2034
	25	April	4334	2012
	26	April	3331	1113
	27	April	3433	3234
	28	April	4443	4344
	29	April	<b>6444</b>	4454
	30	April	4433	3232
	1	May	4233	4434
	2	May	4443	4433
	3	May	2323	2123
	4	May	3110	1112
	5	May	2110	110
	6	May	110	1003
	7	May	1133	1000
	8	May	2033	1220
	9	May	2122	2233
	10	May	1133	2202
	11	May	1012	100
	12	May	2	20
	13	May	135	3343
	14	May	245	3433
	15	May	1232	2000
	16	May	1001	2143
	17	May	4343	3310
	18	May	0	0
	19	May	1101	11
	20	May	11	1000
	21	May	2	3210
	22	May	3233	2122
	23	May	3334	4323
	24	May	3233	4344
	25	May	4423	2433
	26	May	2243	3444
	27	May	4334	4234
	28	May	4333	3344
	29	May	4333	3143
	30	May	3133	2323
	31	May	2134	5432
	1	June	3355	5513
	2	June	4333	<b>3546</b>
	3	June	1031	144
	4	June	1023	<b>5655</b>
	5	June	<b>5767</b>	<b>5766</b>
	6	June	5554	2104
	7	June	2244	2233
	8	June	2222	3452

	9	June	<b>6334</b>	3553
	10	June	<b>4356</b>	<b>5456</b>
	11	June	<b>6544</b>	4344
	12	June	4324	4444
	13	June	<b>6566</b>	<b>6574</b>
	14	June	4321	1000
	15	June	1243	2310
	16	June	1	1
	17	June	2214	<b>5566</b>
	18	June	3432	1243
	19	June	3444	3434
	20	June	4323	1132
	21	June	5233	2333
	22	June	3322	2223
	23	June	3335	4345
	24	June	5433	3233
	25	June	4324	2234
	26	June	4223	3333
	27	June	3112	113
	28	June	2321	11
	29	June	0	1011
	30	June	3323	2445
	1	July	3320	2232
	2	July	133	3234
	3	July	3234	3233
	4	July	4222	2211
	5	July	11	1100
	6	July	1012	1222
	7	July	1200	1123
	8	July	3233	<b>3565</b>
	9	July	<b>2376</b>	5555
	10	July	4323	3110
	11	July	3234	3212
	12	July	2235	3332
	13	July	<b>4456</b>	<b>5755</b>
	14	July	5555	4333
	15	July	3322	1011
	16	July	2222	333
	17	July	4443	3334
	18	July	3212	2244
	19	July	4434	4354
	20	July	3443	3333
	21	July	3433	3234
	22	July	3333	3224
	23	July	4222	3330
	24	July	1012	212
	25	July	1122	2221
	26	July	100	1
	27	July	1001	123
	28	July	1220	2
	29	July	1120	2
	30	July	2231	1020
	31	July	1020	2002

	1	August	3222	2544
	2	August	4354	4424
	3	August	4233	3434
	4	August	4443	2343
	5	August	3433	3234
	6	August	5334	3222
	7	August	2442	1103
	8	August	3222	2102
	9	August	2322	3222
	10	August	1131	1201
	11	August	4334	3311
	12	August	3334	5455
	13	August	4122	1011
	14	August	21	1435
	15	August	3544	3334
	16	August	4432	2223
	17	August	2333	3233
	18	August	3222	2254
	19	August	<b>4375</b>	4322
	20	August	<b>2157</b>	<b>6344</b>
	21	August	5455	3222
	22	August	4544	2223
	23	August	3323	1011
	24	August	3220	2122
	25	August	2223	1012
	26	August	1223	2121
	27	August	3321	1554
	28	August	3221	2233
	29	August	123	2323
	30	August	1223	4354
	31	August	2254	3334
	1	September	5422	3355
	2	September	3343	3212
	3	September	322	1224
	4	September	2232	2213
	5	September	3332	2232
	6	September	2312	2323
	7	September	3222	2111
	8	September	2222	3453
	9	September	3334	<b>4346</b>
	10	September	5543	3334
	11	September	4224	3232
	12	September	2233	1212
	13	September	2122	1133
	14	September	4334	4433
	15	September	3221	1122
	16	September	1122	1022
	17	September	2110	1001
	18	September	111	1012
	19	September	3213	3113
	20	September	1311	1
	21	September	2002	1001
	22	September	1012	2201
	23	September	1001	1

	24	September	2112	1122
	25	September	2323	4555
	26	September	4443	3443
	27	September	4434	5543
	28	September	4434	3344
	29	September	3222	3434
	30	September	2333	3343
	1	October	3232	<b>3266</b>
	2	October	5434	4432
	3	October	2333	2133
	4	October	2332	4254
	5	October	5233	2321
	6	October	2113	3534
	7	October	4433	4232
	8	October	3243	<b>3463</b>
	9	October	3423	2212
	10	October	3333	3332
	11	October	2223	1222
	12	October	2112	12
	13	October	1112	2011
	14	October	2111	2132
	15	October	2221	1121
	16	October	2211	1111
	17	October	1122	4222
	18	October	4323	3322
	19	October	2223	2223
	20	October	3235	4332
	21	October	2213	3243
	22	October	3334	3332
	23	October	2232	1335
	24	October	4343	4333
	25	October	5333	4335
	26	October	3243	3334
	27	October	5534	3444
	28	October	<b>3446</b>	<b>6844</b>
	29	October	<b>5664</b>	<b>4664</b>
	30	October	2123	4544
	31	October	4255	<b>3446</b>
	1	November	<b>5346</b>	<b>6776</b>
	2	November	<b>6541</b>	2333
	3	November	2224	3233
	4	November	2334	2355
	5	November	5333	3332
	6	November	2332	2323
	7	November	3322	1222
	8	November	2255	<b>7679</b>
	9	November	<b>7667</b>	5544
	10	November	3244	4333
	11	November	3223	3455
	12	November	3231	12
	13	November	1123	4423
	14	November	4322	4224
	15	November	3234	4434

	16	November	4234	3333
	17	November	3334	3332
	18	November	3333	3343
	19	November	5344	<b>4654</b>
	20	November	1232	2444
	21	November	2344	<b>4756</b>
	22	November	4435	5223
	23	November	3344	3333
	24	November	2221	2332
	25	November	1231	1322
	26	November	1312	2210
	27	November	1011	222
	28	November	1012	2234
	29	November	3311	3223
	30	November	2222	2224
	1	December	2222	2223
	2	December	3323	5333
	3	December	2223	3233
	4	December	3222	2233
	5	December	2201	1221
	6	December	2102	1001
	7	December	1111	1122
	8	December	1032	3311
	9	December	1234	2333
	10	December	3222	2333
	11	December	3332	2334
	12	December	3322	2334
	13	December	3233	3333
	14	December	1122	2443
	15	December	3212	2000
	16	December	112	4543
	17	December	4344	4343
	18	December	2233	3230
	19	December	1034	3321
	20	December	222	3332
	21	December	3344	3313
	22	December	2132	112
	23	December	2232	1122
	24	December	2323	2110
	25	December	22	2222
	26	December	1222	2233
	27	December	5334	4554
	28	December	3113	4344
	29	December	5433	4445
	30	December	4333	4233
	31	December	3112	3323



Year	Date		K-index	
1992	1	January	3122	2224
	2	January	5435	3331
	3	January	3213	2124
	4	January	3233	2133
	5	January	3222	2432
	6	January	2221	3333
	7	January	2202	2232
	8	January	3233	3232
	9	January	2200	2123
	10	January	3223	2223
	11	January	2213	3343
	12	January	3245	4442
	13	January	3333	3433
	14	January	3333	4434
	15	January	3233	4331
	16	January	1233	4344
	17	January	2222	2122
	18	January	1122	100
	19	January	1221	1201
	20	January	2223	3222
	21	January	1000	2223
	22	January	2122	2010
	23	January	22	1021
	24	January	1002	103
	25	January	2101	1001
	26	January	1	4423
	27	January	4434	2234
	28	January	2322	3332
	29	January	2232	3244
	30	January	3323	3333
	31	January	2232	2131
	1	February	2234	<b>5645</b>
	2	February	<b>3536</b>	<b>5466</b>
	3	February	<b>4565</b>	<b>6566</b>
	4	February	3343	3355
	5	February	3112	2001
	6	February	122	2112
	7	February	2234	3211
	8	February	3342	<b>5745</b>
	9	February	<b>6565</b>	3445
	10	February	3423	4432
	11	February	2222	2322
	12	February	3222	2303
	13	February	3234	2011
	14	February	133	3321
	15	February	122	2100
	16	February	1012	1111
	17	February	1245	<b>6322</b>
	18	February	3322	2312
	19	February	3233	3222
	20	February	5544	<b>5565</b>
	21	February	<b>6575</b>	5333
	22	February	4443	3233

	23	February	2332	1225
	24	February	3133	<b>3556</b>
	25	February	<b>5644</b>	4244
	26	February	3343	<b>4676</b>
	27	February	<b>6467</b>	3553
	28	February	2222	2012
	29	February	2215	5543
	1	March	2323	2223
	2	March	1232	3221
	3	March	2222	1221
	4	March	1133	3432
	5	March	1231	2332
	6	March	3131	1011
	7	March	1122	2324
	8	March	2223	3122
	9	March	3335	3442
	10	March	2333	2244
	11	March	3344	4331
	12	March	2233	2110
	13	March	122	1000
	14	March	1	111
	15	March	1133	2332
	16	March	1123	4342
	17	March	2015	4344
	18	March	4343	3211
	19	March	0	201
	20	March	1011	111
	21	March	2244	5554
	22	March	4312	2043
	23	March	4434	2244
	24	March	3423	3345
	25	March	4323	2211
	26	March	1224	3242
	27	March	2110	1143
	28	March	3122	1123
	29	March	3222	3342
	30	March	1311	2133
	31	March	4213	2333
	1	April	2323	2122
	2	April	1121	331
	3	April	1144	4542
	4	April	1233	3322
	5	April	2134	4224
	6	April	3453	3311
	7	April	2343	3221
	8	April	3332	2241
	9	April	1111	2112
	10	April	1111	1110
	11	April	1100	0
	12	April	1111	1200
	13	April	132	1011
	14	April	21	122
	15	April	3223	1101

	16	April	1111	1200
	17	April	0	202
	18	April	2223	4323
	19	April	4232	2334
	20	April	3322	3223
	21	April	3322	1100
	22	April	3223	2233
	23	April	2010	1322
	24	April	3333	2332
	25	April	2233	2113
	26	April	1022	1032
	27	April	2010	1132
	28	April	2123	2122
	29	April	2120	122
	30	April	2123	3101
	1	May	1132	2342
	2	May	3231	1111
	3	May	2112	2222
	4	May	2412	2201
	5	May	202	111
	6	May	11	1112
	7	May	2232	3243
	8	May	1233	4444
	9	May	3302	<b>3465</b>
	10	May	<b>4477</b>	<b>6666</b>
	11	May	<b>6532</b>	4443
	12	May	4421	1223
	13	May	3423	3113
	14	May	1101	0
	15	May	11	1000
	16	May	1	0
	17	May	11	11
	18	May	1011	135
	19	May	4311	1221
	20	May	3112	2113
	21	May	2021	23
	22	May	1444	5442
	23	May	2231	2351
	24	May	3321	1001
	25	May	3132	2221
	26	May	12	2123
	27	May	1132	2211
	28	May	2133	2222
	29	May	2231	3332
	30	May	1121	3222
	31	May	3210	200
	1	June	3321	1000
	2	June	1000	112
	3	June	1121	110
	4	June	0	1012
	5	June	1012	2211
	6	June	21	100
	7	June	122	1143

	8	June	5343	<b>3446</b>
	9	June	4243	1122
	10	June	1334	3322
	11	June	2312	2255
	12	June	5243	<b>4422</b>
	13	June	1210	1133
	14	June	2011	112
	15	June	3320	2221
	16	June	1101	1000
	17	June	110	110
	18	June	1111	<b>3365</b>
	19	June	3112	1231
	20	June	1211	2101
	21	June	3100	102
	22	June	3202	2111
	23	June	2311	1233
	24	June	2333	2332
	25	June	4222	2222
	26	June	1021	2113
	27	June	1012	2122
	28	June	1244	2212
	29	June	3432	2444
	30	June	4443	2203
	1	July	3322	2243
	2	July	2432	2002
	3	July	2100	0
	4	July	1	11
	5	July	2202	2012
	6	July	1001	1000
	7	July	10	101
	8	July	0	1001
	9	July	1101	1101
	10	July	1210	10
	11	July	1010	0
	12	July	2222	3122
	13	July	1343	2333
	14	July	3323	1231
	15	July	2201	0
	16	July	23	2231
	17	July	2100	1200
	18	July	101	1
	19	July	1020	11
	20	July	2201	2222
	21	July	122	2332
	22	July	2133	3253
	23	July	3433	2132
	24	July	2012	2211
	25	July	2012	2332
	26	July	1001	0
	27	July	2	13
	28	July	3432	1123
	29	July	0	1002
	30	July	3101	2032
	31	July	2022	1324

	1	August	3212	1011
	2	August	2	1121
	3	August	11	1100
	4	August	3101	3444
	5	August	4444	3123
	6	August	333	2222
	7	August	4334	4222
	8	August	2333	1333
	9	August	3113	2221
	10	August	2002	1012
	11	August	3122	2323
	12	August	2221	0
	13	August	12	3423
	14	August	3212	2420
	15	August	2030	33
	16	August	1122	1001
	17	August	2101	1
	18	August	1111	1021
	19	August	111	1122
	20	August	3544	4211
	21	August	1212	2441
	22	August	1234	4455
	23	August	<b>6762</b>	3132
	24	August	1123	1233
	25	August	1201	1001
	26	August	3233	1022
	27	August	1223	3232
	28	August	1200	12
	29	August	4323	2013
	30	August	1010	2021
	31	August	101	0
	1	September	1001	0
	2	September	1123	3444
	3	September	3345	4454
	4	September	4343	3235
	5	September	4333	2233
	6	September	3221	2243
	7	September	2233	3332
	8	September	4322	2232
	9	September	<b>4557</b>	5454
	10	September	5354	<b>5566</b>
	11	September	<b>6532</b>	1433
	12	September	3210	11
	13	September	1100	11
	14	September	122	1123
	15	September	2222	2220
	16	September	1122	2333
	17	September	4455	<b>4576</b>
	18	September	4434	3133
	19	September	3212	2231
	20	September	1122	2023
	21	September	1021	24
	22	September	4422	1123

	23	September	1213	121
	24	September	0	11
	25	September	2123	2233
	26	September	3200	1310
	27	September	12	2001
	28	September	22	3334
	29	September	3553	4434
	30	September	3333	4444
	1	October	3332	2341
	2	October	2120	112
	3	October	10	11
	4	October	2322	2000
	5	October	1111	1212
	6	October	2212	2111
	7	October	1122	1121
	8	October	3111	133
	9	October	<b>3336</b>	3343
	10	October	233	2012
	11	October	1113	4452
	12	October	3334	5422
	13	October	3111	3553
	14	October	3322	2145
	15	October	5333	3245
	16	October	5333	2313
	17	October	2223	3332
	18	October	2011	1323
	19	October	4223	3323
	20	October	3332	12
	21	October	1122	1212
	22	October	2112	3321
	23	October	1121	1002
	24	October	1100	2
	25	October	3122	1122
	26	October	3233	1233
	27	October	4333	2432
	28	October	3222	1222
	29	October	2333	2454
	30	October	2222	2323
	31	October	1022	2211
	1	November	1102	<b>1326</b>
	2	November	4522	2133
	3	November	4333	3022
	4	November	2122	3424
	5	November	3233	2121
	6	November	1122	2323
	7	November	2221	2213
	8	November	2221	1224
	9	November	3354	5334
	10	November	4223	2332
	11	November	3324	2322
	12	November	3213	3234
	13	November	2224	4222
	14	November	1223	3232

	15	November	2122	3434
	16	November	3220	1133
	17	November	2222	1122
	18	November	2012	1330
	19	November	123	2221
	20	November	1001	22
	21	November	3200	11
	22	November	1243	4333
	23	November	3533	4432
	24	November	2232	2332
	25	November	2133	3222
	26	November	2212	3012
	27	November	1111	2100
	28	November	1112	2121
	29	November	1122	3110
	30	November	23	2351
	1	December	3234	3313
	2	December	3212	2222
	3	December	1303	3322
	4	December	1133	3223
	5	December	3211	100
	6	December	1001	1111
	7	December	43	5135
	8	December	4323	3344
	9	December	3223	3323
	10	December	2224	1443
	11	December	2212	1222
	12	December	2211	2122
	13	December	3202	1211
	14	December	2111	2232
	15	December	3223	3133
	16	December	1222	0
	17	December	154	<b>4653</b>
	18	December	3212	1243
	19	December	1212	3244
	20	December	2232	2222
	21	December	1133	3442
	22	December	2122	3211
	23	December	1123	3221
	24	December	212	3231
	25	December	122	1222
	26	December	1001	111
	27	December	10	34
	28	December	3133	<b>4655</b>
	29	December	4333	3522
	30	December	2132	3211
	31	December	2132	3311



**ESKOM Transmission Group**

**TECHNOLOGY SERVICES  
DIVISION**

**SUBSTATION ENGINEERING  
DEPARTMENT**

**REPORT SE91/26**

**Alpha and Beta 765kV Reactors  
Investigations and Recommendations**

P V Goosen

R J C Moore

C E Odendaal

November 1991

REPORT ON FAILURE INVESTIGATION  
OF 765 KV REACTORS AT BETA SUBSTATION

CONTENTS PAGE

SUMMARY 1

BACKGROUND 2

ADDITIONAL INFORMATION RECEIVED FROM SITE 2

INSPECTION AT ROTK 2

FAULT SCENARIO 4

RECOMMENDATIONS 4

APPENDIX 1 5

APPENDIX 2 6

APPENDIX 3 7

R J C MOORE  
C E ODENDAAL  
P V GOOSEN

APPENDIX D

### S U M M A R Y

The cause of failure of two 765 kV shunt reactors at Beta Subst has been investigated by ESKOM and Toshiba.

This report covers these investigations and recommends that all Toshiba reactors be brought to Rotek for modifications as per T recommendations

P V GOOSEN  
R J MOORE  
C E ODENDAAL

## 1. BACKGROUND

Reactor No. 2 (Blue Phase Serial No. 85900082) failed on 18 April 1991. A Buchholz alarm was received approximately 1½ hours before failure occurred and the operator had requested National Control permission to switch out the reactor.

The reactor tripped on Buchholz and tank pressure protection. Tests carried out on site indicated failure and the unit was brought to Rotek for repair.

Reactor No. 2 (Red Phase Serial No. 85900002) was removed from service on 23 September 1991 approximately 1 hour after a Buchholz alarm. Oil testing of hydro carbon gases indicated overheating.

## 2. ADDITIONAL INFORMATION RECEIVED FROM SITE

According to site measurements no abnormal voltage conditions were recorded on the system prior to the faults nor at any previous occasion.

It was reported that the neutral earthing reactors on each three phase reactor bank had faulted during the past twelve months.

There were also reports of a high temperature alarm received on the Alpha 2 reactor on 30 January 1991.

## 3. INSPECTION AT ROTTEK

REACTOR SE. NO. 85900082 ET 1370

The following observations were made :

- 3.1 The windings near the top of the coil were severely twisted and bent. Flash marks were evident on the copper conductors.
- 3.2 The upper yoke was damaged at two places where overheating of the laminations had occurred to the extent that they had melted leaving cavities measuring approximately 100 x 50 mm.
- 3.3 The upper shunts controlling the leakage flux from the winding returning to the yokes showed signs of overheating. The shunt insulation had also deteriorated.



- 3.4 At the tips of three upper magnetic shunts on the line side, a number of laminations had spread open and bent towards the yoke. They had penetrated the insulation causing electrical contact. The yoke laminations had melted at these points.
- 3.5 Molten metal particles from the yoke laminations were found between some of the winding conductors.
- 3.6 The top wooden clamping ring was broken and showed signs of electrical tracking.
- 3.7 The oil had discoloured.
- 3.8 The lower magnetic shunts were slightly discoloured, but appeared normal.

REACTOR SE. NO. 85900002 271311

The following observations were made :

- 3.9 There was no apparent damage to the winding.
- 3.10 The winding insulation was contaminated with carbon deposits.
- 3.11 The upper yoke was damaged at two places where overheating and deterioration of the insulation had occurred.
- 3.12 The upper shunts controlling the leakage flux showed signs of overheating.
- 3.13 At the tips of three upper magnetic shunts on the line side, a number of laminations had spread open and bent towards the yoke. One shunt on the neutral side had bent in a similar manner. They had penetrated the insulation causing electrical contact. The yoke laminations had showed signs of overheating at these points.
- 3.14 The lower magnetic shunts were slightly discoloured, but appeared normal.

## FAULT SCENARIO

REACTOR SE. NO. 85900082

From the available evidence the mode of failure is as follows :

The shunts collecting the stray flux from the winding situated at the top neutral end of the winding overheated due to a high flux density. This region also corresponds to the highest oil temperature at the top of the winding. This caused the glue between laminations to fail allowing a number of laminations to bend towards the yoke as a result of magnetic forces. In the process they pressed their way through the insulation and made electrical contact with the yoke. This in turn set up local circulating currents which overheated and melted the yoke laminations at the points of contact. Molten metal dropped onto the windings causing interturn short circuits resulting in total winding failure.

REACTOR SE. NO. 85900002

A similar process had developed with this reactor resulting in yoke damage when the shunts bent to make electrical contact. There was evidence of local overheating, but melting had not occurred. Gas from the faults tripped the reactor by Buchholz protection.

## RECOMMENDATIONS

### PART A: TECHNICAL

1. IT IS RECOMMENDED THAT TOSHIBA'S PROPOSALS FOR REFURBISHMENT AND IMPROVEMENT OF THE EIGHT UNITS ON SITE AT BETA BE IMPLEMENTED WITHOUT CHANGES.

These are applicable to all operating reactors at Beta:

- 1.1 Remove reactor to Rotek
  - 1.2 Untank and remove winding (1st three under Toshiba supervision)
  - 1.3 Execute modifications around upper and lower magnetic shunts as per Toshiba improved design.
  - 1.4 Re-install original lower shunts
  - 1.5 Install winding
  - 1.6 Install new horizontally-stacked shunts ex Toshiba (original design) to replace thermally damaged units.
  - 1.7 Vapour phase
  - 1.8 Transport to BBT Pretoria and test as per Toshiba recommendations.
  - 1.9 Transport to Beta and re-install and commission.
2. SOURCE NEW REACTOR WINDING AS PER TOSHIBA ORIGINAL DESIGN FROM BBT/PRETORIA OR TOSHIBA/JAPAN AND REPAIR IMPROVE PROCESS AND TEST FIRST FAILED REACTOR AS PER ABOVE.
  3. REPAIR SECOND FAILED REACTOR AS PER TOSHIBA RECOMMENDATIONS AND IMPROVE AS ABOVE.
  4. REFILL ALL BETA REACTORS WITH NEW VIRGIN OIL. (8 X 30 KL)
  5. IMPROVE REACTOR COOLING WITH THE ADDITION OF FORCED AIR COOLING AS PER TOSHIBA'S RECOMMENDATION TO REDUCE THE OPERATING TEMPERATURE BY APPROXIMATELY 15 DEG CELSIUS.

#### PART B: OPERATIONAL

1. Operate the 765 kV system with a nominal target voltage of 765 kV.
2. Install protection to avoid overfluxing of reactors due temporary over voltages (eg 10 minutes @ 1.05 pu of 800 kV)
3. Modify the alarm functions of Buchholz relays on all 765 kV reactors and transformers to initiate trips and configure the tripping logic appropriately to avoid consequential overvoltages following such tripping.
4. Convert BOTH 765 kV lines to 400 kV operation in order to facilitate the expeditious modification to all reactors in a target time of 12 months (subject to confirmation) without complex operating restrictions

#### PART C: PURCHASE OF BBT SPARE REACTORS

1. Proceed with purchase of two units from BBT

PART D: NEGOTIATIONS WITH TOSHIBA

1. Ratify verbal approval given to Toshiba to proceed with immediate manufacture of replacement shunts.
2. COST SHARING ESKOM/TOSHIBA
  - 2.1 Negotiate for free delivery of all Toshiba repair/replacement/improvement material to Rotek.
  - 2.2 Negotiate best price for one replacement winding required for repair of first faulted reactor.  
(BBT or Toshiba)
  - 2.3 Negotiate for free Toshiba quality control on winding if supplied by BBT/Pretoria.
  - 2.4 Negotiate for free supervision of repair/refurbishment of first three reactors with training being transferred to nominated Rotek personnel.
  - 2.5 We recommend that Eskom pay all transport, testing, workshop and re-installation and recommissioning costs
  - 2.6 Negotiate for 50% sharing of cost for the supply of forced air cooling equipment and fittings to Beta site with installation and commissioning at Eskom's cost.
  - 2.7 Risks of equipment damage during refurbishment/repair actions to be carried by Eskom.
  - 2.8 Cost of new oil to be carried by Eskom.

#### PART E: ALPHA SUBSTATION REACTOR PROBLEM

1. Negotiate with Fuji to obtain technical details of internal designs to evaluate gassing problem.
2. Transport worst case Fuji Reactor to Rotek for inspection in January 1992.
3. Negotiate with Fuji to have designers available at Rotek for inspection in February 1992.
4. Treat other Fuji reactors at Alpha subject to findings.

#### PART F: VISIT TO TOSHIBA AND FUJI/JAPAN

It is recommended that a combined technical and commercial team be sent to Japan in January 1992 for negotiating with Toshiba and conducting technical discussions with Fuji.

#### PART G: PROJECT ESTABLISHMENT

In view of the importance, magnitude and logistics involved in executing the above recommendations (+/- R 15m), it is recommended that a project complete with vote and budget be established and a formal Project Leader be appointed.

#### COSTS AND TIME SCHEDULES

These are being prepared by Rotek.

# ESTIMATED COSTS OF REPAIRS FOR SERIAL NO. 85900002

	(RAND)
Dismantle (Beta)	150 000
Transport Beta - Rotek	43 000
Rotek workshop charges	] 592 000
Rotek labour charges	
Transport (Rotek - BBT)	18 000
BBT Testing	60 000
Transport (BBT - Beta)	43 000
Installation charges	190 000
Filling of new oil (30 kl)	43 000
Recommissioning charges	13 000
Toshiba Materials	(To be negotiated)
Toshiba supervision (first 3 units only)	70 000
Supply of cooling fans	] 120 000
Installation of cooling fans	
Substation Technology Technical Supervision (One man month per reactor)	8 000
	-----
TOTAL	1 350 000

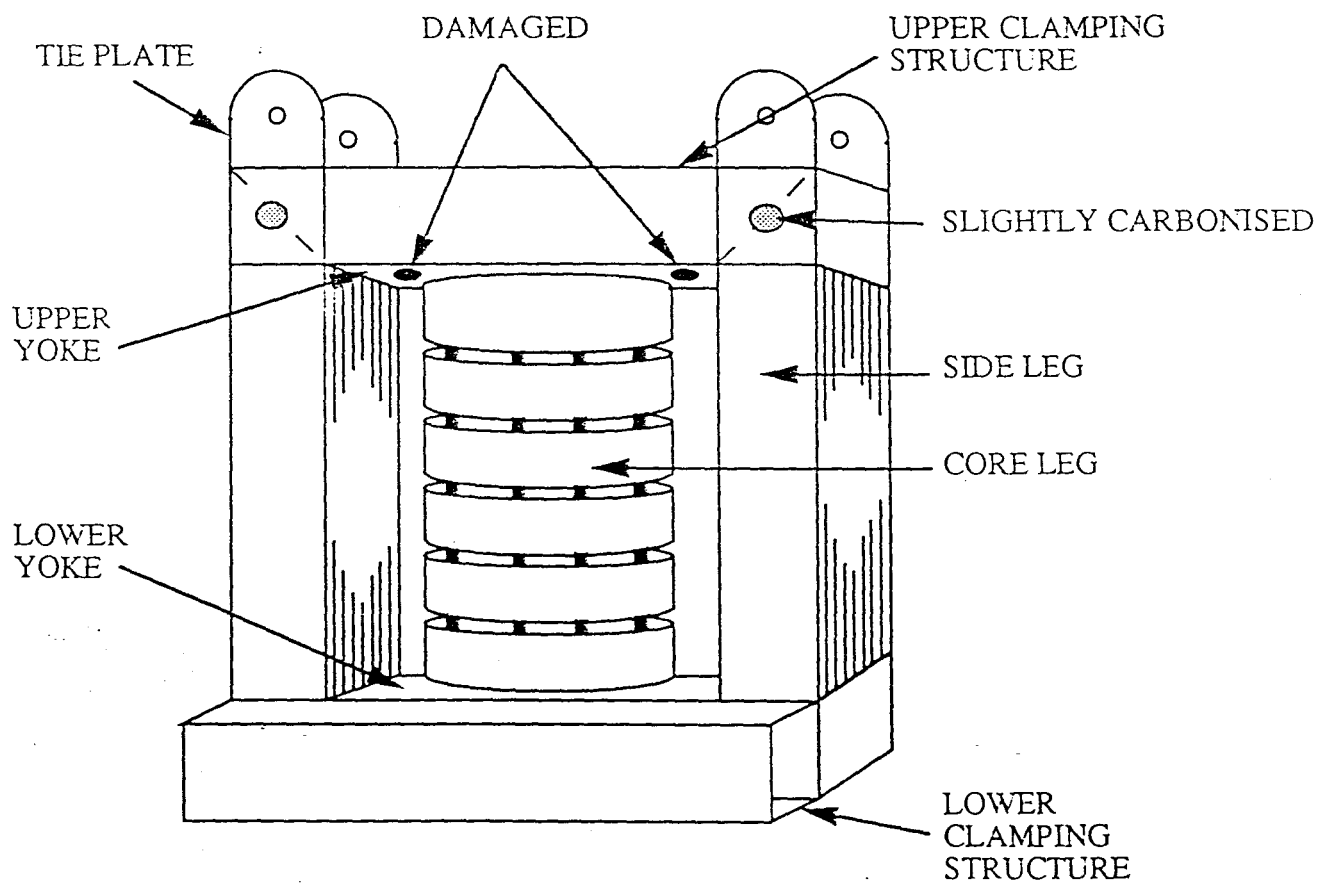
# ESTIMATED COSTS OF REPAIRS FOR REMAINING UNITS AT BETA

## ESTIMATED COST PER SINGLE PHASE UNIT (FOR EIGHT UNITS)

	(RAND)
Dismantle (Beta)	150 000
Transport Beta - Rotek	43 000
Rotek workshop charges ]	375 000
Rotek labour charges ]	
Transport (Rotek - BBT)	18 000
BBT Testing	60 000
Transport (BBT - Beta)	43 000
Installation charges	190 000
Filling of new oil (30 kl)	43 000
Recommissioning charges	13 000
Toshiba Materials	(To be negotiated)
Toshiba supervision (first 3 units only)	70 000
Supply of cooling fans ]	120 000
Installation of cooling fans ]	
Substation Technology Technical Supervision (One man month per reactor)	5 000
	-----
TOTAL	1 130 000



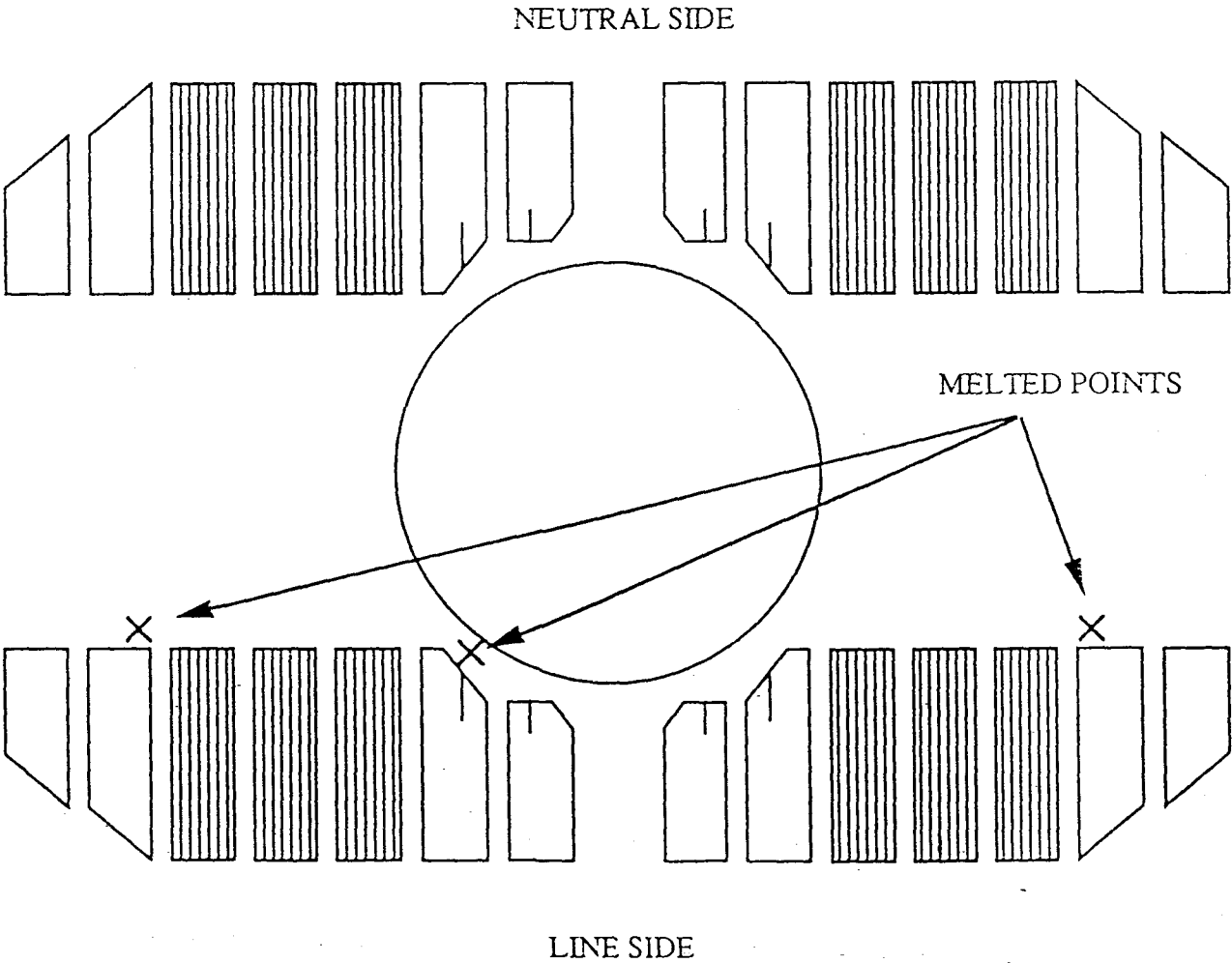
CORE CLAMPING CONSTRUCTION



TEST ITEM

1. MEASUREMENT OF WINDING RESISTANCE
2. MEASUREMENT OF REACTANCE (ABOVE 2000)
3. DIELECTRIC LOSS ANGLE ( $\tan \delta$ ) TEST (including capacitance)
4. SEPARATE SOURCE VOLTAGE WITHSTAND TEST ACCORDING TO IEC REDUCED VOLTAGE (95 kV x 0.8)
5. IMPULSE VOLTAGE WITHSTAND TEST  
1950 kV x 0.8
6. SWITCHING IMPULSE VOLTAGE WITHSTAND TEST  
1425 kV x 0.8

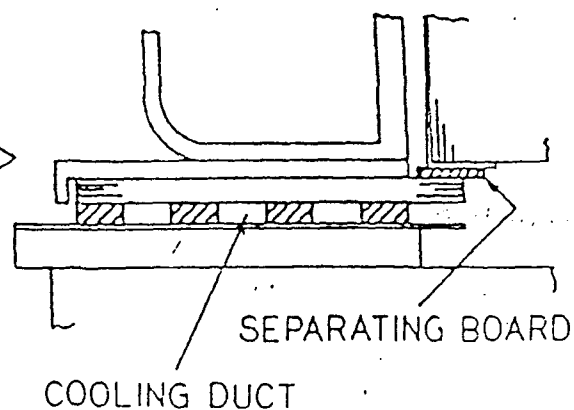
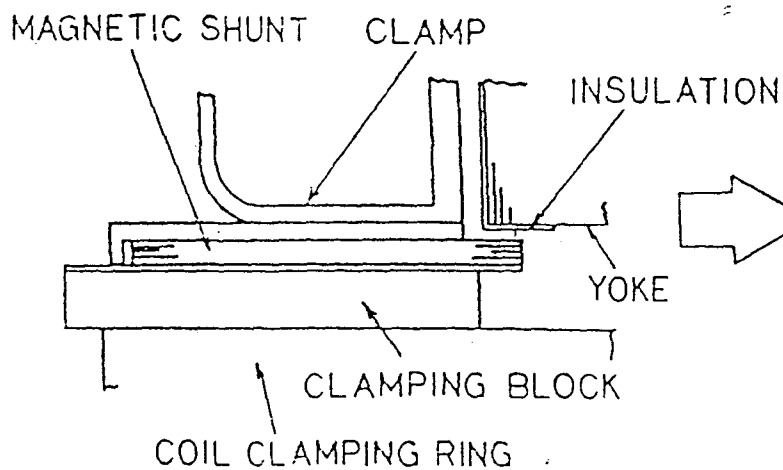
UPPER MAGNETIC SHUNT



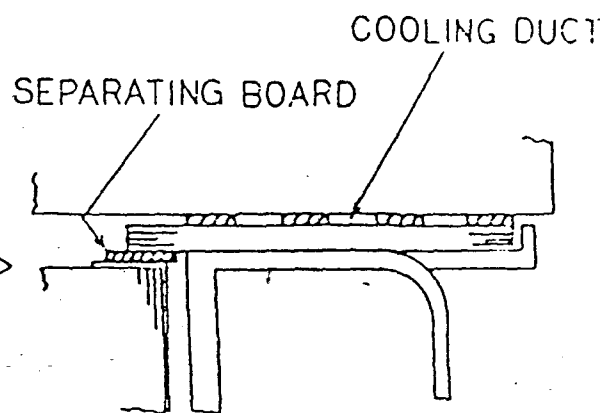
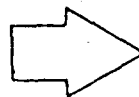
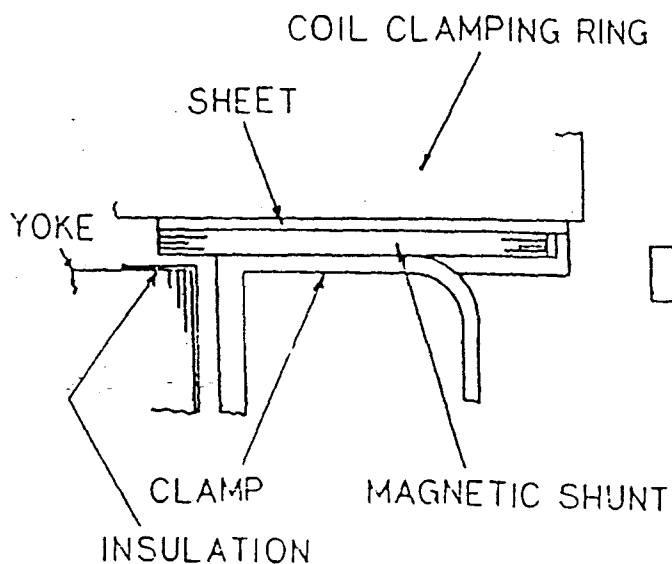
# CLAMP CONSTRUCTION

## EXISTING CONSTRUCTION

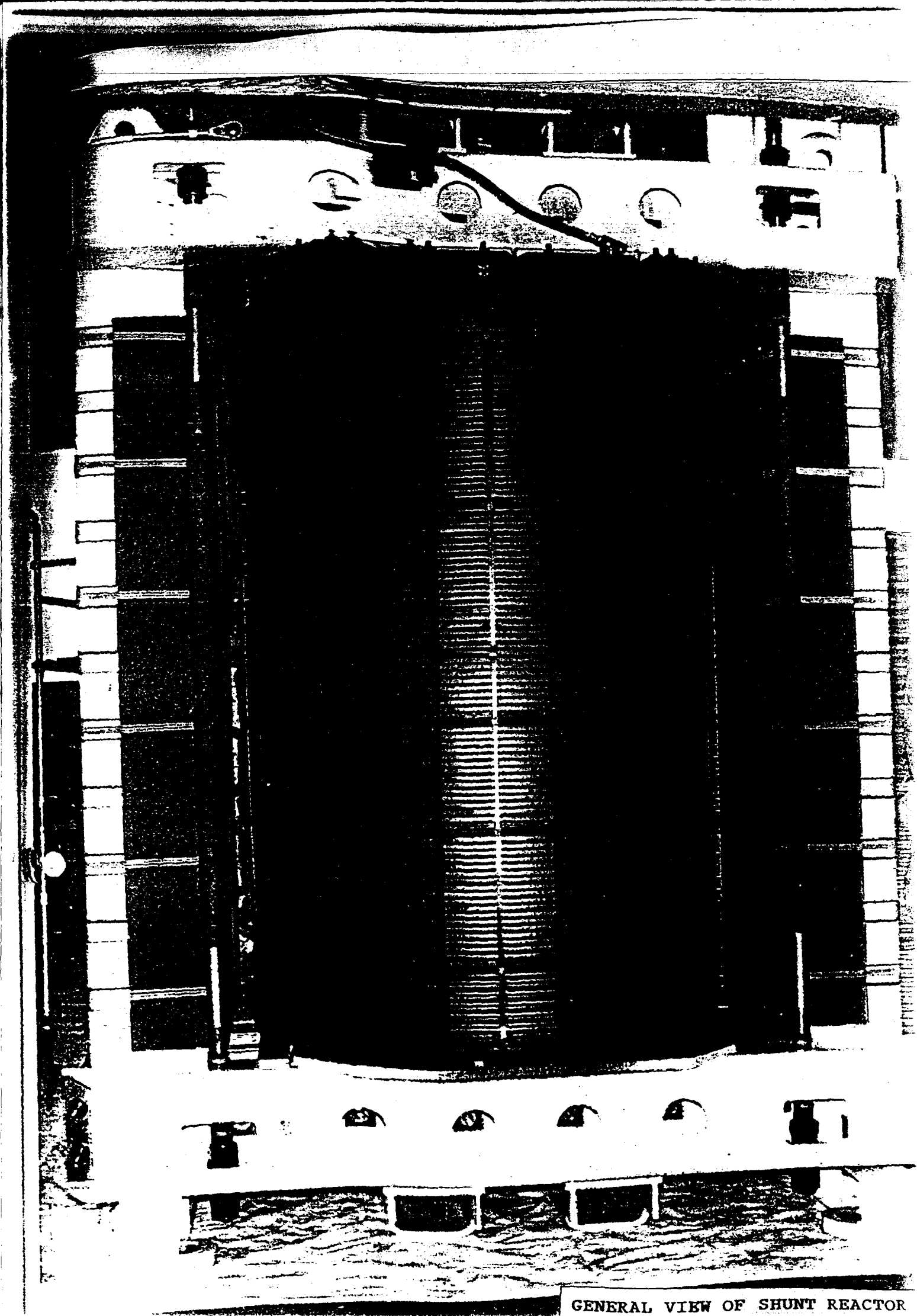
## NEW CONSTRUCTION



## UPPER SIDE



## LOWER SIDE



GENERAL VIEW OF SHUNT REACTOR



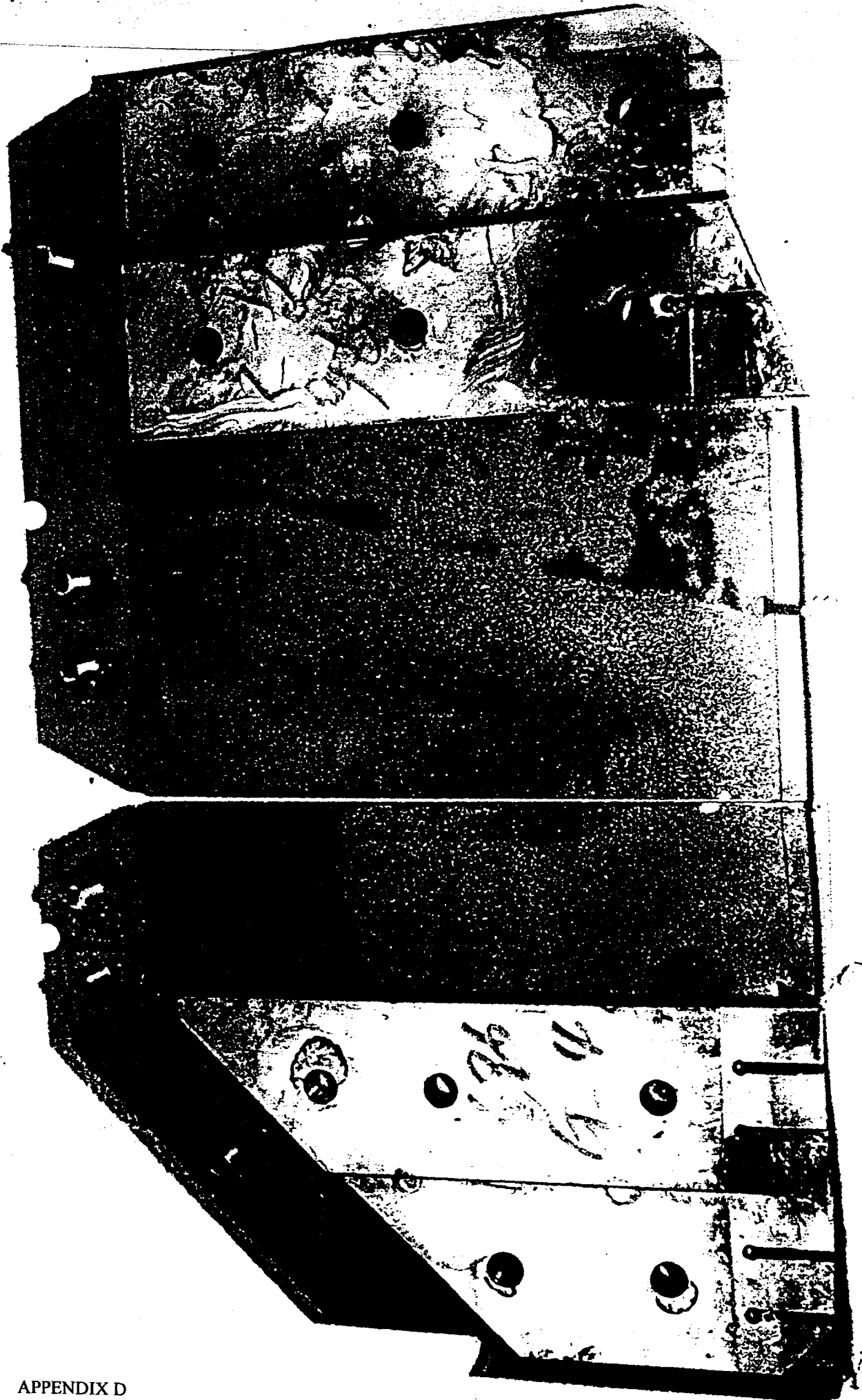
APPENDIX D

TIPS OF DAMAGED SHUNTS

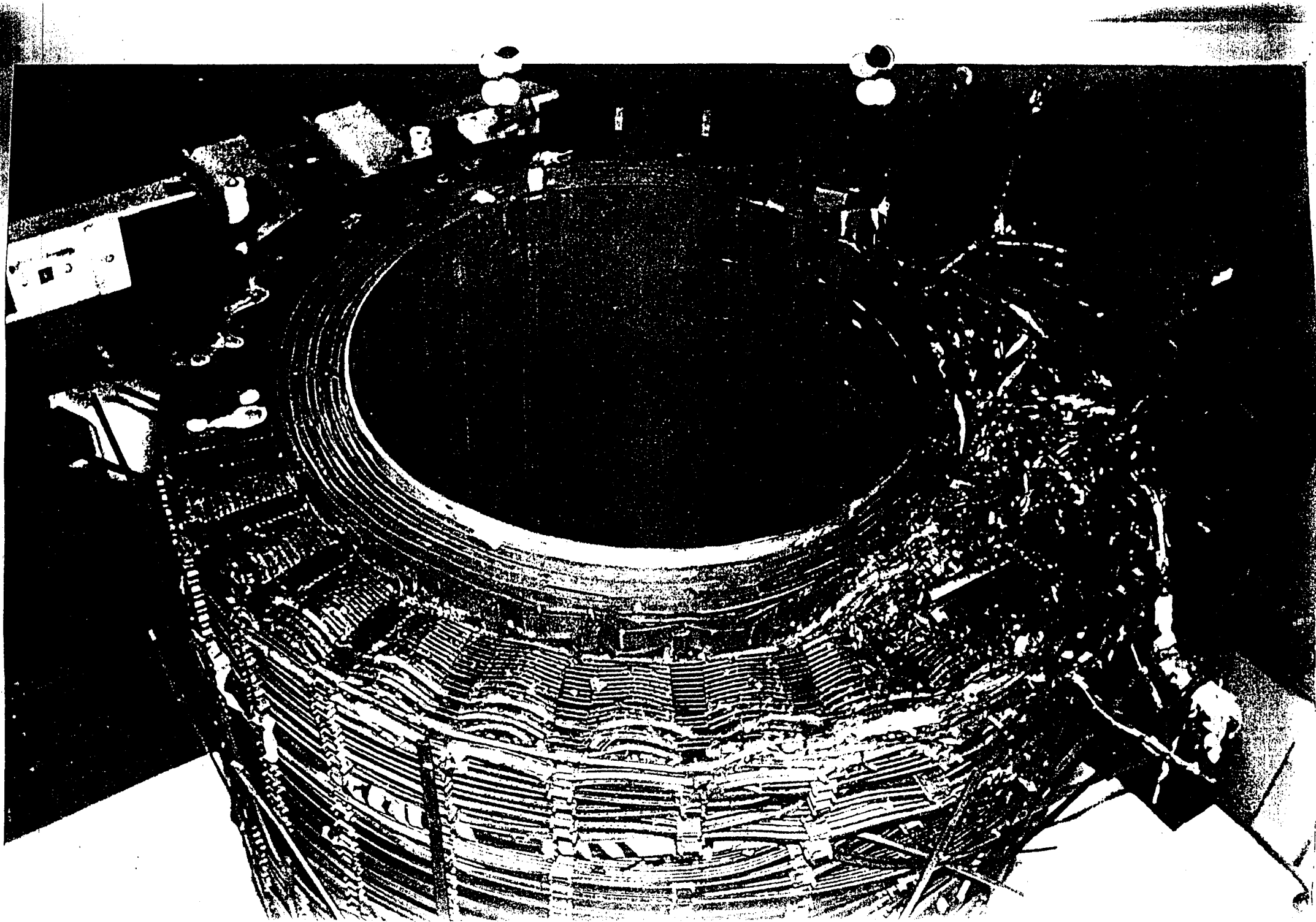


POINT OF SHUNT CONTACT TO YORE  
SHOWING OVERHEATING AND DAMAGE  
INSULATION

11







## APPENDIX E:

### CALCULATING THE ELECTRIC FIELD

The following calculation is a simplified example to illustrate the use of the equations in section 4.3. This procedure to calculate the electric field has been derived by Viljanen and Pirjola [68]. The earth is described as a half-space with a constant conductivity of  $\sigma$  and the geomagnetic field propagates as a vertical plane wave in the earth. Using Cartesian co-ordinates, the x-axis is directed to the magnetic north, y to the magnetic east and z downwards. The electric field is then obtained by

$$E(T_N) = \frac{2}{\sqrt{\pi \mu_0 \sigma \Delta}} (R_{N-1} - R_N - \sqrt{M} b_{N-M}) \quad \dots(1)$$

where  $\Delta$  is the sampling interval,  $N$  is the sample number,  $M = 10$  [66] and

$$R_N = \sum_{n=N-M+1}^N b_n \sqrt{N-n+1} \quad \dots(2)$$

where  $b_n = B_n - B_{n-1}$  ( $B$  being the magnetic component).

Since magnetic and electric fields are perpendicular,  $E_x$  will be calculated from  $B_y$  and  $E_y$  from  $B_x$ . This calculation was done to obtain the eastern electric field ( $E_y$ ) from data on the northern magnetic field ( $B_x$ ) as found in table 2 (none real values are used to simplify the example).

**Table E1** Five samples of northern magnetic field.

N	1	2	3	4	5
$B_x$ [nT]	300	320	290	300	330

The following assumptions and constants are used:

$N = 5$  (sampling number),

$\sigma = 0.001$  (conductivity, i.e.  $\rho = 1000 \Omega.m$ ),

$\mu_0 = 4\pi \times 10^{-7}$  (vacuum permeability),

$\Delta = 10$  s (sampling interval), and,

$M = 3$  ( $M=3$  to simplify the calculation, normally  $M = 10$ ).

Then:

$$E(T_5) = \frac{2}{\sqrt{\pi \mu_0 \sigma \Delta}} (R_4 - R_5 - \sqrt{3} b_2)$$

$$b_2 = B_2 - B_1 = 20 \times 10^{-9} T$$

$$R_4 = \sum_{n=4-3+1}^4 b_n \sqrt{4-n+1}$$

$$R_4 = b_2 \sqrt{3} + b_3 \sqrt{2} + b_4 \sqrt{1} = 2.215 \times 10^{-9}$$

$$\text{similarly } R_5 = -7.819 \times 10^{-9}$$

$$E_y(T_5) = 10066 \times (R_4 - R_5 - \sqrt{3} b_2) = -0.25 V / km$$

## APPENDIX F

### Magnetic Data Used for Example in Chapter 4

Sample	$B_x$ [nT]	$dB_x/dt$ [nT/min]	$E_y$ [V/km]	$B_y$ [nT]	$dB_y/dt$ [nT/min]	$E_x$ [V/km]	$I_{glc} = aE_x + bE_y$ [A]
0	9846			-4325			
1	9854	4	-0.009	-4332	-4	0.033	-4
2	9856	1	0.024	-4337	-3	0.019	-8
3	9865	4	-0.051	-4339	-1	0.033	5
4	9877	6	-0.059	-4345	-3	0.034	6
5	9892	7	-0.069	-4350	-3	0.032	8
6	9880	-6	-0.013	-4342	4	-0.006	4
7	9866	-7	0.024	-4339	2	-0.012	-3
8	9854	-6	0.046	-4329	5	-0.030	-4
9	9851	-2	0.030	-4325	2	-0.028	-1
10	9852	1	0.025	-4317	4	-0.048	3
11	9854	1	0.029	-4308	4	-0.052	3
12	9842	-6	0.042	-4284	12	-0.101	8
13	9842	0	0.004	-4258	13	-0.116	18
14	9843	0	0.015	-4249	5	-0.089	12
15	9852	5	-0.034	-4239	5	-0.085	20
16	9866	7	-0.047	-4242	-1	-0.050	17
17	9867	1	-0.018	-4243	-1	-0.024	8
18	9872	3	-0.042	-4245	-1	-0.007	9
19	9880	4	-0.044	-4245	0	-0.014	11
20	9847	-16	0.074	-4226	10	-0.049	-7
21	9843	-2	0.025	-4218	4	-0.031	0
22	9852	4	-0.001	-4227	-5	0.004	-1
23	9866	7	-0.034	-4271	-22	0.145	-17
24	9901	18	-0.103	-4329	-29	0.206	-13
25	9936	17	-0.137	-4384	-28	0.279	-18
26	9956	10	-0.165	-4427	-21	0.280	-13
27	9952	-2	-0.063	-4448	-11	0.235	-26
28	9984	16	-0.167	-4453	-3	0.143	10
29	10003	10	-0.139	-4442	6	0.035	22
30	9971	-16	0.035	-4390	26	-0.117	12
31	10065	47	-0.307	-4374	8	-0.080	74
32	10041	-12	-0.033	-4373	1	-0.081	20
33	9958	-41	0.209	-4354	9	-0.112	-23
34	9931	-14	0.108	-4338	8	-0.115	-3
35	9957	13	-0.027	-4343	-2	-0.025	10
36	10081	62	-0.312	-4358	-8	0.000	62
37	10001	-40	0.158	-4337	10	-0.080	-18
38	9979	-11	0.031	-4278	30	-0.202	27
39	9954	-12	0.075	-4202	38	-0.313	36
40	9916	-19	0.152	-4176	13	-0.192	1
41	9921	2	0.110	-4172	2	-0.163	5
42	9897	-12	0.127	-4140	16	-0.213	9
43	9872	-12	0.185	-4113	14	-0.181	-7

44	9789	-41	0.271	-4013	50	-0.372	7
45	9777	-6	0.160	-4001	6	-0.156	-6
46	9773	-2	0.166	-4039	-19	-0.008	-32
47	9843	35	-0.163	-4108	-34	0.142	9
48	9871	14	-0.067	-4126	-9	0.081	0
49	9850	-11	-0.026	-4143	-8	0.150	-19
50	9860	5	-0.078	-4119	12	0.050	7
51	9824	-18	0.052	-4091	14	-0.036	-4
52	9800	-12	0.106	-4091	0	-0.018	-18
53	9784	-8	0.105	-4104	-6	0.016	-23
54	9781	-2	0.073	-4123	-9	0.060	-24
55	9751	-15	0.133	-4153	-15	0.096	-42
56	9735	-8	0.111	-4169	-8	0.116	-41
57	9733	-1	0.067	-4173	-2	0.086	-27
58	9725	-4	0.057	-4192	-10	0.110	-29
59	9720	-3	0.059	-4199	-3	0.067	-23
60	9717	-1	0.035	-4201	-1	0.048	-15
61	9707	-5	0.049	-4209	-4	0.049	-18
62	9695	-6	0.065	-4219	-5	0.065	-24
63	9683	-6	0.059	-4231	-6	0.064	-22
64	9673	-5	0.061	-4249	-9	0.094	-27
65	9678	3	0.022	-4270	-10	0.108	-22
66	9671	-4	0.046	-4301	-15	0.155	-34
67	9676	3	-0.005	-4334	-16	0.172	-27
68	9702	13	-0.074	-4339	-3	0.108	-3
69	9710	4	-0.048	-4327	6	0.038	3
70	9699	-5	0.002	-4320	4	0.020	-4
71	9683	-8	0.029	-4314	3	0.002	-6
72	9691	4	-0.028	-4332	-9	0.041	-1
73	9793	51	-0.301	-4356	-12	0.092	45
74	9803	5	-0.097	-4362	-3	0.054	11
75	9824	10	-0.181	-4368	-3	0.056	27
76	9863	19	-0.239	-4371	-2	0.048	39
77	9872	4	-0.131	-4344	13	-0.071	38
78	9820	-26	0.063	-4317	14	-0.095	3
79	9821	0	0.004	-4300	8	-0.092	14
80	9829	4	-0.009	-4306	-3	-0.039	8
81	9838	5	-0.008	-4313	-3	-0.035	7
82	9854	8	-0.021	-4310	1	-0.036	10
83	9859	3	-0.055	-4283	13	-0.082	24
84	9872	6	-0.085	-4257	13	-0.097	33
85	9875	2	-0.045	-4247	5	-0.085	23
86	9850	-13	0.044	-4250	-2	-0.050	-1
87	9841	-5	0.053	-4242	4	-0.063	0
88	9828	-7	0.050	-4241	1	-0.029	-5
89	9824	-2	0.059	-4247	-3	0.009	-13
90	9821	-2	0.046	-4245	1	-0.007	-8